International Journal of Photoenergy

Advanced Oxidation Processes for Wastewater Treatment 2014

Guest Editors: Muruganandham Manickavachagam, Mika Sillanpaa, Meenakshisundaram Swaminathan, and Bashir Ahmmad

Advanced Oxidation Processes for Wastewater Treatment 2014

International Journal of Photoenergy

Advanced Oxidation Processes for Wastewater Treatment 2014

Guest Editors: Muruganandham Manickavachagam, Mika Sillanpaa, Meenakshisundaram Swaminathan, and Bashir Ahmmad

Editorial Board

Contents

Hindawi Publishing Corporation
International Journal of Photoenergy
Volume 2015, Article ID 363167, 1 page
http://dx.doi.org/10.1155/2015/363167

Editorial

Advanced Oxidation Processes for Wastewater Treatment 2014

Muruganandham Manickavachagam,[1] Mika Sillanpaa,[2] Meenakshisundaram Swaminathan,[3] and Bashir Ahmmad[4]

[1] *Water and Environmental Technology (WET) Center, College of Engineering, Temple University, Philadelphia, PA 19122, USA*
[2] *Laboratory of Green Chemistry, Faculty of Technology, Lappeenranta University of Technology, 50130 Mikkeli, Finland*
[3] *Department of Chemistry, Annamalai University, Annamalai Nagar 608002, India*
[4] *Graduate School of Science and Engineering, Yamagata University, 4-3-16 Jonan, Yamagata 992-8510, Japan*

Correspondence should be addressed to Muruganandham Manickavachagam; mmuruganandham@temple.edu

Received 6 April 2015; Accepted 6 April 2015

Growing concern of various environmental issues leads to developing various advanced technologies. Water contamination is a common and ubiquitous problem worldwide, although many water treatment technologies have been used for water treatment. Thus, one of the notable advanced water treatment processes is using Advanced Oxidation Processes (AOPs) for the treatment of wastewater with high degree of pollutants. AOPs offer various advantages over conventional water treatment processes and various aspects of AOPs have been studied and reported in the literature. Two successful special issues had been published earlier and this is the third special issue in this journal.

Electrochemical treatment of spent caustic from two hydrocarbon industries using Ti/BDD electrode was studied and reported by A. Medel et al. In their article, they discussed electrochemical degradation of contaminants and analyzed various water quality parameters. Souz et al., reported inactivation of microorganisms such as *E. Coli*, total coliforms and coliphages using peracetic acid (PAA) in the presence and absence of UV light. They concluded that the combined PAA/UV process provided superior efficacy compared to individual process.

Ozonation of indigo carmine using a Fe/*Pimenta dioica* L. Merrill catalyst was studied and reported by T. Torres-Blancas et al. The authors tested a new catalyst for the catalytic ozonation process and characterized it with suitable analytical methods. Recommendation is being made for effective removal of dye pollutants. Another interesting research has been published by H. A. Kabuk et al. They have used a fuzzy logic model to determine the biological treatability of textile wastewater. They have used a membrane bioreactor (MBR) for biological treatment after the ozonation of the wastewater. The COD, BOD, and color removal efficiencies in the treatment process was studied. The removal of polyvinyl alcohol using an innovative paired photoelectrochemical oxidative system in a divided electrochemical cell was reported by K.-Y. Huang et al. They reached conclusion from their studies that the synergistic effect of combination process of MEO and PEO could be a promising treatment method for PVA removal from wastewater.

Acknowledgment

We are much grateful to the scientific colleagues, who reviewed the manuscripts by sparing their valuable time.

Muruganandham Manickavachagam
Mika Sillanpaa
Meenakshisundaram Swaminathan
Bashir Ahmmad

Hindawi Publishing Corporation
International Journal of Photoenergy
Volume 2015, Article ID 608412, 9 pages
http://dx.doi.org/10.1155/2015/608412

Research Article

Ozonation of Indigo Carmine Enhanced by Fe/*Pimenta dioica* L. Merrill Particles

Teresa Torres-Blancas,[1] Gabriela Roa-Morales,[1] Carlos Barrera-Díaz,[1] Fernando Ureña-Nuñez,[2] Julian Cruz-Olivares,[1] Patricia Balderas-Hernandez,[1] and Reyna Natividad[1]

[1] *Universidad Autónoma del Estado de México (UAEMex), Centro Conjunto de Investigación en Química Sustentable (CCIQS), UAEM-UNAM, Carretera Toluca-Atlacomulco, Km 14.5, 50200 Toluca, MEX, Mexico*
[2] *Instituto Nacional de Investigaciones Nuclearles (ININ), Carretera México-Toluca s/n, 52750 La Marquesa Ocoyoacac, MEX, Mexico*

Correspondence should be addressed to Gabriela Roa-Morales; groam@uaemex.mx and Reyna Natividad; reynanr@gmail.com

Received 2 October 2014; Accepted 17 February 2015

Academic Editor: Meenakshisundaram Swaminathan

Green synthesis of metallic particles has become an economic way to improve and protect the environment by decreasing the use of toxic chemicals and eliminating dyes. The synthesis of metal particles is gaining more importance due to its simplicity, rapid rate of synthesis of particles, and environmentally friendly. The present work aims to report a novel and environmentally friendly method for the synthesis of iron particles using deoiled *Pimenta dioica* L. Merrill husk as support. The indigo carmine removal efficiency by ozonation and catalyzed ozonation is also presented. Synthesized materials were characterized by N_2 physisorption and scanning electron microscopy (SEM/EDS). By UV-Vis spectrophotometry the removal efficiency of indigo carmine was found to be nearly 100% after only 20 minutes of treatment under pH 3 and with a catalyst loading of 1000 mgL^{-1}. Analytical techniques such as determination of the total organic carbon content (TOC) and chemical oxygen demand (COD) showed that iron particles supported on deoiled *Pimenta dioica* L. Merrill husk can be efficiently employed to degrade indigo carmine and achieved a partial mineralization (conversion to CO_2 and H_2O) of the molecule. From the results can be inferred that the prepared biocomposite increases the hydroxyl radicals generation.

1. Introduction

Textile industry is the greatest consumer of high quality fresh water per kg of treated material. Its production processes, due to their nature, significantly contribute to pollution, since the wastewater is a source of persistent organic pollutants. This is reflected on high chemical oxygen demand (COD) values. Textile wastewater also contains chemicals such as formaldehyde, azo dyes, dioxins, and heavy metals [1–3]. These contaminants are mostly toxic, carcinogenic, and persistent. Dyes are mostly complex molecules and are naturally degraded under high temperature, alkaline conditions, ultraviolet (UV) radiation, and other radical initiators generating the formation of by-products many times more toxic to the environment than the original dye [4]. The generated by-products are known to cause perturbations in the aquatic life and food. In addition, textile dyes are designed to be resistant to microbial, chemical, thermal, and photolytic degradation and thus producing recalcitrant compounds [5]. Thus, an effective and economical technique for removing dyes from textile wastewaters is needed. In this sense, several conventional methods for treating textile industry effluents have been studied, such as photodegradation, adsorption, filtration, coagulation, and biological treatments [6, 7]. However, due to the stability of the molecules of dyes some of these methods are not completely effective and/or viable. In this sense, advanced oxidation processes (AOPs) have been studied in order to destroy the dye molecules, decolorize the wastewater, and reduce organic pollution. Among these advanced oxidation processes (AOPs), ozonation has drawn attention. Ozonation is an effective, versatile, and environmentally sound technique that has been proven as a good

method for color removal [8, 9]. It oxidizes organic pollutants via two pathways: direct oxidation with ozone molecules and/or the generation of free-radical intermediates, such as the $HO^{\bullet}$ radical, which is a powerful, effective, and nonselective oxidizing agent [10, 11]. However, the oxidation rate by ozonation is limited by the chemical and molecular stability of the pollutant [2, 12–14]. In order to enhance the ozone oxidation capabilities the addition of metallic particles as catalysts has been suggested [12]. In this context, transition metals are preferred since they exhibit properties that promote free radicals production during the ozonation process. Colloidal particles, either alloyed or core-shelled, have attracted significant attention due to new properties that emerge from the combination of different metals (synergistic effect) in the nanoscale and to the consequent enhancement of the physical and chemical properties of the resulting material [15, 16]. The application of metallic particles supported on solid surfaces has been previously reported [17, 18]. It was found that the substrates containing immobilized particles have several functions in analytical chemistry. In general terms, the immobilization of particles or nanoparticles on a solid substrate shows several advantages for analytical applications [19]. Regarding advanced oxidation processes, metal-catalyzed ozonations have particularly drawn attention for water decontamination and therefore the use of metallic particles is being extensively investigated [20, 21]. In this context, the main aim of this study is to test a new biocomposite material, which consists of stable iron particles using deoiled *Pimenta dioica* L. Merrill husk as support. The evaluation of the removal efficiency using ozonation and catalyzed ozonation of indigo carmine is presented. Allspice (*Pimenta dioica* L. Merrill) belongs to the Myrtaceae family. Mexico exports around 4500 tons per year and half the production is processed in the country. During the oil extraction processes either through steam distillation, hydrodistillation, or supercritical extraction the berry oil yield ranges from 3.0 to 4.5%. The residue of the oil extraction processes is at least 95.5% in weight, reaching annually 1500 tons in Mexico. Exhausted allspice is a fibrous material that contains 23.1% cellulose, 8.5% hemicellulose, and 26.8% lignin and is the essayed biosupport in this work [22].

2. Materials and Methods

2.1. Reagents. The crushed deoiled residue of allspice was obtained as a product of a hydrodistillation process. This waste was first washed with an ethanol-water solution (40–60% v/v), in order to eliminate colored and remaining substances; later on, it was dried at 70°C for 24 h. Once the adsorbent was cooled down, it was sieved through numbers 10, 80, and 170 meshes, obtaining particles sized 2.00, 0.177, and 0.088 mm, respectively. It was then stored in a desiccator. Sodium hydroxide, sulfuric acid, sodium borohydride, iron sulfate, and indigo carmine (IC) dye analytical grade were purchased from Sigma-Aldrich Chemicals. Ozone was generated *in situ* from dry air by an ozone generator (Pacific Ozone Technology), with an average ozone production of 0.005 gdm^{-3}.

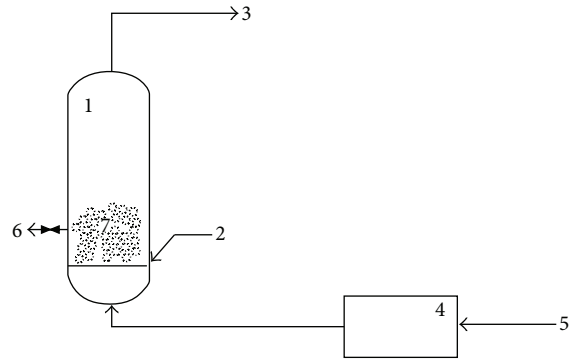

Figure 1: Schematic of the apparatus for the ozonation reaction. (1) Upflow glass bubble column reactor. (2) Porous glass (gas diffuser). (3) Pacific Technology D412 ozone destroyer. (4) Ozone generator. (5) Dry air inlet. (6) Sample valve. (7) Reaction solution.

2.2. Synthesis of Iron Particles and Iron Supported on Deoiled Allspice Husk. Using porous materials is an interesting alternative to control the stability of zero-valent particles [16]. It has been previously reported that the employment of porous materials improves the stability and catalytic properties of supported metal particles and nanoparticles [6]. In this work deoiled allspice husk was employed as porous material for the synthesis and stabilization of metal particles. The synthesis and support of iron particles on deoiled allspice husk were as follows: approximately 10 g of deoiled allspice husk (MPS) was placed in a 500 mL Erlenmeyer flask and mixed with 250 mL of a 0.01 M $FeSO_4$ solution for 24 h under continuous stirring at room temperature and N_2 atmosphere. Then 10 mL of 0.1 NaOH solution was added and the resulting slurry was kept under stirring for further half an hour. After this time, 60 mL of 0.25 M $NaBH_4$ solution was gradually added in order to obtain the metallic particles via reaction (1) [16]. After vacuum filtration, the solid was washed with reagent grade acetone and labelled as MPS/Fe. To synthesize the unsupported iron particles (Fe-NP), 250 mL of 0.01 M $FeSO_4$ solution was mixed with 15 mol of 0.1 NaOH solution and 60 mL of 0.25 M $NaBH_4$. The resulting slurry was also filtered under vacuum and the solid was washed with reagent grade acetone and labelled as Fe-NP:

$$2Fe^{2+} + 2H_2O + BH_4^- + 4e^- \longrightarrow 2Fe_{(s)} + BO_2^- + 4H^+ + 2H_{2(g)} \uparrow \quad (1)$$

2.3. Ozonation. The different ozonation treatments were conducted in a 1 L upflow bubble column reactor (see Figure 1). Ozone was fed through a gas diffuser with a pore size of 2 μm. A heated catalytic ozone destructor (Pacific Technology d41202) was employed in order to destroy the excess of ozone in the outlet of the glass bubble column reactor so there was no ozone being discharged to atmosphere. Samples were taken at specific time intervals to be analyzed. All experiments were carried out at room temperature (19°C ± 2), pH was adjusted at 3.0 with analytical grade sulfuric acid and sodium hydroxide, and the initial IC concentration was 1000 mgL^{-1}. The assessed variables were particle size and

solid concentration. In order to establish the IC adsorption capacity of the synthesized materials, every one of them was placed into an IC solution without feeding ozone. In these experiments the IC concentration at specific time intervals was established by UV-Vis spectrophotometry.

2.4. Chemical Analysis. To determine the concentration of indigo carmine at specific time intervals a spectrophotometric technique was employed. For such a purpose an UV-Vis Perkin Elmer Lambda 25 model spectrophotometer was used. Samples were analyzed in the range of 200 to 900 nm with a scan rate of 960 nms^{-1}. A maximum absorbance of 610 nm was found and ascribed to the indigo carmine (IC) dye. The degree of mineralization of indigo carmine was determined by measuring the total organic carbon with a TOC-LCPH/CPN Shimadzu total organic carbon analyzer. The chemical oxygen demand of the samples was determined by using the American Public Health Association (APHA) standard procedures [23].

2.5. Characterization

2.5.1. Scanning Electron Microscopy (SEM/EDS). Images were obtained in a JEOL JSM 6510LV instrument at 15 kV with 10 mm WD using both secondary and backscattered electron signals. Samples were coated with a 20 nm thin film of gold using Denton Vacuum DESK IV sputtering equipment with a gold target. X-ray energy dispersive spectroscopy analyses were performed in an Oxford PentaFetx5 that was calibrated prior to all analyses with a copper standard.

2.5.2. BET Analysis. Surface area and pore characteristics of deoiled allspice husk original (MPS) and deoiled allspice husk original with iron particles (MPS/Fe) were determined by N_2 gas BET analysis (GEMINI 2360 instrument) obtained from nitrogen adsorption at 77 K. The nitrogen adsorption isotherms were recorded up to a relative pressure to assess the total pore volume. Porosity was determined using the pore volume and density.

3. Results and Discussion

3.1. Ozonation

3.1.1. Effect of Adding Unsupported and Supported Iron Particles on IC Concentration. The ozonation of IC was performed in the bubble column reactor with unsupported iron particles (NP-Fe), original deoiled allspice husk (MPS), and supported iron particles on deoiled allspice husk (MPS/Fe). All experiments were conducted with an initial IC concentration of 1000 mgL^{-1}. The initial absorption spectrum shows IC absorption band with a maximum at 610 nm (see Figure 2). This band was monitored in the ozonation experiments conducted with each material (NP-Fe, MPS, and MPS/Fe). Figure 2 shows that the band at 610 nm decreases significantly for MPS/Fe at 20 minutes compared to others, suggesting greater effectiveness in the degradation of IC. The absorption band with a maximum at 300 nm is associated with π bonds

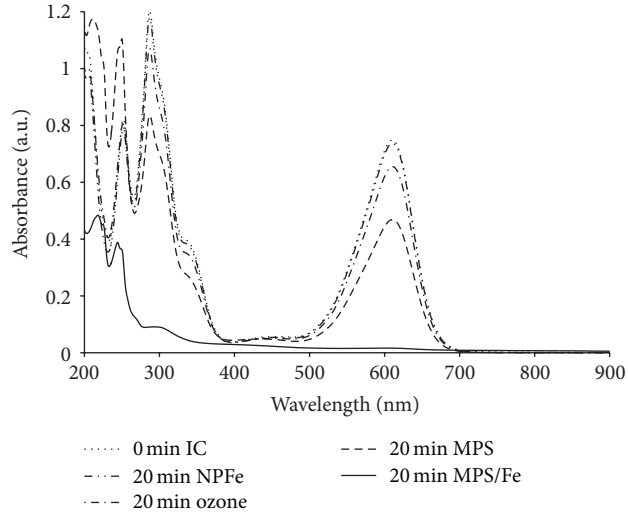

Figure 2: Effect of the addition of unsupported and supported iron particles on UV-Vis spectra of indigo carmine solution after 20 minutes of ozonation.

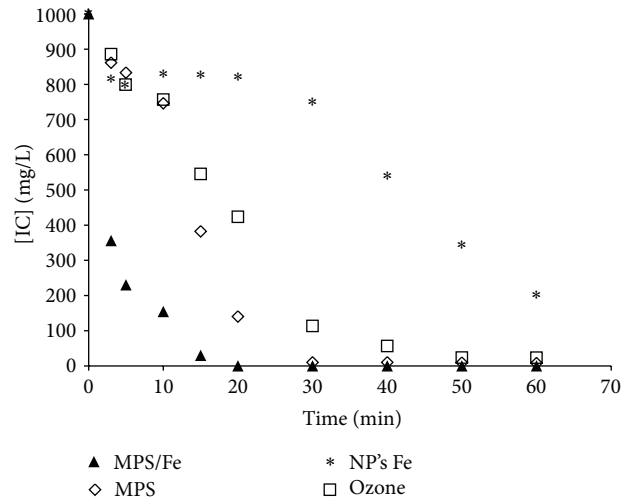

Figure 3: Effect of the material and time on IC concentration [▲] supported on deoiled allspice husk (MPS/Fe), [◇] deoiled allspice husk (MPS), [∗] iron metal particles (NP-Fe), and [□] indigo carmine (IC) only ozone.

and these are decreased by 20% with the application of ozone (O_3), ozone/MPS (O_3/MPS), ozone/iron (O_3/iron particles NP-Fe), indicating that the molecule has not been completely degraded. These π bonds are the result of breaking down the IC molecule by the action of free radicals generated during the ozonation process.

Figure 3 shows the IC concentration profile as function of time. It can be observed that the degradation of IC is fastest when the material with the supported iron particles (MPS/Fe) is employed. MPS/Fe leads to nearly complete degradation of the dye after only 20 min of ozonation. In heterogeneous catalysis the positive effect of the support textural properties on the active sites dispersion and availability is well known. In this context, hydroxo (OH) or oxo (=O) groups in

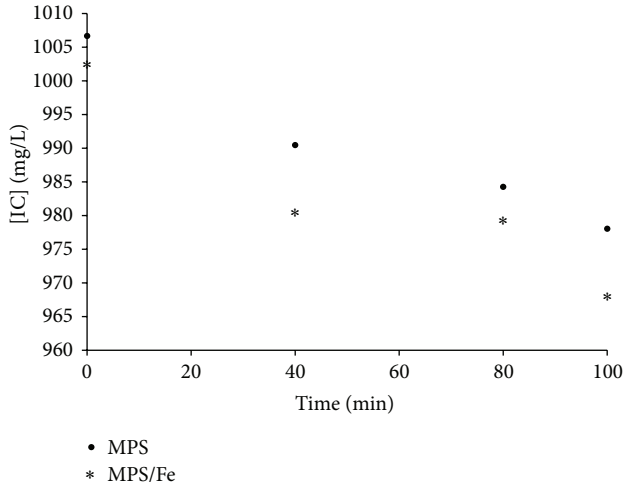

Figure 4: Effect of type of added material and time on IC concentration without ozone.

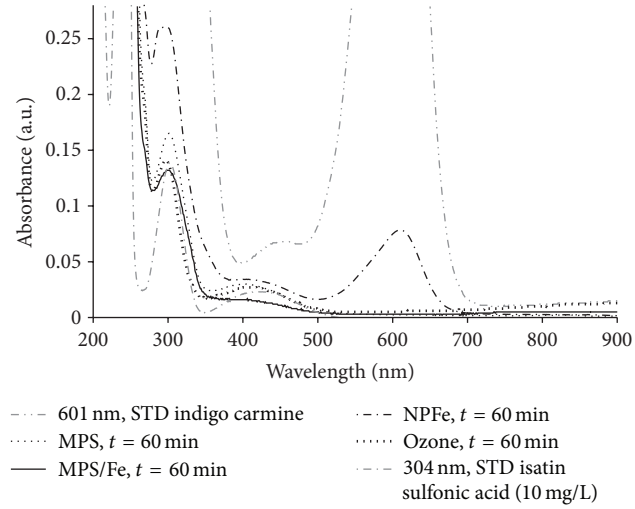

Figure 5: Effect of added material type on the ozonation process on UV-Vis spectra. Reaction time: 60 minutes.

the synthesis stage provide a greater surface area for the synthesis of metal particles onto the material [22].

The adsorption capacity of the MPS and MPS/Fe materials was tested in the absence of bubbling ozone. Figure 4 shows the results for the two types of materials. None of the two materials (MPS or MPS/Fe) shows an important capacity of adsorption during the contact time.

To elucidate the produced compounds reluctant to further degradation during each treatment, the UV-Vis spectra of the reacting solution as function of time were analyzed (Figure 5). It can be seen from this figure that the spectrum corresponding to the IC has two absorption bands with maxima at 610 and 340 nm. The first band is characteristic of IC and the latter can be ascribed to auxochromes (N, SO_3) attached to the benzene ring. One of the main products when the IC is degraded by ozonation is isatin sulfonic acid, which exhibits a maximum of absorption of 304 nm radiation. The presence of this by-product was detected by analysis of a standard reagent grade in UV-Vis.

When only ozone is applied to the IC solution, it was observed that the maximum absorbance at 610 nm decreases and this indicates the characteristic blue color is also decreasing. This may be due to the loss of sulphonate group since this works as auxochrome and therefore increases color intensity. From Figure 6, it is evident that the addition of MPS/Fe to the ozonation process decreases the concentration of isatin sulfonic acid generated by the degradation of IC in greater proportion than the other types of solids. It is worth observing that the support does also have a positive effect on isatin degradation. This, however, is considerably slower than when MPS/Fe is employed. Thus, the use of MPS/Fe not only enhances the IC degradation but also markedly reduces the concentration of the main subproduct (isatin sulfonic acid) generated during the ozonation process.

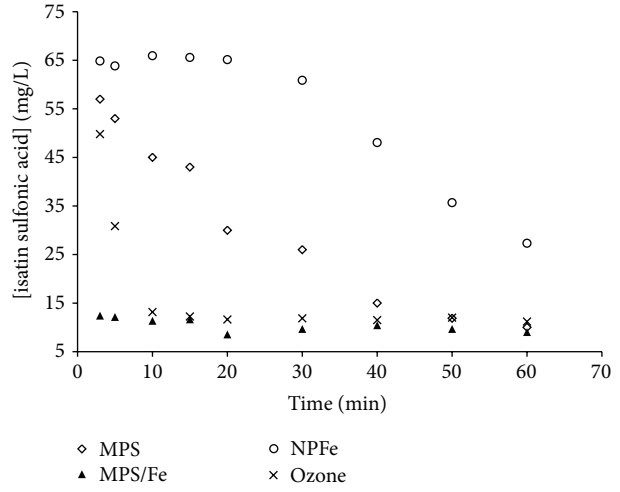

Figure 6: Effect of the tested materials on Isatin sulfonic acid concentration.

Table 1: Effect of solid material on the final total organic carbon content.

	MPS-O_3	MPS/Fe-O_3	NP-Fe	O_3
Total organic carbon (mgL^{-1}) 20 min	272 ± 5	48 ± 5	80 ± 5	202 ± 5
Total carbon (mgL^{-1}) 20 min	274 ± 5	50 ± 5	82 ± 5	205 ± 5
Inorganic carbon (mgL^{-1}) 20 min	3 ± 5	1 ± 5	3 ± 5	3 ± 5

Initial total organic carbon = 202 ± 5 mgL^{-1}.

3.1.2. Effect of Adding Unsupported and Supported Iron Particles on Total Organic Carbon and Chemical Oxygen Demand. Table 1 shows that the use of MPS increases the total carbon (TOC) during the degradation of IC. This can be ascribed to the degradation of the deoiled crushed material during the ozonation process. Nonetheless, the addition of supported iron particles to the ozonation process substantially enhances total organic carbon removal. Table 1 shows that the use

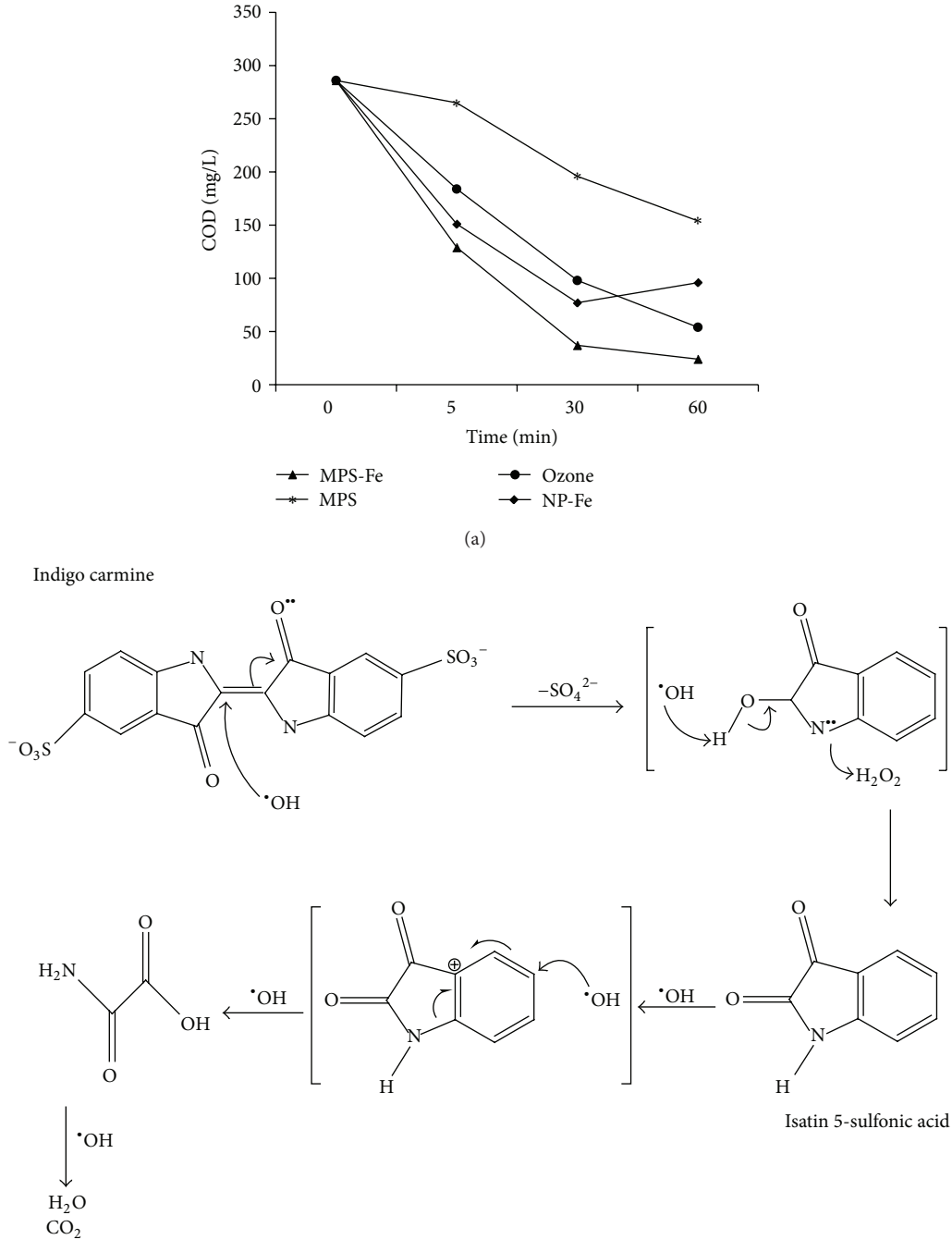

Figure 7: (a) Effect of catalyst type on chemical oxygen demand (COD); (b) proposed indigo carmine degradation mechanism.

of MPS/Fe not only makes IC degradation faster but also inhibits degradation of the support. According to the analysis of total organic carbon the addition of MPS/Fe leads to a 76% removal of TOC after only 20 minutes of treatment. At the same reaction time, ozone alone does not reduce TOC at all. This can be ascribed to the ozone incapacity to further degrade the isatin molecule.

Figure 7 confirms that the IC oxidation degree strongly depends on the type of added material during the ozonation process and this is given in terms of chemical oxygen demand (COD). These results are in concordance with TOC measurements. The effect of the addition of MPS/Fe on the removal of indigo carmine by ozonation offers a synergistic action that increases the rate of degradation of indigo carmine (Figure 7). The formation of reactive oxidizing species, that is, free radicals ($HO^{\bullet}$) during the ozonation process, concomitantly generates other radicals and hydrogen peroxide. Hence, the use of MPS/Fe introduces new reactions, mainly fenton

type, that positively impact the mineralization and oxidation degree of the IC solution.

The effect of the addition of MPS/Fe to the ozonation process generates a production of free radicals not governed by the reaction (2)–(4). The ozone reacts in solution to generate the hydroxyl radical ($HO^{\bullet}$) and radicals superoxide (2), which are consumed in the production of hydrogen peroxide (2)-(3):

$$O_3 + H_2O \longrightarrow 2HO^{\bullet} + O_2 \quad (2)$$

$$O_3 + HO^{\bullet} \longrightarrow HO_2^{\bullet} + O_2 \longleftrightarrow O_2^{\bullet} + H^+ \quad (3)$$

$$2HO_2^{\bullet} \longrightarrow O_2 + H_2O_2 \quad (4)$$

The synthesized zero-valent particles (Fe^0) are expected to be readily oxidized. However, the IC degradation results suggest that the support allows the iron particles to exhibit a catalytic effect on the generation of free radicals ($HO^{\bullet}$). This effect may be related to the interaction of the iron particles with the support surface [24, 25]. As consequence, this catalytic capability is rather diminished when the iron particles are not supported. Actually, because of previous reports [24, 26, 27], when the ozone is combined with MPS/Fe, the intensification of $HO^{\bullet}$ production was expected. The ferrous specie in the composite MPS/Fe by means of the following reactions may produce the ferrous specie involved in reaction

$$6H^+ + O_3 + FeO \longrightarrow FeO^{2+} + 3H_2O \quad (5)$$

So that FeO^{2+} reacts with hydrogen peroxide (traces of oxygen peroxide generated from ozone reactions (2)–(4)) to generate free radicals. Then the degradation of organic matter via free radicals as shown in the following reaction becomes plausible [12, 28, 29]:

$$FeO^{2+} + H_2O_2 \longrightarrow FeO^{3+} + HO^{\bullet} + OH^- \quad (6)$$

Fe^{3+} species may be going back to Fe^{2+} by means of the following reaction [27]:

$$Fe^{3+} + H_2O_2 \longrightarrow Fe^{2+} + HO_2^{\bullet} + H^+ \quad (7)$$

$$RH + HO^{\bullet} \longrightarrow R^{\bullet} + H_2O \quad (8)$$

Therefore, when adding the MPS/Fe to the ozonation process this is catalyzed. This catalytic effect of Fe^{2+} on ozonation has been previously recognized [9, 12]. Therefore, the synergistic effect for the generation of free radicals ($HO^{\bullet}$, $HO_2^{\bullet}$) via ozonation reactions (2)–(4) and catalyzed ozonation reactions with supported iron (5)–(7) cannot be neglected.

Under this scheme the degradation of IC towards isatin and its products has been suggested [18] to occur according to the mechanism depicted in Figure 7.

3.1.3. Effect of Particle Size. Also the effect of particle size of the MPS/Fe material was evaluated. Three different particle sizes were tested 2.00, 0.177, and 0.088 mm. The initial concentration of IC was 1000 mgL^{-1} and the reaction time was 60 min. The results are shown in Figure 8 and suggest

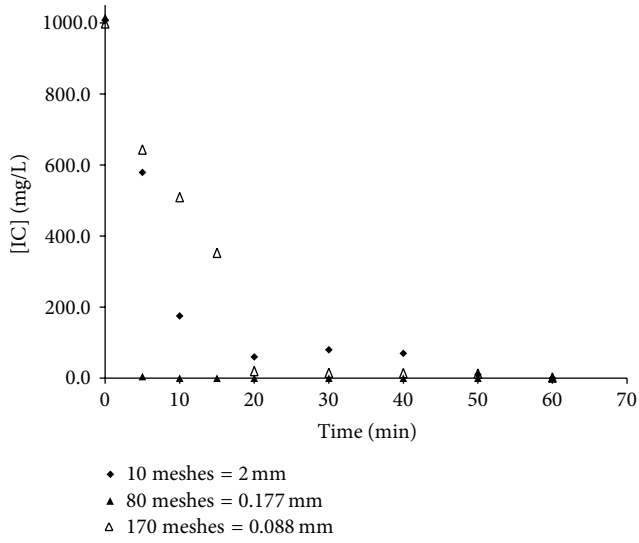

Figure 8: Effect of particle size of supported iron particles on indigo carmine concentration profile.

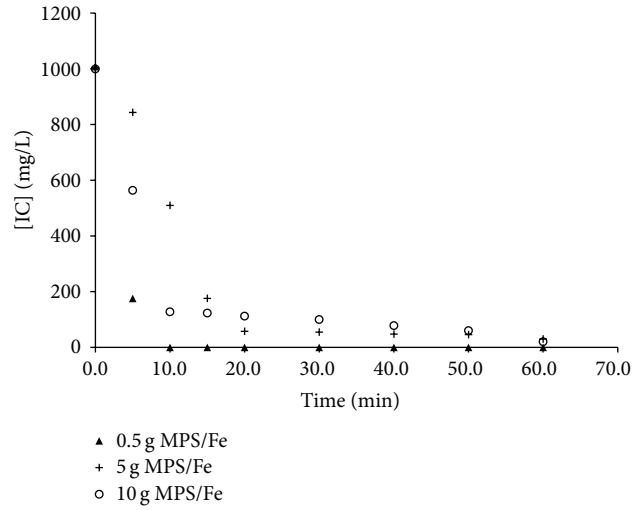

Figure 9: Effect catalyst loading on indigo carmine concentration profile.

the presence of liquid-solid and intraparticle mass transport resistances that are presumably minimized when the particle size is 0.177 mm (80 mesh) as a result of the best and faster degradation of the dye used over the others conditions tested. It is worth noticing that the effect of adsorption was evaluated for all tested materials without the presence of ozone. The results indicated that this phenomenon is negligible for all materials. The unsupported iron particles (NP-Fe) did not exhibit good efficiency in contrast to the supported MPS/Fe.

3.1.4. Effect of Catalyst Concentration. In order to study the effect of this variable three experiments with their corresponding repetitions were conducted. At all experiments the initial concentration of IC were 1000 mgL^{-1} and the reaction time was 60 min. Figure 9 shows the positive effect

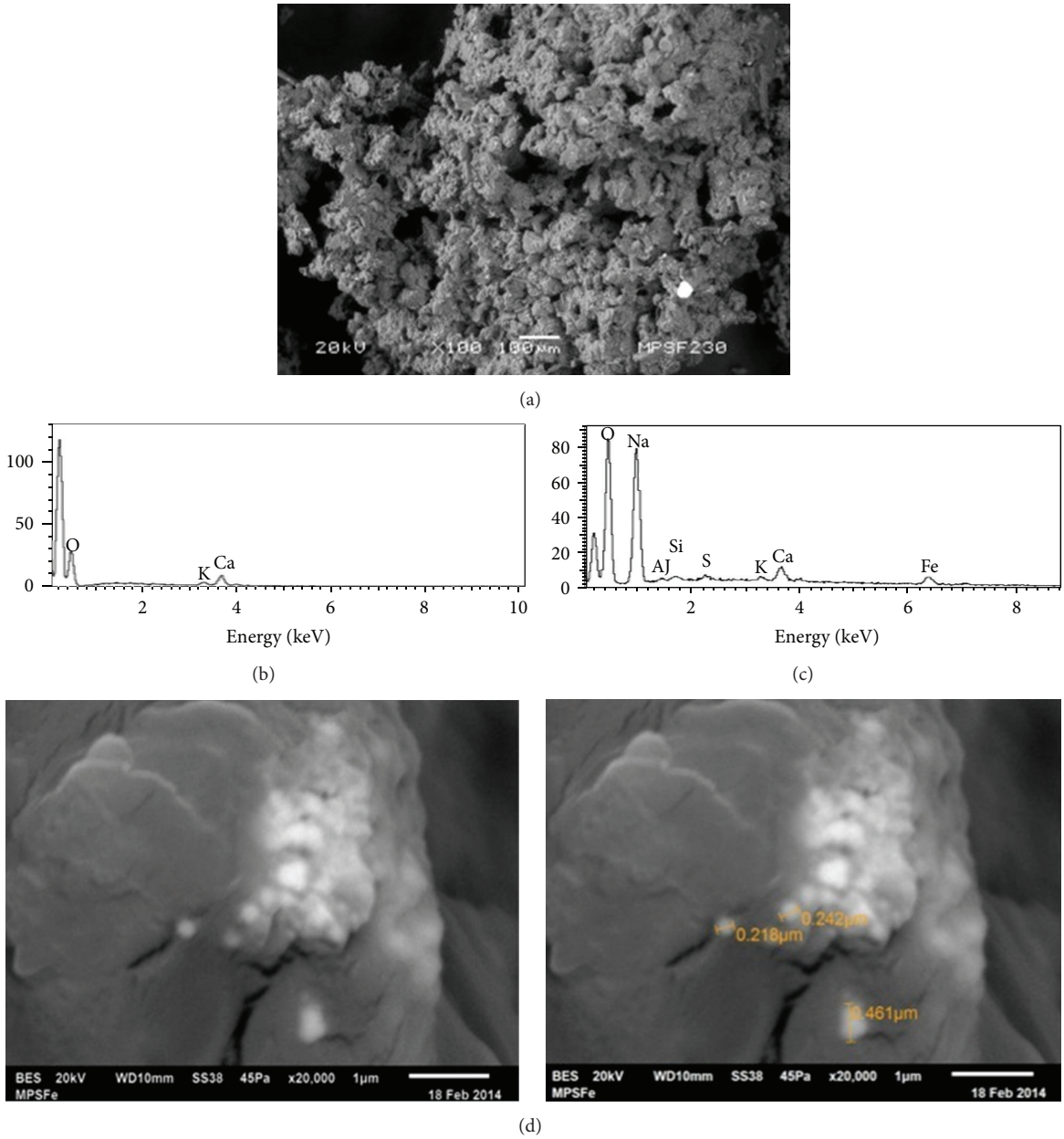

Figure 10: SEM/EDS images for the synthesized materials.

on IC removal when using a [MPS/Fe] = 1000 mgL^{-1}. The presence of the MPS/Fe enhances the ozonation process, and its concentration has a strong influence over the dye degradation. The IC degradation rate increases when mass of MPS/Fe increases and this is also an indicative of the liquid-solid mass transfer resistance being negligible. It is worth pointing out that the removal of IC by adsorption onto the MPS/Fe particles was found to be negligible. Only 1.8% of IC was removed by this phenomenon.

3.2. Materials Characterization

3.2.1. SEM/EDS and Elemental Analysis. SEM micrographs of MPS and MPS/Fe materials in Figure 10(a) show the parent supports as amorphous. These remained unchanged after the deposition of iron. In the elemental analysis it was found that the material elements of the MPS might be acting as natural material (peaks of C, O, K, and Ca, which are typical elements of the natural materials) as shown in Figure 10(b). As expected, iron was detected on the MPS/Fe sample (see Figure 10(c)). The SEM/EDS analysis allows identifying iron particles of approximately 250 nm in size (Figure 10(d)). It is important to note that the increase in oxygen observed in the MPS/Fe sample suggests the presence of FeO^{2+} species in contrast with the support alone (MPS). The decrease in weight percent of carbon observed in the MPS/Fe sample (see Table 2) may be due to the coating of the surface by iron particles.

Table 2: Characteristics of catalytic materials.

	MPS	MPS/Fe
Specific surface area (m^2g^{-1})	2.40	4.58
Cumulative pore volume (cm^3 (STP) g^{-1})	0.55	1.05
Mean pore diameter (nm)	4.45	6.61
Total pore volume (p/p_o) = 0.990 (cm^3g^{-1})	$2.67E-03$	$7.58E-3$
Carbon	54.61%	17.29%
Oxygen	42.84%	59.65%
Sodium	0.57%	20.76%
Calcium	1.99%	0.58%
Iron	0%	1.72%

3.2.2. N_2 Physisorption. The results in Table 2 show that MPS/Fe has a greater specific surface area. This increase may be the consequence of the chemical treatment conducted on the husk during the catalytic system preparation.

4. Conclusions

Unsupported and supported iron particles were synthesized via a relatively low cost method. Indigo carmine removal by ozonation and ozonation with unsupported and supported Fe on a biomaterial was studied. MPS/Fe substantially improves the degradation of indigo carmine and of the generated subproducts during the ozonation process. Catalyzed ozonation leads to attain a reaction rate twice faster than ozonation alone. The use of the MPS/Fe allows the removal of 76% of TOC after only 20 min of ozonation. It was found that the synthesized materials did not exhibit significant adsorption properties.

Conflict of Interests

The authors declare that there is no conflict of interests regarding the publication of this paper.

Acknowledgments

The first author acknowledges the scholarship 248402 from CONACyT to pursue her postgraduate studies. PRODEP is also acknowledged for financial support through project 103.5/13/5257.

References

[1] C. Tang and V. Chen, "Nanofiltration of textile wastewater for water reuse," *Desalination*, vol. 143, no. 1, pp. 11–20, 2002.

[2] A. Bes-Piá, J. A. Mendoza-Roca, M. I. Alcaina-Miranda, A. Iborra-Clar, and M. I. Iborra-Clar, "Reuse of wastewater of the textile industry after its treatment with a combination of physico-chemical treatment and membrane technologies," *Desalination*, vol. 149, no. 1–3, pp. 169–174, 2002.

[3] P. C. Vandevivere, R. Bianchi, and W. Verstraete, "Review: treatment and reuse of wastewater from the textile wet-processing industry: review of emerging technologies," *Journal of Chemical Technology & Biotechnology*, vol. 72, no. 4, pp. 289–302, 1998.

[4] K. Santhy and P. Selvapathy, "Removal of reactive dyes from wastewater by adsorption on coir pith activated carbon," *Bioresource Technology*, vol. 97, no. 11, pp. 1329–1336, 2006.

[5] A. D. Bokare, R. C. Chikate, C. V. Rode, and K. M. Paknikar, "Iron-nickel bimetallic nanoparticles for reductive degradation of azo dye Orange G in aqueous solution," *Applied Catalysis B: Environmental*, vol. 79, no. 3, pp. 270–278, 2008.

[6] F. Pena-Pereira, R. M. B. O. Duarte, and A. C. Duarte, "Immobilization strategies and analytical applications for metallic and metal-oxide nanomaterials on surfaces," *TrAC—Trends in Analytical Chemistry*, vol. 40, pp. 90–105, 2012.

[7] A. Majcen, L. Marechal, and B. Križanec, "Textile finishing industry as an important source of organic pollutants," in *Organic Pollutants Ten Years after the Stockholm Convention—Environmental and Analytical Update*, InTech, 2012.

[8] P. Cañizares, R. Paz, C. Sáez, and M. A. Rodrigo, "Costs of the electrochemical oxidation of wastewaters: a comparison with ozonation and Fenton oxidation processes," *Journal of Environmental Management*, vol. 90, no. 1, pp. 410–420, 2009.

[9] A. C. Quiroz, C. Barrera-Díaz, G. Roa-Morales, P. B. Hernández, R. Romero, and R. Natividad, "Wastewater ozonation catalyzed by iron," *Industrial and Engineering Chemistry Research*, vol. 50, no. 5, pp. 2488–2494, 2011.

[10] W. P. Kwan and B. M. Voelker, "Rates of hydroxyl radical generation and organic compound oxidation in mineral-catalyzed fenton-like systems," *Environmental Science and Technology*, vol. 37, no. 6, pp. 1150–1158, 2003.

[11] A. H. Gemeay, I. A. Mansour, R. G. El-Sharkawy, and A. B. Zaki, "Kinetics and mechanism of the heterogeneous catalyzed oxidative degradation of indigo carmine," *Journal of Molecular Catalysis A: Chemical*, vol. 193, no. 1-2, pp. 109–120, 2003.

[12] M. Bernal, R. Romero, G. Roa, C. Barrera-Díaz, T. Torres-Blancas, and R. Natividad, "Ozonation of indigo carmine catalyzed with Fe-pillared clay," *International Journal of Photoenergy*, vol. 2013, Article ID 918025, 7 pages, 2013.

[13] M. Faouzi, P. Cañizares, A. Gadri et al., "Advanced oxidation processes for the treatment of wastes polluted with azoic dyes," *Electrochimica Acta*, vol. 52, no. 1, pp. 325–331, 2006.

[14] N. Gandra, A. T. Frank, O. Le Gendre et al., "Possible singlet oxygen generation from the photolysis of indigo dyes in methanol, DMSO, water, and ionic liquid, 1-butyl-3-methylimidazolium tetrafluoroborate," *Tetrahedron*, vol. 62, no. 46, pp. 10771–10776, 2006.

[15] R. Sankar, P. Manikandan, V. Malarvizhi, T. Fathima, K. S. Shivashangari, and V. Ravikumar, "Green synthesis of colloidal copper oxide nanoparticles using *Carica papaya* and its application in photocatalytic dye degradation," *Spectrochimica Acta—Part A: Molecular and Biomolecular Spectroscopy*, vol. 121, pp. 746–750, 2014.

[16] V. K. Vidhu and D. Philip, "Catalytic degradation of organic dyes using biosynthesized silver nanoparticles," *Micron*, vol. 56, pp. 54–62, 2014.

[17] G. Carja, E. Husanu, C. Gherasim, and H. Iovu, "Layered double hydroxides reconstructed in NiSO4 aqueous solution as highly efficient photocatalysts for degrading two industrial dyes," *Applied Catalysis B: Environmental*, vol. 107, no. 3-4, pp. 253–259, 2011.

[18] C. Flox, S. Ammar, C. Arias, E. Brillas, A. V. Vargas-Zavala, and R. Abdelhedi, "Electro-Fenton and photoelectro-Fenton

degradation of indigo carmine in acidic aqueous medium," *Applied Catalysis B: Environmental*, vol. 67, no. 1-2, pp. 93–104, 2006.

[19] X. Weng, Z. Chen, M. Megharaj, and R. Naidu, "Clay supported bimetallic Fe/Ni nanoparticles used for reductive degradation of amoxicillin in aqueous solution: characterization and kinetics," *Colloids and Surfaces A: Physicochemical and Engineering Aspects*, vol. 443, pp. 404–409, 2014.

[20] P. Vasileva, B. Donkova, I. Karadjova, and C. Dushkin, "Synthesis of starch-stabilized silver nanoparticles and their application as a surface plasmon resonance-based sensor of hydrogen peroxide," *Colloids and Surfaces A: Physicochemical and Engineering Aspects*, vol. 382, no. 1–3, pp. 203–210, 2011.

[21] A. R. Khataee, V. Vatanpour, and A. R. A. Ghadim, "Decolorization of C.I. Acid Blue 9 solution by UV/Nano-TiO_2, Fenton, Fenton-like, electro-Fenton and electrocoagulation processes: a comparative study," *Journal of Hazardous Materials*, vol. 161, no. 2-3, pp. 1225–1233, 2009.

[22] T. Torres-Blancas, G. Roa-Morales, C. Fall, C. Barrera-Díaz, F. Ureña-Nuñez, and T. B. Pavón Silva, "Improving lead sorption through chemical modification of de-oiled allspice husk by xanthate," *Fuel*, vol. 110, pp. 4–11, 2013.

[23] American Public Health Association American Water Works Association/Water Environment Federation, *Standard Methods for the Examination of Water and Wastewater*, American Public Health Association American Water Works Association/Water Environment Federation, 20th edition, 1998.

[24] W. P. Kwan and B. M. Voelker, "Influence of electrostatics on the oxidation rates of organic compounds in heterogeneous fenton systems," *Environmental Science and Technology*, vol. 38, no. 12, pp. 3425–3431, 2004.

[25] P. Cañizares, M. Hernández-Ortega, M. A. Rodrigo, C. E. Barrera-Díaz, G. Roa-Morales, and C. Sáez, "A comparison between conductive-diamond electrochemical oxidation and other advanced oxidation processes for the treatment of synthetic melanoidins," *Journal of Hazardous Materials*, vol. 164, no. 1, pp. 120–125, 2009.

[26] M. A. Al-Shamsi, N. R. Thomson, and S. P. Forsey, "Iron based bimetallic nanoparticles to activate peroxygens," *Chemical Engineering Journal*, vol. 232, pp. 555–563, 2013.

[27] J. De Laat, H. Gallard, S. Ancelin, and B. Legube, "Comparative study of the oxidation of atrazine and acetone by H_2O_2/UV, Fe(III)/UV, Fe(III)/H_2O_2/UV and Fe(II) or Fe(III)/H_2O_2," *Chemosphere*, vol. 39, no. 15, pp. 2693–2706, 1999.

[28] M. A. García-Morales, G. Roa-Morales, C. Barrera-Díaz, B. Bilyeu, and M. A. Rodrigo, "Synergy of electrochemical oxidation using boron-doped diamond (BDD) electrodes and ozone (O_3) in industrial wastewater treatment," *Electrochemistry Communications*, vol. 27, pp. 34–37, 2013.

[29] K. C. Pillai, T. O. K. Kwon, and I. S. Moon, "Degradation of wastewater from terephthalic acid manufacturing process by ozonation catalyzed with Fe^{2+}, H_2O_2 and UV light: direct versus indirect ozonation reactions," *Applied Catalysis B: Environmental*, vol. 91, no. 1-2, pp. 319–328, 2009.

Hindawi Publishing Corporation
International Journal of Photoenergy
Volume 2015, Article ID 860845, 7 pages
http://dx.doi.org/10.1155/2015/860845

Research Article

Water and Wastewater Disinfection with Peracetic Acid and UV Radiation and Using Advanced Oxidative Process PAA/UV

Jeanette Beber de Souza,[1] Fernanda Queiroz Valdez,[2] Rhuan Felipe Jeranoski,[1] Carlos Magno de Sousa Vidal,[1] and Grasiele Soares Cavallini[3]

[1]*Department of Environmental Engineering, Universidade Estadual do Centro-Oeste, PR 153, km 07, Riozinho, P.O. Box 21, 84500-000 Irati, PR, Brazil*
[2]*Department of Hydraulics and Sanitation, the São Carlos Engineering School, São Paulo University, P.O. Box 359, 13566-590 São Carlos, SP, Brazil*
[3]*Department of Environmental Chemistry, Federal University of Tocantins (UFT), Campus Gurupi, P.O. Box 66, 77402-970 Gurupi, TO, Brazil*

Correspondence should be addressed to Jeanette Beber de Souza; jeanettebeber@yahoo.com.br

Received 6 October 2014; Revised 14 December 2014; Accepted 28 December 2014

Academic Editor: Meenakshisundaram Swaminathan

The individual methods of disinfection peracetic acid (PAA) and UV radiation and combined process PAA/UV in water (synthetic) and sanitary wastewater were employed to verify the individual and combined action of these advanced oxidative processes on the effectiveness of inactivation of microorganisms indicators of fecal contamination *E. coli*, total coliforms (in the case of sanitary wastewater), and coliphages (such as virus indicators). Under the experimental conditions investigated, doses of 2, 3, and 4 mg/L of PAA and contact time of 10 minutes and 60 and 90 s exposure to UV radiation, the results indicated that the combined method PAA/UV provided superior efficacy when compared to individual methods of disinfection.

1. Introduction

Waters that do not present good quality represent a menace to the human health, due to the possibility of contamination of populations through waterborne diseases. According to the Trata Brasil Institute, 88% of the deaths caused by diarrhea worldwide are caused by unsuitable sanitation. In 2011, in Brazil, 396.048 people were infected with diarrhea, and 35% of these patients were children under 5 years old [1].

One of the main sources of water contamination is the release of raw domestic sewage or wastewater that have not undergone efficient treatment, thus constituting a potential load of pathogenic organisms excreted by infected individuals [2, 3].

In such context, the interest in wastewater disinfection processes has become increasingly higher.

Chlorine is the most widely employed disinfectant to treat water and wastewater all over the world. This is due to its largely known technology, low cost, and proved efficiency in inactivating a great variety of pathogenic microorganisms [3–5].

However, the use of chlorine to disinfect sanitary sewage requires dechlorination prior to the effluent release in the receptor body; even at low concentrations, chlorine is toxic to the water life. Regarding drinking water, there is a concern about this disinfectant oxidizing some kinds of organic matter, mainly humic and fulvic acids, and forming trihalomethanes, which are highly carcinogenic compounds [5, 6].

Due to this problem, new studies have been developed, seeking alternative disinfectants to the chlorine, such as ultraviolet (UV) radiation, peracetic acid (PAA), and advanced oxidative processes as the PAA/UV proposal analyzed in this study.

UV radiation is a physical mechanism that transfers electromagnetic energy to the microorganisms' genetic material, through special mercury vapor lamps. When the UV radiation penetrates the cell wall, it destroys the microorganism ability to reproduce [7].

UV radiation presents the advantages of being efficient to inactivate a great variety of microorganisms without provoking residual effects that might be harmful to human being or water life; it is easy to operate and requires short contact time for disinfection, which implies smaller units in the water or wastewater treatment plants [7].

However, small doses might not be efficient in inactivating some viruses, spores, and cysts, and some organisms might reverse the radiation effect through the photoreactivation or dark repair. Besides that, turbidity and total suspended solids present in the sewage might reduce the efficacy of disinfection through radiation. And, regarding drinking water, the main inconvenience is the absence of disinfectant residual along the distribution system. UV radiation is more expensive than chlorination, but the costs become competitive when dechlorination is taken into consideration [4, 6, 7].

Peracetic acid (CH_3CO_3H) is a strong oxidant which presents advantages: the treatment being easy to implement (without the need of high investment), the large spectrum of microbial activity even in the presence of heterogeneous organic matter, absence of residual or toxic and/or mutagenic by-products, not requiring dechlorination, presenting low dependency on pH, and short contact time [8].

There are no reports in the literature pointing PAA as carcinogenic or that it presents toxicity in the reproduction and human development.

When surveying studies on the use of PAA to disinfect wastewater, Cavallini et al. [9] observed that the toxicity results and the formation of by-products were very low when compared with chlorine, which might be ascribed to the PAA composition and its fast decomposition in the effluent.

The disadvantages of using PAA in wastewater disinfection are the increase in the effluent organic content, enhancing microbial regrowth, higher cost when compared to chloride and lower efficiency against some viruses and parasites [8, 10], and, in water disinfection, the absence of disinfectant residual.

In the literature, some advanced oxidative processes (AOPs) have been proposed (UV/H_2O_2, O_3/H_2O_2, O_3/UV, and TiO_2/UV). The AOPs are based on the use of secondary oxidants, such as free radicals (OH), which can be generated by the interaction of UV radiation with a chemical disinfectant able to release such radicals. Hydroxyl radicals are highly reactive oxidant agents which can be used to oxidize organic and inorganic compounds and other toxic or pollutants or resistant to biological treatment and as disinfectants [11, 12].

In the PAA/UV sequential process there is PAA photolysis under the action of the UV light. According to Caretti and Lubello [11] there is an interruption in the bond O–O of the PAA molecule, with the subsequent formation of the hydroxyl radical. The presence of PAA hydrogen contributes not only to the formation of PAA again as soon as it is consumed, but also to the formation of new hydroxyl radicals.

The use of two or more disinfectants, simultaneously or sequentially applied, characterizes the disinfection method named by USEPA [7] as interactive or combined and presents the increase in microbial inactivation efficiency in some groups of microorganisms as an advantage; this includes the possibility of synergism to occur, minimization of disinfection by-products formation, and the use of smaller doses of disinfectant agents.

The sublethal damage to the cell wall of the microorganism provided by a disinfecting agent can improve the sensitivity of the organism to the action of other disinfectants and then synergism occurs.

However, despite the promising advantages of the use of combined processes, they do not present global improvement of disinfection in all situations. Thus, research in this area, involving different disinfection methods in combination, as it is the case of PAA/UV in different groups of indicator microorganisms, is highly relevant.

This study presents tests with wastewater and synthetic water disinfection using peracetic acid (PAA), UV radiation and employing the sequential PAA/UV process to the inactivation of indicator microorganisms: *E. coli*, total coliforms, and coliphages.

2. Materials and Methods

2.1. Experimental Conditions. Disinfection experiments, both in water and in wastewater, were carried out individually with PAA, UV radiation and using the sequential PAA/UV method. The individual assays with PAA and UV radiation were performed in order to calculate the synergism, once the method employed takes into account individual disinfection tests, as will be seen in Section 3.

The water under study, named synthetic water, was composed of deionized water and specific salts, according to the *Standard Methods for the Examination of Water and Wastewater* [13], and added to the indicator microorganisms strains: *E. coli* strain ATCC 11229 (bacteria indicator) and coliphages (virus indicator) isolated from wastewater, using the *E. coli* CIP 55.30 as the host strain.

The wastewater was collected at the output of a municipal wastewater treatment plant (WTP) consisting of a biological secondary treatment: a fluidized bed anaerobic reactor (FBAR) and an upflow anaerobic sludge blanket (UASB) in parallel, followed by stabilization pond, and the sewage samples were collected at the output of this pond.

For the UV radiation disinfection tests, a laboratory bench reactor measuring 45 cm × 40 cm × 15 cm was employed, operating in a batch mode, made of stainless steel, with removable aluminum lid, containing six emerged 15 W mercury vapor lamps.

The UV reactor was filled up with both effluent and synthetic water up to the point where liquid reached 4 cm, which made up a total volume of 7,5 liters. In order to carry out the experiments, the six lamps in the reactor were turned on for 30 minutes in advance to produce heat and stabilize. The times of exposure employed were 60 and 90 seconds, which in experiments with wastewater characterized doses of 125,16 and 187,74 mWs/cm^2 for test 1 and 109,89 and 164,84 mWs/cm^2 for test 2. Regarding the water experiments, the same times of exposure, 60 and 90 s, characterized doses of 282,58 and 423,87 mWs/cm^2, respectively, in test 1 and 217,71 and 326,56 mWs/cm^2 in test 2.

Table 1: *E. coli*, TC, and coliphages inactivation employing, individually, PAA and UV radiation in tests with wastewater.

		N_o	Peracetic acid Concentration (mg/L)			UV radiation Exposure (s)	
			2	3	4	60	90
Test 1	*E. coli*	$1{,}1 \times 10^4$	$3{,}4 \times 10^3$	$3{,}7 \times 10^3$	$1{,}3 \times 10^2$	6	4
	TC	$2{,}25 \times 10^5$	7×10^4	$2{,}12 \times 10^4$	$6{,}2 \times 10^3$	$5{,}1 \times 10^3$	$3{,}9 \times 10^3$
	Coliphages	$3{,}15 \times 10^2$	$1{,}35 \times 10^2$	$1{,}25 \times 10^2$	$2{,}4 \times 10^2$	5	10
Test 2	*E. coli*	3×10^4	—	<1	—	10	10
	TC	$3{,}6 \times 10^5$	—	$5{,}2 \times 10^4$	—	200	160
	Coliphages	$1{,}27 \times 10^3$	—	320	—	<1	<1

—: not carried out; <1: lower than the detection limit of the method used.

Throughout the exposure time, the liquid was kept under magnetic agitation, preventing the sedimentation of solids. After the exposure time was over, samples were collected for the microbiological examination.

Radiation intensity measurements were carried out with a radiometer (Vilber Lourmat) with UV radiation detector sensor at the 254 nm wavelength. To determine the UV radiation dose, the route described by Daniel [14], as well as the study carried out by Souza et al. [15], was followed.

PAA disinfection tests were carried out in a batch mode employing the commercial product PROXITANE 1512 which is a quaternary mixture in equilibrium containing peracetic acid (15%), hydrogen peroxide (23%), acetic acid (16%), and stabilizing vehicle. In the experiments with wastewater, PAA doses applied were 2, 3, and 4 mg/L in test 1 and 3 mg/L in test 2; the contact time employed was 10 minutes for all doses. In experiments with water, in both tests carried out, PAA doses employed were 2, 3, and 4 mg/L and contact time was 10 minutes. To inactivate the residual PAA, after the contact time specified, sodium thiosulfate (1%) was added at the proportion 0,1 mL for each 100 mL sample. The residual PAA was measured through the spectrophotometric method, using the chromophore N,N-diethyl-p-phenylenediamine (DPD) ($(C_2H_5)_2C_6H_4NH_2$, 97% ALDRICH) [9].

In the combined method, the same procedures were employed as the individual methods, PAA was the primary disinfectant employed, and, after the contact time, the effluent was exposed to the previously set UV radiation doses.

2.2. Sample Characterization. The physicochemical characterization of samples was carried out according to the procedures indicated in the *Standard Methods for the Examination of Water and Wastewater* [13], and turbidity, total suspended solids, chemical oxygen demand (COD), and absorbance 254 nm analyses were performed for the wastewater and turbidity, pH, COD, and absorbance 254 nm, for the water. Besides that, total coliforms, *E. coli*, and coliphages were quantified in the wastewater and *E. coli* and coliphages in water.

In order to quantify *E. coli* and total coliforms (TC) the membrane filtration technique was employed using the culture medium Agar Hicrome Selective ECC Base CAT.M1294 (Himedia) which enables the simultaneous determination of total coliforms and *E. coli*.

For the quantification of coliphages, the plates test was carried out according to the CETESB L5.225 Norm [16] and the culture medium employed was modified *Tryptic Soy Agar* (TSA).

3. Results and Discussion

3.1. Tests of Wastewater Disinfection Employing the PAA and UV Radiation Individual Methods. For the wastewater, results of the physicochemical analyses of turbidity, SST, COD, and absorbance 254 nm varied, respectively, from 8,43 to 71,7 NTU, 15 to 140 mg/L, 53 to 164 mg/L, and 0,313 to 0,364 from the first to the second test.

In Table 1 the results of microbial inactivation employing the PAA and UV individual methods are presented, and for the inactivation calculation the equation $-\log(N/N_o)$ was used, where N_o corresponds to the microorganisms initial number (gross sample) and N the microorganisms after disinfection.

In relation to the results in UV tests, good global efficiency inactivation was observed in test 2, reaching 3,48 log *E. coli* inactivation values for both doses of UV used, 3,1 log coliphages, also for both UV doses, and 3,35 log total coliforms for the 164,84 mWs/cm^2 dose.

In test 1, despite the coliphages inactivation presenting lower values, its inactivation was efficient (Table 1). This is due to the fact that the coliphages concentration in the gross effluent was not really high. On the other hand, in the same test, UV radiation was not very efficient to remove total coliforms (maximum inactivation log 1,76). The biggest difficulty to the inactivation of total coliforms is also observed in several other studies in the area specific literature, including Souza et al. [15].

In test 2, although the effluent turbidity was much higher than in test 1, the UV disinfection did not have its efficiency reduced in this case.

In relation to the inactivation of indicator microorganisms *E. coli*, TC, and coliphages, in both PAA tests and with all doses applied, inactivation below 2 log was observed for all microorganisms, except for the *E. coli* in the second test, in which 4,48 log was observed. Regarding specifically the coliphages Souza and Daniel [17] also observed results of low inactivation of such viral indicators, employing 3 and 4 mg/L PAA concentrations and 20-minute contact time.

Table 2: *E. coli,* TC, and coliphages inactivation, employing the PAA/UV sequential method in tests with wastewater.

		N_o	Sequential PAA/UV					
			2 (60)	2 (90)	3 (60)	3 (90)	4 (60)	4 (90)
Test 1	*E. coli*	$1{,}1 \times 10^4$	410	7	5	<1	<1	<1
	TC	$2{,}25 \times 10^5$	$2{,}24 \times 10^4$	$2{,}9 \times 10^3$	$7{,}1 \times 10^3$	$2{,}35 \times 10^3$	$3{,}1 \times 10^2$	$1{,}1 \times 10^2$
	Coliphages	$3{,}15 \times 10^2$	10	5	<1	5	5	< 1
Test 2	*E. coli*	3×10^4	—	—	<1	<1	—	—
	TC	$3{,}6 \times 10^5$	—	—	140	20	—	—
	Coliphages	$1{,}27 \times 10^3$	—	—	<1	<1	—	—

—: tests not carried out.

Gehr et al. [18] who analyzed different disinfection processes, amongst them PAA, ozone, and UV radiation, to treat effluents in a municipal WTP which employed physicochemical treatment (ferric coagulation or with aluminum) to treat domestic and industrial effluents altogether observed high negative influence of the organic matter on the PAA disinfection, even making the adoption of PAA in this case unviable as an alternative disinfectant for the STS under study. It is important to highlight that in that study all sewage samples presented high concentrations of dissolved organic carbon (DOC) (124–240 mg/L), SS (16–45 mg/L), and turbidity (16–31 NTU).

Regarding PAA tests, samples were collected for the analyses of COD and residual.

The PAA residual, after 10-minute contact, was low; it varied from <0,1 to 0,92 mg/L in test 1 and was 0,34 mg/L in test 2, indicating that a considerable part of the PAA applied was consumed in the wastewater oxidation/disinfection phases. After disinfection with PAA, the COD increased with the increase in the concentration of the PAA applied (in test 1, e.g., from 53 mg/L in gross sewage to 70 mg/L after application of 4 mg/L PAA). This fact was observed in other studies developed by the authors of this study, with special attention to the study of Cavallini et al. [19] who analyzed the disinfection of wastewater with PAA and observed that the application of different PAA doses to the wastewater with 20-minute contact time resulted in 15% average increase in the COD at each 10 mg/L PAA applied.

According to Kitis [8] the increase in organic content in the PAA disinfected sewage samples, associated with the microbial potential regrowth, is the biggest inconvenience of the use of this disinfectant. The author ascribes this increase to the presence of acetic acid, which is a biodegradable compound, present both in the PAA composition and in its decomposition product.

However, the authors of this work do not ascribe the COD elevation only to the acetic acid, as proposed by Kitis [8], once the PAA is a percarboxylic acid which also contributes to the organic load of the disinfected effluent. Thus, it is not possible to relate the COD elevation only to the acetic acid.

3.2. PAA/UV Sequential Disinfection of Wastewater. In Table 2, results obtained with the PAA/UV sequential method in both tests with wastewater are presented.

For *E. coli* 4,5 log inactivation was obtained for both PAA/UV doses employed in experiment 2, in which 100% inactivation was reached. Also, for the three last combined doses employed of 3(187,74), 4(125,16), and 4(187,74), despite the lower inactivation log(4,04), 100% *E. coli* inactivation efficiency was also reached.

For total coliforms, inactivation of up to 4,25 log with the 4(187,74) dose was obtained, and, for coliphages, 3,1 log inactivation for both doses applied in experiment 2, and 2,5 log for doses 3(125,16) and 4(187,74) employed in experiment 1.

In general, disinfection tests with the sequential method were proved more efficient than the experiments in which disinfectants were used separately. In most cases, the highest inactivation log reached using only one disinfectant was overcome in the sequential method with the use of smaller doses of each disinfectant. This result demonstrates that the sequential method can bring economic benefit, once the doses needed of each disinfectant were smaller in this process than in the disinfection with only PAA or only UV radiation.

3.3. Synergy Verification. With the inactivation results of the sequential disinfection tests, it was possible to verify the occurrence or nonoccurrence of synergy for the method used. According to Finch et al. [20], synergy is verified from the premise that the inactivation resulting from the sequential action must be higher than the sum of individual inactivation. Consider

$$\text{Synergy} = I_r - (I_1 + I_2), \quad I = -\log\left(\frac{N}{N_o}\right), \tag{1}$$

where I_r is sequential process resulting inactivation, I_1 is primary disinfectant resulting inactivation, I_2 is secondary disinfectant resulting inactivation, N is organism final number, and N_o is organism initial number.

Results of synergy verification for both tests are presented in Table 3.

According to the results obtained, very little synergy was observed, occurring only for the *E. coli* with the dose 3(187,74) and for coliphages with the doses 3(125,16) and 1(187,74), in the first test. And, in test 2, there was synergy only in the inactivation of total coliforms, with the dose 3(164,84). That is, in most cases, the inactivation provided by the sequential method was lower than the sum of inactivation in the individual disinfection processes.

Table 3: Synergy verification.

	Doses APA/UV							
	Test 1						Test 2	
	2 (125,16)	2 (187,74)	3 (125,16)	3 (187,74)	4 (125,16)	4 (187,74)	3 (109,89)	3 (164,84)
E. coli	−2,34	−0,75	−0,39	0,13	−1,15	−1,33	−3,48	−3,48
TC	−1,15	−0,38	−1,16	−0,8	−0,34	−0,01	−0,68	0,06
Coliphages	−0,66	−0,06	0,3	−0,1	−0,12	0,88	−0,6	−0,6

Table 4: *E. coli* and coliphages inactivation employing PAA and UV radiation individually in tests with water.

			Peracetic acid Concentration (mg/L)			UV radiation Exposure (s)	
		N_o	2	3	4	60	90
Test 1	*E. coli*	5×10^2	10	<1	<1	$3{,}7 \times 10^2$	<1
	Coliphages	—	—	—	—	—	—
Test 2	*E. coli*	9×10^3	60	40	10	100	<1
	Coliphages	2×10^3	235	70	<1	5	<1

N_o: microorganisms initial number in gross water; —: test not carried out.

However, although the sequential method almost did not present synergy, it was proved more efficient in the disinfection than the individual methods. The sequential method provided higher inactivation values obtained amongst the three methods analyzed, and these are 4,48 log for *E. coli*, 4,25 log for total coliforms, and 3,1 log for coliphages.

In the case of wastewater experiments, the low residual value of PAA in the effluent did not permit the formation of AOP and its potential effect added to the microbial inactivation.

Caretti and Lubello [11] proposed an advanced treatment for wastewater, aiming at complete reuse in agriculture, and evaluated the efficiency of the PAA and UV disinfectants in the configuration: PAA/UV and UV/PAA, and, considering the same doses, observed that the levels of inactivation reached when the PAA was added before the UV radiation were higher. The effect of inactivation resulting from the PAA/UV method overcame the sum of these disinfectants individual effects, confirming the synergy between these two treatments. The highest efficiency of the PAA/UV combined method was ascribed to the formation of free radicals due to the PAA photolysis, in the presence of UV rays.

Koivunen and Heinonen-Tanski [12], with the PAA/UV combined method, observed synergic effects against enteric bacteria, reaching values over 2 log inactivation for *E. coli*. However, the coliphages inactivation presented much lower synergy values.

3.4. Tests of Water Disinfection Employing the Individual Methods PAA and UV Radiation. Regarding the experiments with synthetic water, the turbidity was 0,52 NTU in the first test and 0,82 in the second test; the COD varied between 367 and 377 mg/L in the first test and 655 and 665 mg/L in the second; the absorbance in 254 nm varied from 0,069 to 0,107 in the first test and 0,136 to 0,158 in the second.

High COD and absorbance values in the synthetic water were due to the cultures media present in the microorganism strains added to the water, which also provided higher turbidity to the water in test 2, and the COD had its valued doubled, in test 2, proportionally to the elevation of *E. coli* concentration and coliphages in water prior to disinfection.

Table 5: PAA residual in mg/L for both tests with water.

PAA applied concentration (mg/L)	1st test	2nd test
0	0	0
2	0,75	0,2
3	1,66	1,45
4	2,4	2,11

In Table 4, the results of microbial inactivation in the synthetic water disinfection tests employing the individual methods PAA and UV radiation are presented.

In test 1 the UV radiation provided 0,13 log *E. coli* inactivation after 60 s exposure and total efficacy at 90 s, with approximately 2,7 log, with significant improvement of this microorganism inactivation being noted with the increase in the UV dose.

According to data presented in Table 4, the UV system was highly efficient in terms of *E. coli* and coliphages inactivation regarding the 90 s exposure time, in which radiation doses above 300 $mW \cdot s \cdot cm^{-2}$ were generated for both tests.

In experiments with PAA in test 1, the concentration of 2 mg/L PAA provided 1,7 log *E. coli* inactivation and for the concentrations 3 and 4 mg/L total inactivation was reached (2,7 log). Regarding the second test, only the dose 4 mg/L resulted in coliphages maximum inactivation (3,3 log) and 2,95 log for *E. coli*.

In Table 5, PAA residuals present in samples after disinfection for the different doses applied are presented.

PAA was not totally consumed (after 10-minute contact time) at any of the concentrations applied; a certain pattern of PAA consumption was even observed: for doses 2, 3,

Table 6: *E. coli* and coliphages inactivation with the sequential PAA/UV method with synthetic water.

Concentration (mg/L)	Radiation contact time (s)	*E. coli* inactivation $[-\log(N/N_o)]$	Coliphages inactivation $[-\log(N/N_o)]$	PAA residual (mg/L)
2	0	2,17	0,93	0,1
	60	5	5	
	90	5	5	
3	0	2,35	1,46	0,94
	60	5	5	
	90	5	5	
4	0	2,95	5	1,58
	60	5	5	
	90	5	5	

and 4 mg/L applied in the first test, the consumption was, respectively, 1,25; 1,34; and 1,6 mg/L PAA, and in the second test, which presented higher microorganisms density in the samples prior to disinfection, the PAA residual was lower, and the consumption was 1,8; 1,55; and 1,89 mg/L, respectively, for the same doses previously employed. The PAA consumption, in this study, was always below 2 mg/L, which seems to mean that only certain percentage of the PAA applied is really used to satisfy the demand and disinfect; the remaining PAA is available in residual form in the water or wastewater, not presenting antibacterial effect.

After this observation, it is important to highlight that the use of PAA in full scale, for different water or wastewater characteristics, requires the evaluation of its real consumption, which depends amongst other factors on the characteristics of the organic matter and the microbial density, so that the best dosage to be employed is set for each case, aiming to avoid, mainly, unnecessary costs with the use of chemical product.

3.5. Sequential PAA/UV Disinfection with Synthetic Water. In Table 6, the microorganisms *E. coli* and coliphages inactivation values in the sequential PAA/UV disinfection, as well as the PAA residual, are presented.

The *E. coli* and coliphages inactivation results with PAA treated water (2, 3, and 4 mg/L) followed by UV radiation were considered excellent, once 5 log microorganism reduction was reached with all combined doses employed, and in all situations the detection limit of the method employed was reached, after 60-second UV radiation exposure, suggesting that it is possible to reduce the UV radiation time.

As PAA residual was detected after the contact period of 10 minutes, the higher inactivation values obtained in this experiment are ascribed to the occurrence of OH radical formation provided by the AOP PAA/UV.

4. Conclusion

This study enabled us to conclude that the *E. coli*, TC, and coliphages microorganisms inactivation through the advanced PAA/UV oxidative process is an alternative which presents high efficacy of microbial inactivation once it resulted in maximum disinfection values. The absence of suspended solids in the synthetic water provided, in general, better microbial inactivation results when compared to the experiments carried out with wastewater. This is probably due to the shield effect provided by the suspended particles which protect the microorganisms from the action of the disinfectant agents, both chemical, and especially of the UV radiation.

The possibility of synergy occurrence when employing AOPs such as the PAA/UV proposal is a very important tool, which should be better investigated, as it can guarantee higher global disinfection efficacy even when lower doses of disinfectant are applied, which might lower the cost of the process. Although economic viability has not been evaluated in this study, it is a relevant aspect, mainly in the case of WTP; this factor might be the one to rule the disinfection systems maintenance in such units.

Conflict of Interests

The authors declare that there is no conflict of interests regarding the publication of this paper.

References

[1] Trata Brasil, *Situação do Saneamento no Brasil*, 2012, http://www.tratabrasil.org.br/saneamento-no-brasil.

[2] J. B. Costa, *Avaliação ecotoxicológica de efluente de tratamento secundário de esgoto sanitário após desinfecção com ácido peracético, cloro, ozônio e radiação ultravioleta [Tese de Doutorado]*, Escola de Engenharia de São Carlos, Universidade de São Paulo, São Carlos, Brazil, 2007.

[3] R. F. Gonçalves, *Desinfecção de efluentes sanitários*, vol. 1, PROSAB/FINEP, ABES, RiMa, Rio de Janeiro, Brazil, 2003.

[4] M. V. Sperling, *Introdução a Qualidade das Águas e ao Tratamento de Esgotos*, Universidade Federal de Minas Gerais, Belo Horizonte, Brazil, 3rd edition, 2005.

[5] USEPA—U.S. Environmental Protection Agency, *Wastewater Technology Fact Sheet Chlorine Disinfection*, Washington, DC, USA, 1999.

[6] N. Fischer, *Sinergismo em desinfecção sequencial com aplicação de cloro e radiação ultravioleta*, Monografia (Graduação em Engenharia Ambiental), Escola de Engenharia de São Carlos, Universidade de São Paulo, São Carlos, Brazil, 2010.

[7] (USEPA) U.S. Environmental Protection Agency, *Wastewater Technology Fact Sheet Ultraviolet Disinfection*, USEPA, Washington, DC, USA, 1999.

[8] M. Kitis, "Disinfection of wastewater with peracetic acid: a review," Environment International, 2003, http://www.sciencedirect.com.

[9] G. S. Cavallini, S. X. Campos, J. B. Souza, and C. M. Vidal, "Utilização do ácido peracético na desinfecção de esgoto sanitário: uma revisão," *Semina: Ciências Exatas e Tecnológicas*, vol. 33, no. 1, pp. 27–40, 2012.

[10] J. B. Souza, *Avaliação de métodos para desinfecção de água, empregando cloro, ácido peracético, ozônio e o processo de desinfecção combinado ozônio/cloro [Doutorado Tese em Hidráulica e Saneamento]*, Escola de Engenharia de São Carlos, Universidade de São Paulo, São Carlos, Brazil, 2006.

[11] C. Caretti and C. Lubello, "Wastewater disinfection with PAA and UV combined treatment: a pilot plant study," *Water Research*, vol. 37, no. 10, pp. 2365–2371, 2003.

[12] J. Koivunen and H. Heinonen-Tanski, "Inactivation of enteric microorganisms with chemical disinfectants, UV irradiation and combined chemical/UV treatments," *Water Research*, vol. 39, no. 8, pp. 1519–1526, 2005.

[13] APHA/AWWA/WEF, *Standard Methods of the Examination of Water and Wastewater*, CD-ROM, APHA (American Public Health Association), Washington, DC, USA, 20th edition, 1998.

[14] L. A. Daniel, *Processos de desinfecção e desinfetantes alternativos na produção de água potável*, PROSAB, São Paulo, Brazil, 2001.

[15] J. B. Souza, C. M. S. Vidal, G. S. Cavallini, L. Quartaroli, and L. R. C. Marcon, "Avaliação do emprego da radiação ultravioleta na desinfecção de esgoto sanitário," *Semina: Ciências Exatas e Tecnológicas*, vol. 33, no. 2, pp. 117–126, 2012.

[16] CETESB (Companhia de Tecnologia de Saneamento Ambiental), "Determinação de colifagos em amostras de água," Método de ensaio L5/225, CETESB, São Paulo, Brazil, 1990.

[17] J. B. Souza and L. A. Daniel, "Comparação entre hipoclorito de sódio e ácido peracético na inativação de *E. coli*, colifagos e *C. perfringens* em água com elevada concentração de matéria orgânica," *Engenharia Sanitária e Ambiental*, vol. 10, pp. 111–117, 2005.

[18] R. Gehr, M. Wagner, P. Veerasubramanian, and P. Payment, "Disinfection efficiency of peracetic acid, UV and ozone after enhanced primary treatment of municipal wastewater," *Water Research*, vol. 37, no. 19, pp. 4573–4586, 2003.

[19] G. S. Cavallini, S. X. de Campos, J. B. de Souza, and C. M. de Sousa Vidal, "Evaluation of the physical-chemical characteristics of wastewater after disinfection with peracetic acid," *Water, Air, & Soil Pollution*, vol. 224, no. 10, article 1752, 2013.

[20] G. R. Finch, L. R. J. Liyanage, L. L. Gyurék, and J. S. Bradbury, *Synergistic Effects of Multiple Disinfectants*, AWWA Research Foundation and American Water Works Association, Denver, Colo, USA, 2000.

Hindawi Publishing Corporation
International Journal of Photoenergy
Volume 2015, Article ID 829136, 18 pages
http://dx.doi.org/10.1155/2015/829136

Research Article

Novel Electrochemical Treatment of Spent Caustic from the Hydrocarbon Industry Using Ti/BDD

Alejandro Medel,[1] Erika Méndez,[2] José L. Hernández-López,[1] José A. Ramírez,[1] Jesús Cárdenas,[1] Roberto F. Frausto,[1] Luis A. Godínez,[1] Erika Bustos,[1] and Yunny Meas[1]

[1]*Centro de Investigación y Desarrollo Tecnológico en Electroquímica, S.C., Parque Tecnológico, Querétaro-Sanfandila, 76703 Pedro Escobedo, QRO, Mexico*
[2]*Facultad de Ciencias Químicas, Laboratorio de Investigación Electroquímica, Universidad Autónoma de Puebla, Ciudad Universitaria, Edificio 105-i., 72570 Puebla, PUE, Mexico*

Correspondence should be addressed to Alejandro Medel; alejandromedelreyes@gmail.com
and Yunny Meas; yunnymeas@cideteq.mx

Received 10 October 2014; Accepted 26 November 2014

Academic Editor: Mika Sillanpää

During the crude oil refining process, NaOH solutions are used to remove H_2S, H_2S_{aq}, and sulfur compounds from different hydrocarbon streams. The residues obtained are called "spent caustics." These residues can be mixed with those obtained in other processes, adding to its chemical composition naphthenic acids and phenolic compounds, resulting in one of the most dangerous industrial residues. In this study, the use of electrochemical technology (ET), using BDD with Ti as substrate (Ti/BDD), is evaluated in electrolysis of spent caustic mixtures, obtained through individual samples from different refineries. In this way, the Ti/BDD's capability of carrying out the electrochemical destruction of spent caustics in an acidic medium is evaluated having as key process a chemical pretreatment phase. The potential production of $^{\bullet}OH$s, as the main reactive oxygen species electrogenerated over Ti/BDD surface, was evaluated in HCl and H_2SO_4 through fluorescence spectroscopy, demonstrating the reaction medium's influence on its production. The results show that the hydrocarbon industry spent caustics can be mineralized to CO_2 and water, driving the use of ET and of the Ti/BDD to solve a real problem, whose potential and negative impact on the environment and on human health is and has been the environmental agencies' main focus.

1. Introduction

The aqueous residues produced by the hydrocarbon industry, which involve the use of sodium hydroxide (NaOH) to remove hydrogen sulfide (H_2S), sulfhydric acid (H_2S_{aq}), and sulfur compounds, found in different fractions of crude oil, are known as spent caustics. The process of producing said residues begins when an aqueous solution of NaOH is mixed with a fraction of oil. Although the oil itself can contain sulfur, the process is commonly carried out after the oil fraction is distilled, due to its contact with air, allowing the formation of H_2S, which is very corrosive and difficult to remove. If the H_2S is formed, the NaOH reacts with it to form sodium sulfide, which is water soluble. The spent caustics are also obtained from different and specific processes, whereby they are classified as sulfidic spent caustics (removal of H_2S and mercaptans from hydrocarbons), naphthenics (removal of naphthenic acids from kerosene and diesel), and cresylic spent caustics (removal of organic acids, phenols, cresols, and xylenols). In the case of naphthenics and cresylics, the NaOH reacts with the naphthenic acids, leading to the formation of sodium naphthenates and phenolates, respectively. Accordingly and depending on the quantity and type of products processed, a refinery can generate spent caustics with multiple characteristics containing sulfide (S^{2-}, 1–4 wt%), mercaptans (0.1–4 wt%), phenols (0–2,000 mg L^{-1}), total organic carbon (TOC, 6,000–20,000 mg L^{-1}), chemical oxygen demand (COD, 20,000–60,000 mg L^{-1}), biochemical oxygen demand (BOD, 5,000–15,000 mg L^{-1}), and potentially toxic elements (PTEs) such as Cu, Ni, Cd, Pb, and Cr, among

others [1], which require unconventional handling and treatment due to their highly toxic nature and unpleasant odor (the mercaptans can be detected in ppb). In the specific case of spent caustics produced from olefins plants, large amounts of S^{2-} (14,000–21,000 mg L^{-1}), pH values of 13.5 to 13.7, and emulsified hydrocarbons have also been reported [2]. With regard to the phenolic content, depending on the refining process, it can reach up to 30,600 mg L^{-1} [3]. The potential danger of the spent caustics can be understood considering the fact that, by not having technology for its treatment *in situ*, the different types of spent caustics can be combined, resulting in the production of highly toxic mixtures. On the other hand, when the spent caustics are not treated immediately, these are temporarily stored or confined by authorized companies, with their transport and storage being a latent threat due to the possibility of spillage, which has already been recorded in history with a highly negative impact on human health. A concentration of phenol ranging from 5 to 25 mg L^{-1} is as toxic for aquatic life as it is for humans [4, 5]. For this reason, the maximum limits allowed of phenol residues found in industrial discharges vary between 0.5 and 1.0 mg L^{-1} [5]. In the case of potable drinking water, the European Union (EU), in its 80/778/EC Directive, assigned a maximum limit allowed of <0.0005 mg L^{-1} for phenol in all of its forms [4], given that the consumption of water containing these compounds can induce cancer or death [6]. At the same time, the elevated danger of this contaminant for aquatic life has marked phenol and some phenolic compounds as priority contaminants, in agreement with the criteria of the Environmental Protection Agency (EPA) of the United States [4, 5]. In a conventional manner, the treatment of spent caustics from refineries has been carried out in three steps: (1) wet air oxidation (WAO), (2) acid neutralization (AN), and (3) biological oxidation (BO). On occasions, step (2) can be followed by steam stripping. After AN, stripping removes residual H_2S and mercaptans. The liquid effluent obtained has high BOD and COD concentrations because the major portion of the organic constituents is unaffected by the stripping process. Although WAO can treat spent caustic to lower than 1,000 mg L^{-1} COD in 60 min at 475 K and 28 bar, the process is very expensive, and due to severe reaction conditions, safety is a major concern [2]. At the same time, though the elimination of contaminants in steps (1) and (2) can lead to the obtainment of wastewater easily treatable by BO, this depends strictly on the level of conversion and removal of the contaminants found. For example, if the sulfur content is high and the concentration of phenols is low, the BO (use of bacteria from the genus *Thiobacillus*) is possible. Contrarily, the process can be deactivated when the concentration of phenol is high. It has been reported that effluents containing phenol with a concentration of >3000 mg L^{-1} cannot be treated through BO [4]. Taking this problem into account, different processes have been applied and evaluated for the treatment of effluents from refineries, leaving aside the treatment of the spent caustics. It is important to mention that the physicochemical nature and composition of the spent caustics is not comparable to wastewater produced as part of the extraction processes of crude oil (water produced) or the wastewater produced in other processes. In spent caustics the content of phenolic compounds can reach a value of 30,600 mg L^{-1} [3], while in water produced or any other kind of wastewater this value can oscillate between 20 and 200 mg L^{-1} [7–9]. In the case of wastewaters from refineries, the chemical coagulation using polyaluminium chloride [10], chemical precipitation [11], integrated processes (coagulation-flocculation and flotation) [12], and electrocoagulation (EC) has been reported to remove the high content of the organic material found [13]. At the same time and considering the importance of the phenolic content, as well as the content of commonly found fats and oils [14], the EC has also been evaluated, using NaCl, reaching removal percentages of 91% [15] and 94.5% [16] for synthetic and real samples, respectively. In other studies, the combination of electroflotation (EF) and EC and integrated processes (EC-adsorption-BO) have also been proposed [17, 18]. Although, in spent caustics, the EC has been tested for the removal of sulfides and organic material [1], it is important to highlight that the nature of this process is not destructive, allowing the transference of the pollutants from one phase to another with the subsequent disposal problem. On the other hand and considering the technical difficulties in treating aqueous wastes containing phenol or phenolic compounds through WAO, BO or EC, alternative processes of a destructive nature such as the chemical advanced oxidation processes (AOPs, in the presence or absence of sunlight or assisted light), like the use of hydrogen peroxide (H_2O_2), ozone (O_3), photocatalysis, Fenton process, and the ozonation in alkaline medium, have been amply tested in the treatment of phenols and phenolic compounds. However, the majority of these studies have only been carried out on synthetic samples. In real samples from refineries, applying these processes, only a few studies have been reported [19]. Considering the importance implied in the treatment of real samples, in the last years (2000–2014), different isolated studies have been reported on the treatment of spent caustics using the Fenton process. In this sense, samples containing a COD of 20,160 mg L^{-1} and a total of phenols of 1,800 mg L^{-1} have been successfully treated obtaining removal efficiencies of 90% for COD and 99% for total phenols at a pH of 4 [20]. At the same time, when comparing this process using assisted light (photo-Fenton) in the treatment of sulfidic spent caustics, a greater efficiency was reached with a removal of COD and sulfide up to 97% and 100%, respectively [21]. Applying both processes and despite the excellent results, in practice, the percentage of total destruction of the organic content is strictly dependent on the physicochemical composition of the sample to be treated. An elevated organic charge consumes a large amount of H_2O_2. Also, because of a high concentration of H_2S (up to 20 g L^{-1}), its reaction with ferric ion causes a loss of iron catalyst activity [2]. At the same time, it is necessary to emphasize that the chemical AOPs do not possess the ability to destroy the reaction byproducts. Contrarily, one of the most efficient processes and with the potential to carry out the destruction of any contaminant, including phenol and phenolic compounds, is electrochemical oxidation (EO). Said technology bases its efficiency on the nature of

the material used as anode [22]. In this sense, two types of anodic materials are known: (i) active anodes (Au, Ni, stainless steel (SS), Pt, IrO_2, Ti/RuO_2, and analogous combinations) and, (ii) inactive anodes (Ti/PbO_2, Ti/SnO_2-Sb, and analogous combinations), which are materials with a low or high production of $^{\bullet}$OH radicals ($^{\bullet}$OHs), respectively. The $^{\bullet}$OHs can destroy any toxic pollutant to CO_2 and water, due to its high oxidation potential (2.8 V vs. ENH). For this reason the use of inactive anodes is preferred. Here, it is important to mention that Au, Ni, SS, Pt, and analogous combinations are included, due to their similar active or inactive behavior. These materials are not included in the original reference. Although, in the literature, there are numerous studies related to the EO of phenol in synthetic samples [22–53], only a few studies have been reported applying this technology in the treatment of samples from refineries and, as far as we know, there are no reported studies on the treatment of spent caustics. It is also important to consider that both types of aqueous residues represent a highly complex matrix, whose chemical composition can favor or diminish the process efficiency. According to this, using a titanium (Ti) electrode, coated with titanium oxide and ruthenium oxide (RuO_2), efficiencies of phenol degradation in 99.7% and 94.5% and oxidation percentages of COD in 88.9% and 70.1% were obtained for synthetic and real samples (petroleum refinery wastewater), respectively [54]. In other studies using Ti/TiO_2-RuO_2-IrO_2 for phenol degradation in wastewater samples from refineries, removal percentages of 74.75% and 48% for COD and TOC, respectively, were obtained, even when using high quantities of chloride ions [7]. At the same time, the use of Ti/RuO_2-TiO_2-SnO_2 has also been evaluated in the hydrocarbon industry effluents, obtaining low percentages of phenol degradation around 20–47% [55]. Ruling out the use of active electrodes and mixtures of these [56], a very important option is the use of Ti/SnO_2-Sb and Ti/PbO_2, which possess a high production of $^{\bullet}$OHs; however, the application of these materials continues to be restricted due to structural problems and to the possible release of Pb ions [57–59]. As an alternative anodic material, the boron doped diamond (BDD) has been amply evaluated and accepted due to its unusual properties such as a high corrosion resistance, a low adsorption of organic compounds, generation of oxidizing species (O_3, H_2O_2, and $^{\bullet}$OH) [60], and an elevated overpotential for the reaction of oxygen evolution, ηO_2 [61]. The BDD efficiency is based on its high production of $^{\bullet}$OHs, which are produced through the water oxidation process (1), leading to the complete mineralization of pollutants to CO_2 and water (2), with high current efficiencies [62]. This process is known as electrochemical incineration [22]:

$$H_2O \longrightarrow {}^{\bullet}OH + H^+ + e^- \quad (1)$$

$$R + M\left({}^{\bullet}OH\right) \longrightarrow M + mCO_2 + nH_2O + H^+ + e^- \quad (2)$$

It is important to emphasize that different studies on the oxidation of phenol and phenolic compounds in synthetic samples, using BDD, have been presented from 2000 to 2014 [63–86], demonstrating the capability of the use of BDD for the destruction of these pollutants. When comparing the use of Ti/BDD with Ti/SnO_2-Sb [87, 88] and PbO_2 [89], it was found that the BDD electrode is much better for the destruction of phenol. Although the application of BDD in real samples has been weakly explored, when comparing the BDD with the electro-Fenton process for the treatment of wastewaters from refineries, it has been confirmed that even though the electro-Fenton process can induce a greater phenol degradation in comparison with the BDD electrode, the greater efficiency of degradation of the reaction byproducts (in terms of COD and TOC) occurs with BDD [9, 90]. At the same time, other important studies applying the BDD for the treatment of water produced and typical wastewater from refineries have demonstrated the great efficiency of BDD [91–93]. Said studies and those previously presented not only highlight the effectiveness of the use of the electrochemical technology using BDD but also represent a platform which impulses the use of the BDD, whose scaling potential must be examined in order to advance strategically in solving real problems. According to the above, and based on an extensive review of specialized literature from 1980 to 2014 (use of national and international databases), the object of the present study is to demonstrate the technical feasibility of the use of the Ti/BDD in the electrochemical treatment of spent caustics mixtures, one of the most toxic residues at an industrial level, whose potential and negative impact on the environment and human health is and has been the main focus of environmental agencies.

2. Experimental Details

2.1. Chemicals. Sulfuric acid (H_2SO_4), hydrochloric acid (HCl), NaOH, and phenol (C_6H_5OH) were obtained from J. T. Baker. K_2HPO_4, KH_2PO_4, NH_4OH, potassium ferricyanide ($K_3Fe(CN)_6$), and 4-aminoantipyrine ($C_{11}H_{13}N_3O$) for analysis of phenol in all of its forms were obtained from Aldrich. Coumarin was obtained from Aldrich. The luminescent marine bacteria *Vibrio fischeri* (*Photobacterium phosphoreum*) for toxicity analysis was provided by SDI.

2.2. Instruments. Analysis of phenol in all of its forms was carried out through visible ultraviolet spectroscopy (UV-Vis), using a Lambda XLS$^+$ spectrophotometer. COD and TOC were evaluated using a Hach model DR/200 reactor/Uv-Vis spectrophotometer DR/2010 and Shimadzu Model TOC-VCSN equipment, respectively. COD was obtained using HACH products. Toxicity analysis was done using a DeltaTox kit, provided by SDI. Electrolysis using ultraviolet light (λ = 254 nm) was done by using a Philips mercury lamp with 11 W. Orion Star A215 equipment was used for pH/ORP/conductivity measurements. The electrolysis experiments in galvanostatic mode were performed using Tektronix PWS4323 equipment. The PTEs analyses were performed using a Perkin Elmer Optima 3300 DV model and an Analyst 200/MHS-15 Perkin Elmer. The first equipment was used for the inductively coupled plasma (ICP) analysis and the second for the Hg analyses by hydride generation. The morphology and element analysis of the different electrodes evaluated during the selection of the best anodic material were obtained using a scanning electron microscope (JEOL JMS-6060LV)

(a) (b)

(c)

Figure 1: Handling and control of (a) spent caustics mixture, (b) safety equipment, and (c) specialized infrastructure.

equipped with an energy dispersive spectrometer (EDS). Crystal structure analysis using X-ray diffraction (XRD) was carried out in a Rigaku Minifles, using Cu Kα radiation, with a 30 kV operation voltage and 15 mA of current, at a velocity of 2°/min. Cyclic voltammetry (CV) was carried out with an Autolab PGSTAT 30. The $^{\bullet}$OHs analysis was performed by fluorescence spectroscopy using the equipment HORIBA Jobin MOD Fluorolog 3–22 with double monochromator.

2.3. Characterization of the Spent Caustics

2.3.1. Sample Preparation. A total of 10 samples (20 L each) of spent caustic were obtained from different refineries and stored at room temperature. From these samples, a composite sample was prepared by combining 1 L of each individual sample. The sample obtained (called mixture) is shown in Figure 1(a). This process was carried out using safety equipment (Figure 1(b)) and working under an exhaust hood, which was attached to a gas scrubber containing NaOH (Figure 1(c)).

Before taking each sample, the container was stirred vigorously and the sample was taken immediately. The mixture obtained was also stirred vigorously and stored under refrigeration (4°C) until its analysis.

2.3.2. Physicochemical Analysis. Before carrying out any analysis, the container of the mixture of spent caustics was stirred vigorously. The PTEs analysis was done by using inductively coupled plasma atomic emission spectroscopy (ICP-AES), with the exception of Hg, which was analyzed by hydride generation atomic absorption spectroscopy (HGAAS). The analysis was done prior to digestion of the samples. The concentration of anions present was done through ion chromatography according to the EPA method 300.1 (EPA, 1997). This analysis was performed using a high resolution liquid chromatograph Dionex ICS-2500 HPLC/IC fitted with a Dionex IonPac AS14A column and coupled to a conductivity detector (ED50A). The mobile phase was Na_2CO_3/$NaHCO_3$ (1 mL min^{-1}). The equipment was calibrated using prepared solutions from the 7-Anion Standard of Dionex and the quality of the results was evaluated from the analysis of the certified standard of Inorganic Ventures IC-FAS-1A. The determination of volatile and semivolatile organic compounds (CIDETEQ and Intertek laboratories) in qualitative form was done through gas chromatography mass spectrometry (GC-MS) in accordance with the EPA 5030/EPA 8260C-2006 and EPA 3510/EPA 8270D-2007 procedures. Other physicochemical analyses were done under standard procedures. It is important to highlight that, during the entire

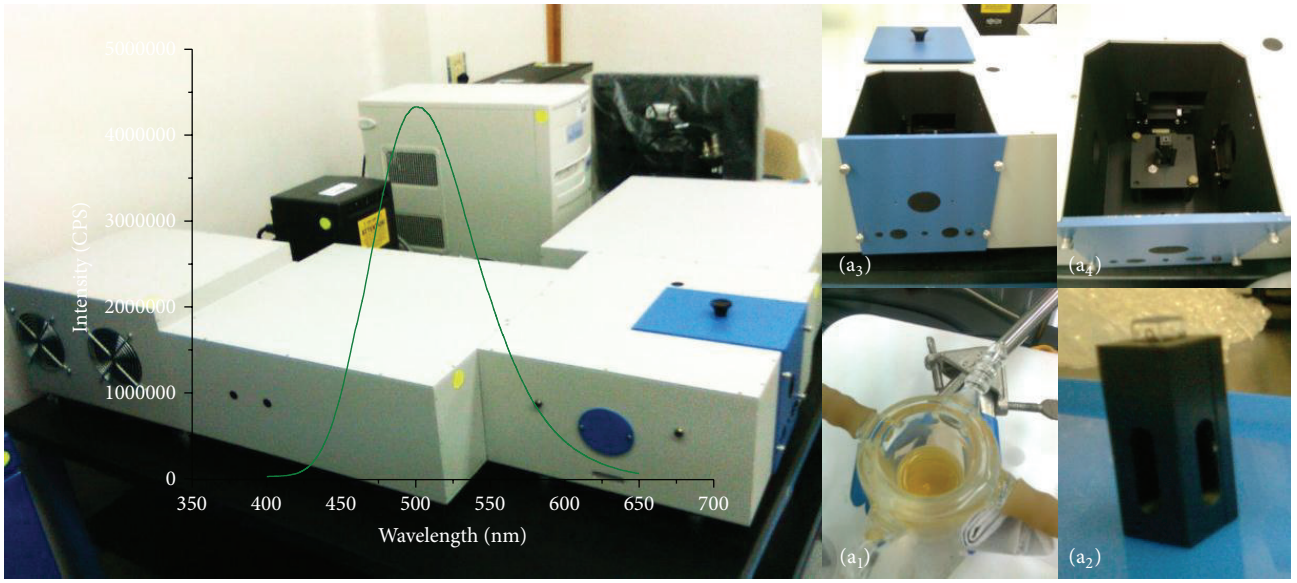

(a)

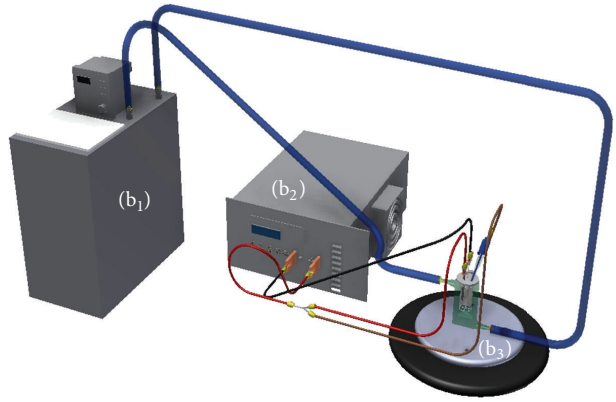

(b)

Figure 2: Experimental system for (a) hydroxyl radicals' analysis by fluorescence spectroscopy, where (a_1)–(a_4) are the steps for analysis of 7-hydroxycoumarin, and (b) electrolysis in galvanostatic mode of spent caustics mixture using Ti/BDD: (b_1) heat exchanger, (b_2) rectifier, and (b_3) electrochemical cell.

process of preparation and analysis of the samples, a strict security protocol was followed, from the use of a personalized infrastructure and safety equipment such as gas masks, nitrile, and neoprene gloves, to that of a special suit.

2.4. Electrochemical Treatment

2.4.1. Selection of the Anode. Morphological, structural, and electrochemical analysis of the different materials evaluated (Ti/IrO_2-Ta_2O_5, Ti/SnO_2-Sb, and Ti/BDD) by SEM-EDS, XRD, and CV were done over the same area (2.185 cm^2). Ti/IrO_2-Ta_2O_5 and Ti/SnO_2-Sb electrodes were synthesized by the thermal deposition method using a special formulation. Polycrystalline boron ((B) = 1300 ppm) doped diamond film (Ti/BDD) of 3 μm thickness, provided by Adamant Technologies, was synthesized by hot filament chemical vapor deposition (HF-CVD). The electroactivity of each material was evaluated by CV using a three-electrode cell (60 mL capacity, with a reaction volume of 50 mL). Ti/IrO_2-Ta_2O_5, Ti/SnO_2-Sb, and Ti/BDD electrodes (2.185 cm^2) were used as anodes, a rod of Ti was used as cathode, and a mercury sulfate electrode ($Hg/Hg_2SO_4/K_2SO_4$ (SAT), E° = 0.640 V vs. SHE) was the reference electrode. The temperature was maintained at 298 K and the voltammetric profiles for each electrode were obtained applying a scan rate of 100 mV s^{-1} using 0.5 M H_2SO_4 as the supporting electrolyte. Before each analysis, the system was deoxygenated using N_2 gas. In this analysis the Ti/BDD was previously activated (to eliminate C-sp^2 impurities) developing a special methodology [94]. Ti/IrO_2-Ta_2O_5 and Ti/SnO_2-Sb were activated by cycling each electrode (50 cycles, 100 mV s^{-1} in 0.5 M H_2SO_4) to stabilize the surface and eliminate impurities.

2.4.2. Selection of the Reaction Medium. Three aspects were taken into account: (i) the pH effect on the chemical state of

phenol, (ii) the pH effect on the electrochemical response of the previously selected electrode, and (iii) the pH effect on the production of $^{\bullet}$OHs. In the first point, analysis by UV-Vis spectroscopy to different pH values was performed with the goal of identifying possible chemical changes on the phenol structure. In this analysis, a synthetic sample was used. The second point was evaluated by the use of CV analyzing two types of acids, HCl and H_2SO_4 (0.5 M), under the same conditions mentioned above. The last point was evaluated through electrolysis experiments, which were performed applying an anodic potential pulse (2.3 V vs. Hg/Hg_2SO_4, polarization time of 10 min, use of a Pt mesh as counter electrode, 298 K). This last analysis was performed through the use of fluorescence spectroscopy using coumarin (3×10^{-5} M) as a probe compound to give way to the formation of the 7-hydroxycoumarin with a wavelength of maximum excitation and emission of 332 nm and 500 nm, respectively (λ_{ex} = 332 nm, λ_{em} = 500 nm). During electrolysis, samples of 10 μL were withdrawn every minute and immediately analyzed. The equipment and the cell used for detection of the 7-hydroxycoumarin are shown in Figure 2(a).

2.4.3. Electrolysis of the Spent Caustic. The electrochemical destruction process of the mixture of spent caustics was done in galvanostatic mode, using the experimental system shown in Figure 2(b). In this process, a cell with a single compartment and a capacity of 120 mL (reaction volume of 100 mL, 8 rpm, 298 K and Ti/Pt (3 cm^2 as counter electrode)) was used. The area of the anode (prior selection) was 3 cm^2. Electrolysis with UV light (λ = 254 nm) was done under the same conditions indicated above. In each experiment, representative samples were taken at different reaction times (t_r), and the degradation of aromatic compounds (phenol and phenolic compounds) and reaction intermediates was done through TOC and COD analysis.

The removal percentages were calculated according to the following formula (3), where C_o is the initial concentration (mg L^{-1}) and C_f is the final concentration (mg L^{-1}) [90]:

$$\%\ \text{removal} = \left[\frac{\left(C_o - C_f\right)}{C_o}\right] * 100. \quad (3)$$

The phenol analysis was done using a standard procedure [95], while the toxicity tests were done using a standard method using a lyophilized bacteria, *Vibrio Fischeri* (*Photobacterium phosphoreum*), of a luminescent nature, where the reduction of light is proportional to the degree of toxicity.

3. Results

3.1. Characterization of the Spent Caustics

3.1.1. Physicochemical Analysis. Table 1 shows the results obtained in the physicochemical characterization of the sample corresponding to the mixture of spent caustics (mixture of 10 samples). Comparatively, it shows the analysis of a simple sample, corresponding to the sample of greater toxicity (preliminary evaluation of the phenolic content), including the reported values in the literature for spent caustics as well as for wastewater from refineries [1, 3, 7, 9, 13, 16–19, 96–98].

The analysis of the mixture showed a phenolic content of 11,041.74 mg L^{-1}, while the simple sample showed a content of 7,270.89 mg L^{-1}. The difference between both samples clearly demonstrates the environmental problem that commonly appears in the hydrocarbon industry. That is to say, residues of low or high toxicity are mixed with each other, resulting in a residue of greater toxicity. Here, the phenol concentration, organic load, and dissolved solids are not comparable with any other residue, including wastewater from different refining processes [90]. The phenol concentration in the samples analyzed suggest that this residue cannot be treated by BO (a concentration >3,000 mg L^{-1} leads to the complete deactivation of the microorganisms). This is confirmed by the result obtained in the toxicity tests (100% toxic) and through the analysis of the BOD_5/COD = 0.09 and 0.07 for the simple sample and the sample corresponding to the mixture, respectively. On the other hand, the elevated alkalinity (52,266.35 mg L^{-1}) and an elevated pH (13–13.5) reflect the reducing nature of these residues, which should be considered in the treatment to be chosen. Many of the contaminants can be fixed at an alkaline pH and be liberated under oxidizing conditions. The reactivity analysis for sulphides and cyanides showed values below the detection limit (<37.29 and <0.25 mg L^{-1}, resp.). Based on the results obtained in this phase of characterization, the samples evaluated were classified as cresylic spent caustics.

3.1.2. Ion Analysis. The analysis of anions, done through ion chromatography, in the case of the simple sample, showed a low content of chlorides (Cl^-) and sulfates (SO_4^{-2}) with values of 86 and 608 mg L^{-1}, respectively, with their concentration being much higher in the mixture, with values of 54,900 and 1,882 mg L^{-1}, respectively. It is necessary to mention that in this case the presence of chlorides is very important. The chlorides, while they can give rise to the presence of compounds of greater toxicity, can also exert a synergic effect during an EO process, giving way to the formation of different oxidizing species [99, 100].

3.1.3. Analysis of Volatile and Semivolatile Organic Compounds. An analysis through GC-MS, corresponding to the mixture of spent caustics, was carried out to determine the different phenolic compounds (reflected in the analysis of phenol in all of its forms, Table 1). Different compounds were considered, of which 43 were for volatile and 62 for semivolatile analysis. The results showed only the presence of 2,4-dimethylphenol, phenol, m-methylphenol, p-methylphenol, and o-methylphenol, all highly toxic compounds. Figure 3 shows the representative chemical structures of each compound identified.

At the same time, a PTEs analysis through ICP was carried out, taking into account that the physicochemical composition of the mixture of spent caustics includes PTEs and possible catalyst traces used in the different processes of hydrocarbon refining. The selection of each PTE was based on an extensive bibliography review. Table 2 shows the main

Table 1: Physicochemical analysis of spent caustics.

Parameter	Value		Value reference	
	Simple sample	Mixture	Spent caustic	Typical refinery wastewater
Total phenol ($mg\,L^{-1}$)	7,270.89	11,041.74	30,600 [3]	13 [16], 172.50 [18], 3.17 [17], 192.90 [9], 141 [7], 113 [19], 23 [96]
Oil and grease ($mg\,L^{-1}$)	239.70	3,399.70	—	85 [97], 1.96 [17], 12.70 [19], 15 [98]
BOD_5 ($mg\,L^{-1}$)	6,930	7,811	—	323 [97], 40.25 [16], 570 [3]
COD ($mg\,O_2\,L^{-1}$)	72,065	98,750–102,842.50	72,450 [1], 320,100 [3]	3,150 [97], 100 [16], 4,450 [18], 2,323 [13], 257 [17], 590 [9], 602 [7], 935 [19], 2,746 [98], 1,220 [96]
BOD_5/COD	0.09	0.07	—	0.60 [19]
Sulfides ($mg\,L^{-1}$)	<37.29	<37.29	34,517 [1], 48,500 [3]	19 [19]
Ammonia ($mg\,L^{-1}$)	—	—	—	13.10 [19]
Cyanides ($mg\,L^{-1}$)	<0.25	<0.25	—	—
pH	13.02	13.50	12.97 [1], 13 [3]	8 [16], 8.60 [18], 8.05 [13], 7.60 [17], 9.20 [7], 8.10 [19], 7.59 [98], 10 [96]
TOC ($mg\,L^{-1}$)	—	20,137.50	53,900 [3]	370 [19], 1,500 [96]
Hydrocarbons ($mg\,L^{-1}$)	—	—	—	11.72 [17], 0.02 [19]
Conductivity ($mS\,cm^{-1}$)	129.20	208.44	126.70 [1]	6 [18], 13.06 [13], 15.63 [7], 1.73 [7], 0.06 [98]
Alkalinity, $CaCO_3$ ($mg\,L^{-1}$)	52,266.35	—	15,500 [3]	3,990 [96]
Total dissolved solid ($mg\,L^{-1}$)	—	169,680	—	5,000 [18], 7,990 [13], 1,333 [7], 4,380 [98]
Settleable solids ($mg\,L^{-1}$)	—	40	—	—
Total suspended solids ($mg\,L^{-1}$)	—	3,940	—	22.80 [16], 35 [18], 100 [13], 1,000 [96]
Toxicity (%)	100	100	—	—
F^- ($mg\,L^{-1}$)	50	135	—	—
Cl^- ($mg\,L^{-1}$)	86	54,900	37,900 [3]	63 [97], 112 [7], 200,000 [96]
Br^- ($mg\,L^{-1}$)	12	<0.30	—	—
NO_3^- ($mg\,L^{-1}$)	11	<0.25	—	—
PO_4^{3-} ($mg\,L^{-1}$)	381	<0.30	4,600 [3]	—
SO_4^{2-} ($mg\,L^{-1}$)	608	1,882	20,300 [3]	1,054.50 [13], 212 [7], 1,650 [96]
ORP (mV)	−334.20	—	—	—
Turbidity (NTU)	—	—	—	6.10 [16], 37 [17], 37 [19]

PTEs identified in the mixture sample. In this analysis, a high amount of Na^+ and Fe with values of 19,148 $mg\,L^{-1}$ and 1,323 $mg\,L^{-1}$, respectively, was identified. The presence of Na^+ confirms the caustic nature of the sample, while the presence of Fe, though it is not an especially toxic element, is commonly controlled by the effect of turbidity caused by the precipitation of oxides and hydroxides. The analysis of Fe was done taking into account its catalytic activity on H_2O_2, to give way for the $^{\bullet}OH$ through the Fenton reaction [90]. Due to this, the presence of Fe could be used to accelerate the mineralization process and decrease the residence times during the EO process.

On the other hand, PTEs like As and Cd remained under the detection limit (<0.098 and <0.114 $mg\,L^{-1}$, resp.), while Cu, Cr, Hg, Ni, and Pb exceeded the maximum limits allowed under the Mexican Regulation [101]. It is important to highlight the elevated toxicity of said elements and, specially, that of the Hg [102, 103] and Pb, which have the ability to enter into the food chains and to concentrate in organisms (magnification process). Considering these analyses, the elevated toxicity of the spent caustics is confirmed, thus justifying the need to direct efforts towards their treatment and/or destruction.

3.2. Electrochemical Treatment

3.2.1. Selection of the Anode. Morphology, elemental composition, crystal structure, and electrochemical analysis. The results corresponding to these analyses are shown in Figure 4. The morphology of metal oxide coatings (Ti/IrO_2-Ta_2O_5 and Ti/SnO_2-Sb) (Figures 4(a) and 4(b), resp.) showed smaller cracks in comparison with Ti/BDD (Figure 4(c)). The latter showed a compact structure, demonstrating the quality of the coating and the adherence of the diamond to the titanium substrate. In parallel, X-ray dot-mapping was used to analyze the distribution of coating elements.

Table 2: Analysis of PTEs in spent caustics mixture.

PTE (mg L^{-1})		MLA (mg L^{-1}) in rivers					
		Agricultural irrigation (A)		Public-urban (B)		Protection of aquatic life (C)	
		p.d	p.m	p.d	p.m	p.d	p.m
Al	15.46	—	—	—	—	—	—
As	<0.098	0.2	0.4	0.1	0.2	0.1	0.2
Cd	<0.114	0.2	0.4	0.1	0.2	0.1	0.2
Co	2.42	—	—	—	—	—	—
Cu*	6.89	4.0	6.0	4.0	6.0	4.0	6.0
Cr*	1.95	1.0	1.5	0.5	1.0	0.5	1.0
Fe	1,323	—	—	—	—	—	—
Mn	7.23	—	—	—	—	—	—
Ca	148.87	—	—	—	—	—	—
Mg	34	—	—	—	—	—	—
Na	19,148	—	—	—	—	—	—
Hg*	0.07	0.01	0.02	0.005	0.01	0.005	0.01
Ni*	6.75	2	4	2	4	2	4
Pb*	1.23	0.5	1	0.2	0.4	0.2	0.4
Zn	4.68	10	20	10	10	20	10
V	0.24	—	—	—	—	—	—

MLA = maximum limits allowed; p.d = per day; p.m = per month.
*Values that exceed the established MLA under Mexican Regulation.

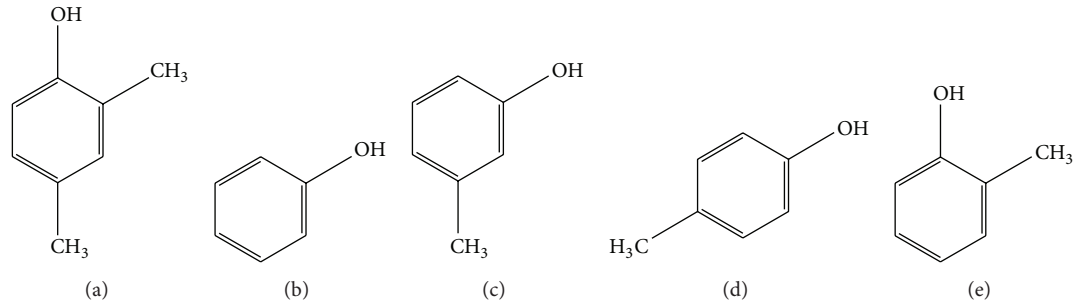

Figure 3: Chemical structure of the main phenolic compounds identified by GC-MS in the spent caustics mixture: (a) 2,4-dimethylphenol, (b) phenol, (c) m-methylphenol, (d) p-methylphenol, and (e) o-methylphenol.

This analysis showed a uniform distribution of Ir (a_1), Ta (a_2), Sn (b_1), B (c_1), and C (c_2). However, the Sb, in the case of Ti/SnO_2-Sb, was not detected. The absence of Sb was probably due to the additive ratio in the coating solution. To verify its presence, an XRD analysis was done demonstrating the presence of SnO_2, Sb_2O_3, and Sb_2O_5. For this specific reason, pretreatment of this electrode was performed before the cyclic voltammetric analysis. At the same time, for both materials (Ti/IrO_2-Ta_2O_5 and Ti/SnO_2-Sb), the wt% of each element was obtained by EDS. In this analysis, the presence of additional elements such as O, Ti, and Si was detected. The results of these analyses (XRD and EDS) have been omitted due to the formulation used. In the case of Ti/BDD, an exhaustive characterization was performed in other studies [94]. The electrochemical characterization of each electrode by CV is shown in Figure 4(d). It shows a comparative analysis of Ti/IrO_2-Ta_2O_5 (d_1), Ti/SnO_2-Sb (d_2), and Ti/BDD (d_3), in 0.5 M H_2SO_4. This graph shows that Ti/BDD has the highest potential window in comparison to Ti/IrO_2-Ta_2O_5 and Ti/SnO_2-Sb. An elevated ηO_2 is important taking into account that the oxidation reaction of the organic compounds during the EO occurs in parallel to the evolution of O_2. Using a material with a high ηO_2, the oxidation reaction is favored over the evolution of O_2, resulting in high current efficiencies. Based on this, it was decided that Ti/BDD was the best material to use in the electrochemical treatment of spent caustic.

3.2.2. Selection of the Reaction Medium. To carry out the electrochemical destruction of the spent caustics using Ti/BDD, the selection of the reaction medium was done taking into account the following approaches: (i) the pH effect on the chemical state of phenol, (ii) the pH effect on the Ti/BDD's electrochemical response, and (iii) the pH effect

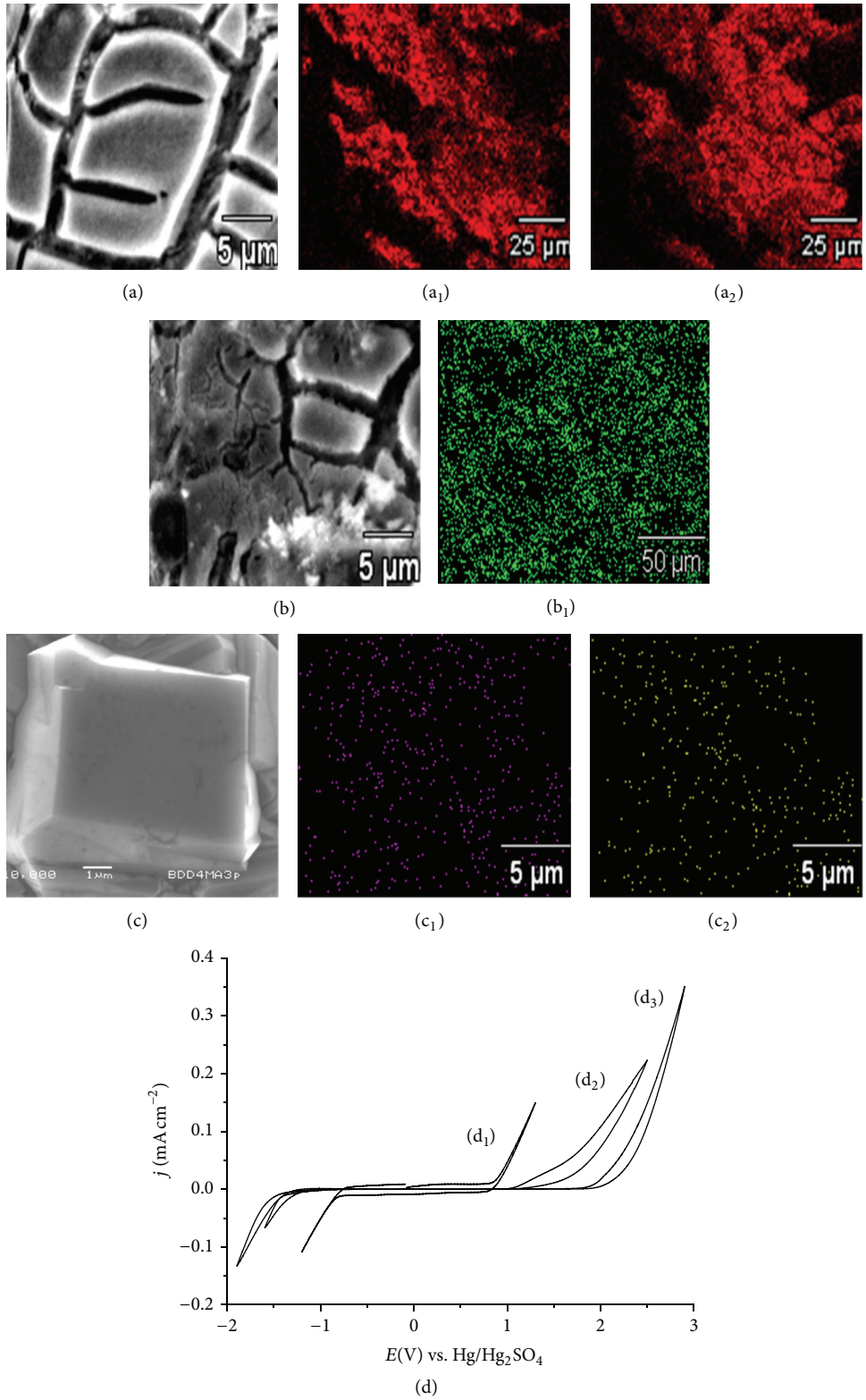

Figure 4: SEM analysis. (a) Ti/IrO_2-Ta_2O_5. (b) Ti/SnO_2-Sb. (c) Ti/BDD, applying 15 kV with its respective micrographies and X-ray dot-mapping analysis, identifying: (a_1) Ir, (a_2) Ta, (b_1) Sn, (c_1) B, and (c_2) C. (d) Cyclic voltammetry analysis for (d_1) Ti/IrO_2-Ta_2O_5, (d_2) Ti/SnO_2-Sb, and (d_3) Ti/BDD in 0.5 M H_2SO_4.

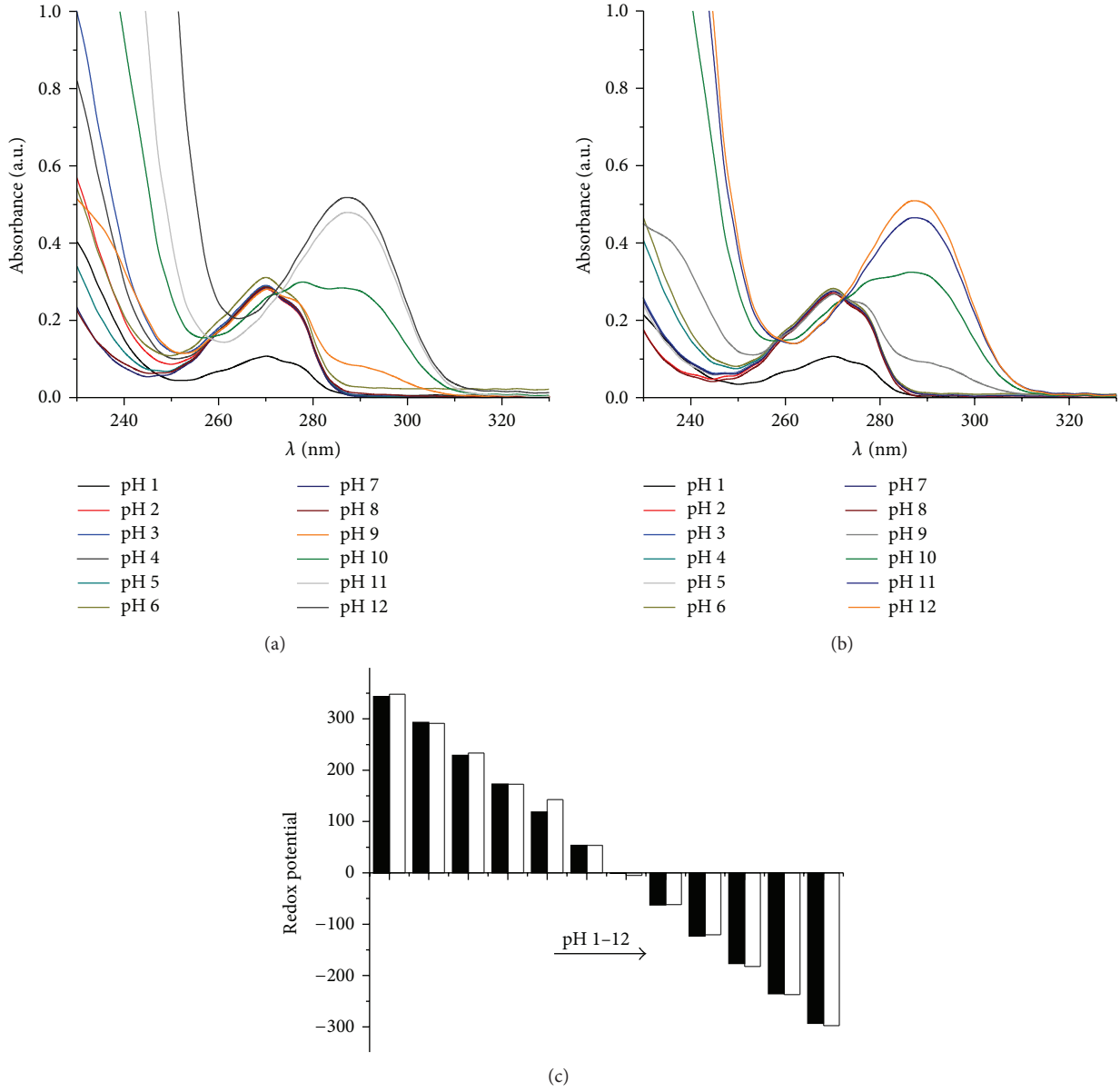

Figure 5: UV-Vis analysis of the pH effect on the chemical state of phenol, using 30 mg L^{-1} of TOC in (a) 0.05 M $NaOH/H_2SO_4$ (pH 12–1), (b) 0.05 M NaOH/HCl (pH 12–1), and (c) ORP analysis under the same conditions to 298 K.

on $^{\bullet}OH$s production. According to the first approach, in an extremely alkaline environment (pH 13–13.5, Table 1), the phenol is chemically transformed into sodium phenolates [90]. Although the electronic state of phenol in an alkaline medium has been shown to be favorable for an EO process using electrodes with a low ηO_2 [28], this does not occur using BDD, where the most degradation efficiency is obtained using an acidic medium [90]. Frequently, in literature, different types of acids have been reported for the EO of phenol, such as $HClO_4$ [63, 104] and HNO_3 [105]; however, for a possible industrial application, the costs of said acids must be considered. For this reason and considering that during the ion analysis a high quantity of chlorides (54,900 mg L^{-1}) and sulfates (1,882 mg L^{-1}) was identified as part of the chemical composition of the spent caustics mixture, HCl and H_2SO_4 were selected as possible acids to carry out the pH adjustment (13, 13.5 to 1). Initially, the acidification process was evaluated using a synthetic sample in order to rule out any chemical change that occurred on the phenol molecule during the acidification process and to avoid an overestimation of the subsequent results. In said analysis, a solution of 0.05 M NaOH containing phenol 30 mg L^{-1} (TOC) was adjusted to different pH values in an interval of 12–1, using 0.5 M HCl and H_2SO_4. The changes that occurred during the acidification process were evaluated through UV-Vis spectroscopy. Figure 5 shows the different UV-Vis absorption spectrums obtained during the adjustment of the pH using H_2SO_4 (Figure 5(a)) and HCl (Figure 5(b)). It is clearly observed that the chemical

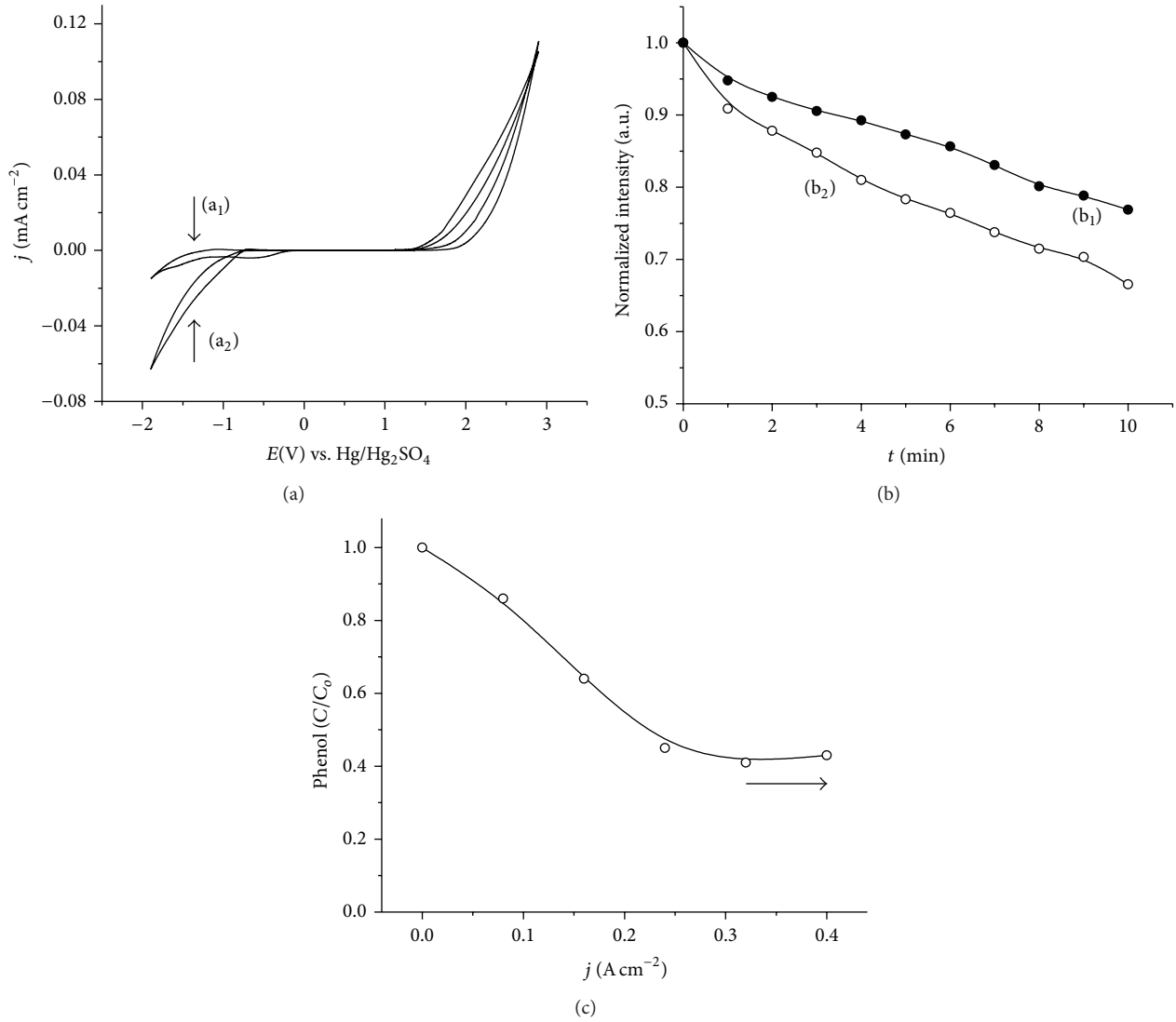

Figure 6: Electrochemical characterization of Ti/BDD by cyclic voltammetric analysis using (a_1) 0.05 M NaOH/HCl (pH 1) and (a_2) 0.05 M NaOH/H_2SO_4 (pH 1). (b) $^{\bullet}$OHs analysis by fluorescence spectroscopy using (b_1) 0.05 M NaOH/HCl (pH 1) and (b_2) 0.05 M NaOH/H_2SO_4 (pH 1). (c) Selection of the current density using synthetic solutions of phenol (30 mg L^{-1} of TOC) in 0.05 NaOH/H_2SO_4 (pH 1).

conversion of sodium phenolates to phenol (λ = 270 nm) is obtained with both types of acids at a pH of 9, reaching the maximum conversion efficiency at a pH of 7.

There were no additional and significant chemical changes observed. In parallel to this measurement, an analysis of the redox potential (ORP) was carried out at 298 K. The result of this analysis is shown in Figure 5(c). The values obtained clearly show that an acidic pH favors highly oxidizing conditions, which is of high importance considering that, albeit, an acidic environment does not alter the chemical structure of phenol, the contaminants associated with the spent caustics can be liberated, whereby, a specialized infrastructure and safety equipment are necessary. Using H_2SO_4, a slight increase in the ORP was observed in comparison with HCl, which is logical considering a greater number of protons. To evaluate the second approach (effect of the pH on the electrochemical response of the Ti/BDD), different voltammograms were obtained through the adjustment of 0.05 M NaOH with 0.5 H_2SO_4 and HCl in a pH range of 12–1 (data not shown). It was observed that when the pH values descended to acidic, the ηO_2 increased considerably [106]. When comparing the window of potential of H_2SO_4 with that of HCl (pH 1) (Figure 6(a)), a difference in overpotential of 0.5 V was obtained. Considering these results and according to the third approach (pH effect on $^{\bullet}$OHs production), an analysis of the generation of the $^{\bullet}$OHs was carried out in both reaction mediums (pH 1). Figure 6(b) shows the influence of the reaction medium on the production of $^{\bullet}$OHs. It is clearly observed that the production of $^{\bullet}$OHs is greater in NaOH/H_2SO_4 (pH 1).

This result is of great importance considering that, with the use of a BDD electrode, the formation of any oxidizing species produced in parallel to the oxidation of organic compounds is strictly dependent on the formation of

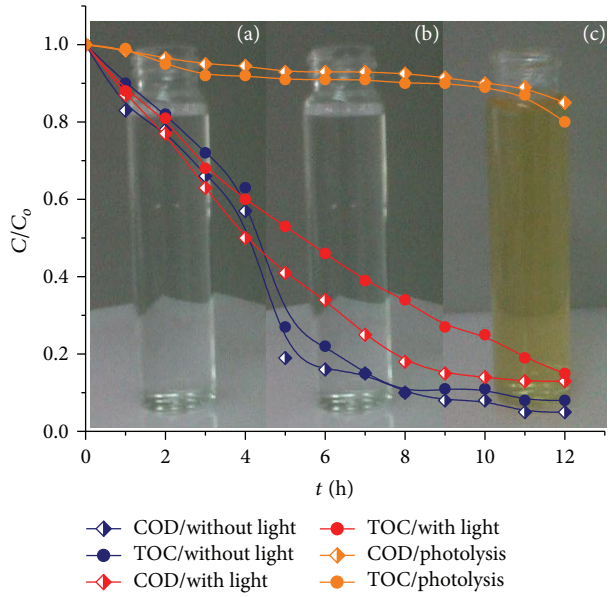

FIGURE 7: Evaluation of the use of UV light (λ = 254 nm). Removal of COD and TOC in spent caustic corresponding to the simple sample using Ti/BDD, applying 0.96 A (j = 0.32 A cm^{-2}), under constant stirring, pH 1 (adjustment with H_2SO_4) and t_r = 12 h. Images of (a) in the absence of UV light, (b) in the presence of UV light (λ = 254 nm), and (c) photolysis.

the $^{\bullet}$OHs. Based on this result, H_2SO_4 was selected to carry out the acidification process.

3.2.3. Electrolysis Using Ti/BDD. Before performing the degradation experiments, a preliminary analysis using a synthetic solution with a phenol concentration of 30 mg L^{-1} of TOC was carried out in NaOH/H_2SO_4 (pH 1) with the goal of identifying the current to be applied. The currents evaluated were 0.24, 0.48, 0.72, 0.96, 1.20, and 1.44 A, for a 2-hour period, under constant stirring. Ti/BDD (3 cm^2) was used as anode and Ti/Pt (3 cm^2) was used as counter-electrode. It was observed that the middle point of the removal was reached at 0.96 A (j = 0.32 A cm^{-2}), as shown in Figure 6(c). After having identified the current to be applied and before carrying out electrolysis of the spent caustics mixture, a preliminary electrolysis was performed using a simple sample (Table 1). The conditions of electrolysis were j = 0.32 A cm^{-2}, pH 1 (adjustment with H_2SO_4). In this analysis, the effect of ultraviolet light was considered for the purpose of favoring the synergic effect on the production of the $^{\bullet}$OH. It has been reported that, in the presence of chlorides, the use of ultraviolet light (λ = 254 nm) can lead to the production of the $^{\bullet}$OH, according to the reaction (4):

$$\mathrm{HOCl} + h\nu \longrightarrow {}^{\bullet}\mathrm{OH} + {}^{\bullet}\mathrm{Cl} \quad (4)$$

Figure 7 shows the degradation profiles (TOC and COD) obtained in the different analyses done in the presence and absence of UV light (λ = 254 nm).

The results obtained in electrolysis in the absence of light were more satisfactory than those obtained in its presence (λ = 254 nm). The results obtained can be attributed to the type of sample analyzed. A real sample is not comparable to a synthetic sample. Here, it is inferred that, due to the high content of organic material, oxidation processes, different from those that occurred in the interface or by the action of the oxidants themselves, are not significant. When analyzing the effect of UV light (λ = 254 nm), without applying a current (photolysis), no significant change was observed.

Figure 8 shows the analysis of images obtained during the different electrolysis carried out.

The initial image (t_r = 0 h) corresponds to the simple sample submitted to a special pretreatment before electrolysis (acidification to pH 1 using H_2SO_4). A dark brown color in the first stages of the phenol electrolysis is related to the formation of byproducts such as benzoquinone and hydroquinone, known as an active redox couple in equilibrium in an aqueous solution [51]. The color degradation in each experiment was gradual. When comparing each image (t_r = 8 h), it is clearly observed that, in electrolysis carried out in the absence of light (Figure 8(a)), the sample turned completely crystalline, indicating a high level of destruction of the organic content. Contrarily, in electrolysis in the presence of light (λ = 254 nm) (Figure 8(b)) and in photolysis experiments (Figure 8(c)), the opposite process was observed. In the presence of light (λ = 254 nm), the degradation time to obtain a visually crystalline sample was greater (t_r = 12 h). Based on these results, the use of UV light (λ = 254 nm) was discarded. On the other hand and considering the results obtained, the possible passivation of Ti/BDD as an important point was also evaluated. In this analysis, the $^{\bullet}$OHs production was performed in function of the interfacial potential or current applied. The result (data not shown) indicates that these species only are generated in the zone corresponding to the decomposition of the medium, whereby, if the domains of the potential or current applied are not the correct ones, the electrode can be completely

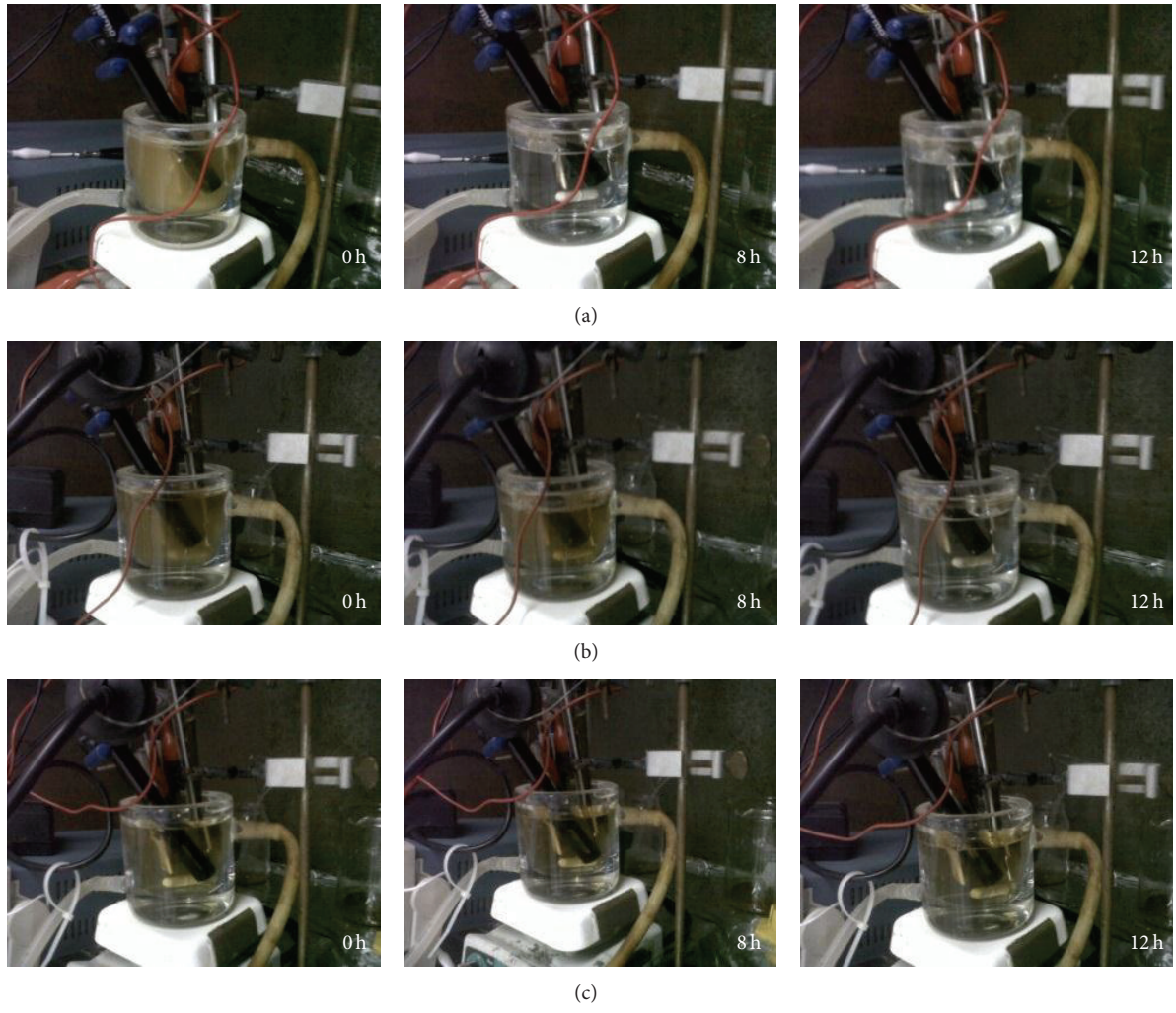

Figure 8: Images of electrolysis of spent caustic corresponding to the simple sample. (a) In the absence of UV light. (b) In the presence of UV light ($\lambda = 254$ nm). (c) Photolysis, using Ti/BDD, applying 0.96 A ($j = 0.32$ A cm^{-2}), under constant stirring, pH 1 (adjustment with H_2SO_4) and $t_r = 12$ h.

Table 3: Electrochemical treatment of spent caustics (mixture) using Ti/BDD.

Sample	COD (mg L^{-1})	COD removal (%)	Total removal efficiency, WT-ET (%)	TOC (mg L^{-1})	TOC removal (%)	Total removal efficiency, WT-ET (%)
Without treatment (WT)	98,750	0	—	20,137.5	0	0
Chemical treatment (CT)*	24,533	75.15	—	15,700	22.03	—
Electrochemical treatment (ET)	2,333	90.40	96.63	2,322	85.21	88.46

* Acidification to pH 1 using H_2SO_4.

passivated. The image analysis of this test is shown in Figure 9. As can be observed (Figure 9(a)), when working with a current, where the production of the $^{\bullet}$OHs does not occur, a thick layer of organic compounds is deposited, causing the deactivation of the electrode.

Contrarily, when the current is applied, inducing a greater interfacial potential by which $^{\bullet}$OHs are electrogenerated, the Ti/BDD electrode can be operated successfully (Figure 9(b)). Finally and according to the previous studies, the electrolysis of the mixture (100 mL) of spent caustics was carried out (pH 1/H_2SO_4, $j = 0.32$ A cm^{-2}). The results obtained in this analysis are shown in Table 3. The results obtained were similar to those from electrolysis of the simple sample.

The analysis of the image of the sample corresponding to the mixture of spent caustics before and after the electrochemical treatment with Ti/BDD ($t_r = 15$ h) is shown in Figures 9(c) and 9(d), respectively. Complementary analyses of toxicity and phenol in all of its forms showed that the sample electrochemically treated is not toxic, presenting a low phenol content (<3 ppm), with this value being

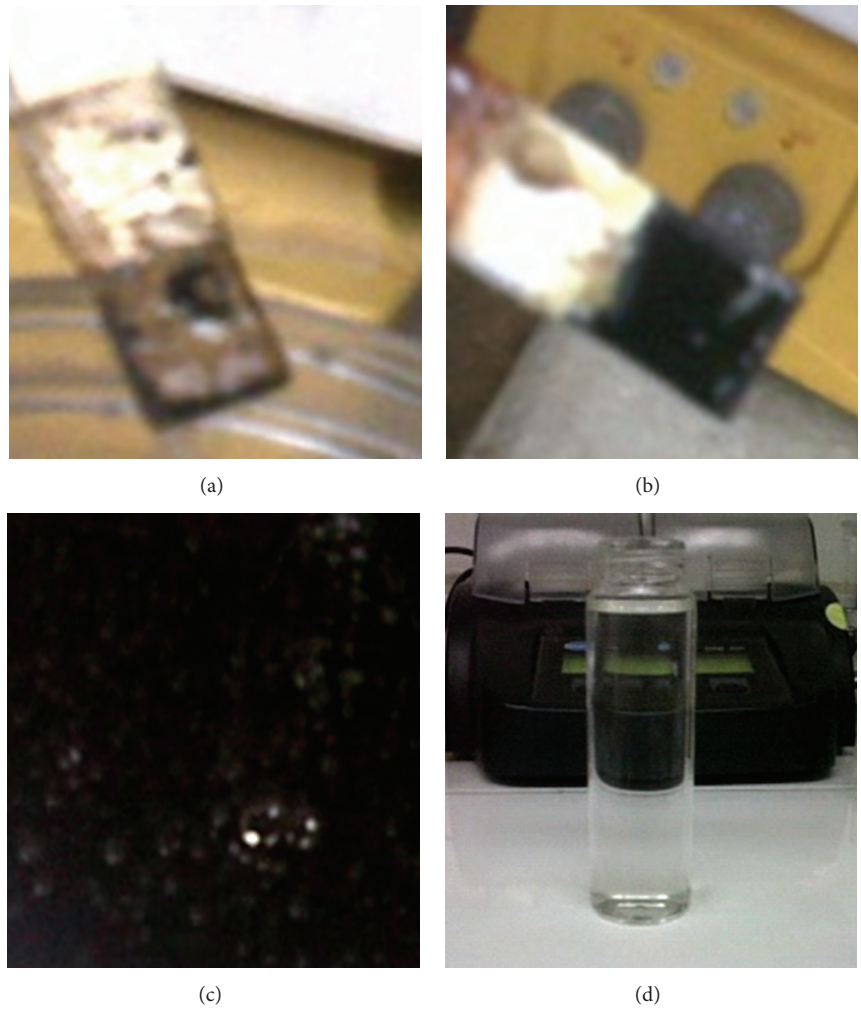

Figure 9: Electrochemical treatment of spent caustics mixture. (a) Applying a current where the $^{\bullet}$OHs are not generated. (b) Applying a current where the $^{\bullet}$OHs are generated. (c) Electrolyzed sample (without pretreatment). (d) Sample obtained after the electrochemical treatment with Ti/BDD applying 0.96 A (j = 0.32 A cm^{-2}), under constant stirring, pH 1 (adjustment with H_2SO_4) and t_r = 15 h.

the minimum standard discharge limit for refinery effluents [107].

4. Conclusions

A greater production of the $^{\bullet}$OH was obtained by using H_2SO_4 as a reaction medium. The degradation of spent caustics in an acidic medium (H_2SO_4, pH 1) using Ti/BDD in simple samples proceeded at 100%, while for the mixture, percentages of destruction of 90.40% and 85.21% for COD and TOC, respectively, were obtained. The use of UV light (λ = 254 nm) did not show an improvement of the process. Further studies are necessary to improve the efficiencies obtained.

Conflict of Interests

The authors declare that there is no conflict of interests regarding the publication of this paper.

Acknowledgments

The authors would like to thank Mexico's National Council of Science and Technology (CONACyT) for its financial support of this research. The authors also thank Ms. Alejandra Rojo (native speaker) for her review of this paper.

References

[1] I. Hariz, A. Halleb, N. Adhoum, and L. Monser, "Treatment of petroleum refinery sulfidic spent caustic wastes by electrocoagulation," *Separation and Purification Technology*, vol. 107, pp. 150–157, 2013.

[2] S.-H. Sheu and H.-S. Weng, "Treatment of olefin plant spent caustic by combination of neutralization and fenton reaction," *Water Research*, vol. 35, no. 8, pp. 2017–2021, 2001.

[3] A. Olmos, P. Olguin, C. Fajardo, E. Razo, and O. Monroy, "Physicochemical characterization of spent caustic from the

OXIMER process and sour waters from mexican oil refineries," *Energy & Fuels*, vol. 18, no. 2, pp. 302–304, 2004.

[4] H. Jiang, Y. Fang, Y. Fu, and Q.-X. Guo, "Studies on the extraction of phenol in wastewater," *Journal of Hazardous Materials*, vol. 101, no. 2, pp. 179–190, 2003.

[5] Y. Han, X. Quan, S. Chen, H. Zhao, C. Cui, and Y. Zhao, "Electrochemically enhanced adsorption of phenol on activated carbon fibers in basic aqueous solution," *Journal of Colloid and Interface Science*, vol. 299, no. 2, pp. 766–771, 2006.

[6] A. Nuhoglu and B. Yalcin, "Modelling of phenol removal in a batch reactor," *Process Biochemistry*, vol. 40, no. 3-4, pp. 1233–1239, 2005.

[7] D. Rajkumar and K. Palanivelu, "Electrochemical treatment of industrial wastewater," *Journal of Hazardous Materials*, vol. 113, no. 1–3, pp. 123–129, 2004.

[8] H. Polat, M. Molva, and M. Polat, "Capacity and mechanism of phenol adsorption on lignite," *International Journal of Mineral Processing*, vol. 79, no. 4, pp. 264–273, 2006.

[9] Y. Yavuz, A. S. Koparal, and Ü. B. Öğütveren, "Treatment of petroleum refinery wastewater by electrochemical methods," *Desalination*, vol. 258, no. 1–3, pp. 201–205, 2010.

[10] H. Farajnezhad and P. Gharbani, "Coagulation treatment of wastewater in petroleum industry using poly aluminum chloride and ferric chloride," *International Journal of Research and Reviews in Applied Sciences*, vol. 13, no. 1, pp. 306–310, 2012.

[11] L. Altaş and H. Büyükgüngör, "Sulfide removal in petroleum refinery wastewater by chemical precipitation," *Journal of Hazardous Materials*, vol. 153, no. 1-2, pp. 462–469, 2008.

[12] C. E. Santo, V. J. P. Vilar, C. M. S. Botelho, A. Bhatnagar, E. Kumar, and R. A. R. Boaventura, "Optimization of coagulation-flocculation and flotation parameters for the treatment of a petroleum refinery effluent from a Portuguese plant," *Chemical Engineering Journal*, vol. 183, pp. 117–123, 2012.

[13] M. H. El-Naas, S. Al-Zuhair, A. Al-Lobaney, and S. Makhlouf, "Assessment of electrocoagulation for the treatment of petroleum refinery wastewater," *Journal of Environmental Management*, vol. 91, no. 1, pp. 180–185, 2009.

[14] C.-L. Yang, "Electrochemical coagulation for oily water demulsification," *Separation and Purification Technology*, vol. 54, no. 3, pp. 388–395, 2007.

[15] M. A. Zazouli, M. Taghavi, and E. Bazrafshan, "Influences of solution chemistry on phenol removal from aqueous environments by electrocoagulation process using aluminium electrodes," *Journal of Health Scope*, vol. 1, no. 2, pp. 66–70, 2012.

[16] O. Abdelwahab, N. K. Amin, and E.-S. Z. El-Ashtoukhy, "Electrochemical removal of phenol from oil refinery wastewater," *Journal of Hazardous Materials*, vol. 163, no. 2-3, pp. 711–716, 2009.

[17] A. Dimoglo, H. Y. Akbulut, F. Cihan, and M. Karpuzcu, "Petrochemical wastewater treatment by means of clean electrochemical technologies," *Clean Technologies and Environmental Policy*, vol. 6, no. 4, pp. 288–295, 2004.

[18] M. H. El-Naas, M. A. Alhaija, and S. Al-Zuhair, "Evaluation of a three-step process for the treatment of petroleum refinery wastewater," *Journal of Environmental Chemical Engineering*, vol. 2, no. 1, pp. 56–62, 2014.

[19] A. Coelho, A. V. Castro, M. Dezotti, and G. L. Sant'Anna Jr., "Treatment of petroleum refinery sourwater by advanced oxidation processes," *Journal of Hazardous Materials*, vol. 137, no. 1, pp. 178–184, 2006.

[20] G. Salas and N. Ale, "Treatment of wastewaters from a pretroleum refinery through advanced oxidation (AOX), using reactive Fenton (H_2O_2/Fe^{2+})," *Peruvian Magazine of Chemistry and Chemical Engineering*, vol. 11, no. 2, pp. 12–18, 2008.

[21] S. Sayid, M. Abu, Z. Noor, S. Noor, and A. Aris, "Fenton and photo-fenton oxidation of sulfidic spent caustic: a comparative study based on statistical analysis," *Environmental Engineering and Management Journal*, vol. 13, no. 3, pp. 531–538, 2014.

[22] C. Comninellis, "Electrocatalysis in the electrochemical conversion/combustion of organic pollutants for waste water treatment," *Electrochimica Acta*, vol. 39, no. 11-12, pp. 1857–1862, 1994.

[23] V. S. de Sucre and A. P. Watkinson, "Anodic oxidation of phenol for waste water treatment," *The Canadian Journal of Chemical Engineering*, vol. 59, no. 1, pp. 52–59, 1981.

[24] B. Fleszar and J. Poszyńska, "An attempt to define benzene and phenol electrochemical oxidation mechanism," *Electrochimica Acta*, vol. 30, no. 1, pp. 31–42, 1985.

[25] H. Sharifian and D. W. Kirk, "Electrochemical oxidation of phenol," *Journal of the Electrochemical Society*, vol. 113, no. 5, pp. 921–924, 1986.

[26] I. F. McConvey, K. Scott, J. M. Henderson, and A. N. Haines, "Electrochemical reaction with parallel reversible surface adsorption: interpretations of the kinetics of anodic oxidation of aniline and phenol to carbon dioxide," *Chemical Engineering and Processing: Process Intensification*, vol. 22, no. 4, pp. 231–235, 1987.

[27] D.-T. Chin, N. R. K. Vilambi, and C. Y. Cheng, "Oxidation of phenol to benzoquinone in a CSTER with modulated alternating voltage," *Journal of Applied Electrochemistry*, vol. 19, no. 3, pp. 459–461, 1989.

[28] C. Comninellis and C. Pulgarin, "Anodic oxidation of phenol for waste water treatment," *Journal of Applied Electrochemistry*, vol. 21, no. 8, pp. 703–708, 1991.

[29] R. Kötz, S. Stucki, and B. Carcer, "Electrochemical waste water treatment using high overvoltage anodes. Part I: physical and electrochemical properties of SnO_2 anodes," *Journal of Applied Electrochemistry*, vol. 21, no. 1, pp. 14–20, 1991.

[30] S. Stucki, R. Kötz, B. Carcer, and W. Suter, "Electrochemical waste water treatment using high overvoltage anodes. Part II: anode performance and applications," *Journal of Applied Electrochemistry*, vol. 21, no. 2, pp. 99–104, 1991.

[31] O. J. Murphy, G. D. Hitchens, L. Kaba, and C. E. Verostko, "Direct electrochemical oxidation of organics for wastewater treatment," *Water Research*, vol. 26, no. 4, pp. 443–451, 1992.

[32] C. Comninellis and C. Pulgarin, "Electrochemical oxidation of phenol for wastewater treatment using SnO_2, anodes," *Journal of Applied Electrochemistry*, vol. 23, no. 2, pp. 108–112, 1993.

[33] K. T. Kawagoe and D. C. Johnson, "Electrocatalysis of anodic oxygen-transfer reactions. Oxidation of phenol and benzene at bismuth-doped lead dioxide electrodes in acidic solutions," *Journal of the Electrochemical Society*, vol. 141, no. 12, pp. 3404–3409, 1994.

[34] C. Comninellis and A. Nerini, "Anodic oxidation of phenol in the presence of NaCl for wastewater treatment," *Journal of Applied Electrochemistry*, vol. 25, no. 1, pp. 23–28, 1995.

[35] N. B. Tahar and A. Savall, "Mechanistic aspects of phenol electrochemical degradation by oxidation on a Ta/PbO_2 anode," *Journal of the Electrochemical Society*, vol. 145, no. 10, pp. 3427–3434, 1998.

[36] U. Schümann and P. Gründler, "Electrochemical degradation of organic substances at PbO_2 anodes: monitoring by continuous

CO_2 measurements," *Water Research*, vol. 32, no. 9, pp. 2835–2842, 1998.

[37] N. B. Tahar and A. Savall, "Electrochemical degradation of phenol in aqueous solution on bismuth doped lead dioxide: a comparison of the activities of various electrode formulations," *Journal of Applied Electrochemistry*, vol. 29, no. 3, pp. 277–283, 1999.

[38] P. Cañizares, J. A. Domínguez, M. A. Rodrigo, J. Villaseñor, and J. Rodríguez, "Effect of the current intensity in the electrochemical oxidation of aqueous phenol wastes at an activated carbon and steel anode," *Industrial & Engineering Chemistry Research*, vol. 38, no. 10, pp. 3779–3785, 1999.

[39] J. Iniesta, J. González-García, E. Expósito, V. Montiel, and A. Aldaz, "Influence of chloride ion on electrochemical degradation of phenol in alkaline medium using bismuth doped and pure PbO_2 anodes," *Water Research*, vol. 35, no. 14, pp. 3291–3300, 2001.

[40] G. A. Bogdanovskii, T. V. Savel'eva, and T. S. Saburova, "Phenol conversions during electrochemical generation of active chlorine," *Russian Journal of Electrochemistry*, vol. 37, no. 8, pp. 865–869, 2001.

[41] Z. Wu and M. Zhou, "Partial degradation of phenol by advanced electrochemical oxidation process," *Environmental Science and Technology*, vol. 35, no. 13, pp. 2698–2703, 2001.

[42] M. H. Zhou, Z. C. Wu, and D. H. Wang, "A novel electrocatalysis method for organic pollutants degradation," *Chinese Chemical Letters*, vol. 12, no. 10, pp. 929–932, 2001.

[43] R. T. Pelegrini, R. S. Freire, N. Duran, and R. Bertazzoli, "Photoassisted electrochemical degradation of organic pollutants on a DSA type oxide electrode: process test for a phenol synthetic solution and its application for the E1 bleach Kraft mill effluent," *Environmental Science and Technology*, vol. 35, no. 13, pp. 2849–2853, 2001.

[44] M.-H. Zhou, Z.-C. Wu, and X.-D. Xuan, "Anodic-cathodic electrocatalytic degradation of phenol with oxygen sparged in the presence of iron (II)," *Chemical Research in Chinese Universities*, vol. 18, no. 3, pp. 262–266, 2002.

[45] R. L. Pelegrino, R. A. Di Iglia, C. G. Sanches, L. A. Avaca, and R. Bertazzoli, "Comparative study of commercial oxide electrodes performance in electrochemical degradation of organics in aqueous solutions," *Journal of the Brazilian Chemical Society*, vol. 13, no. 1, pp. 60–65, 2002.

[46] Y. J. Feng and X. Y. Li, "Electro-catalytic oxidation of phenol on several metal-oxide electrodes in aqueous solution," *Water Research*, vol. 37, no. 10, pp. 2399–2407, 2003.

[47] P. D. P. Alves, M. Spagnol, G. Tremiliosi-Filho, and A. R. de Andrade, "Investigation of the influence of the anode composition of DSA-type electrodes on the electrocatalytic oxidation of phenol in neutral medium," *Journal of the Brazilian Chemical Society*, vol. 15, no. 5, pp. 626–634, 2004.

[48] P. Cañizares, J. García-Gómez, J. Lobato, and M. A. Rodrigo, "Modeling of wastewater electro-oxidation processes part I. General description and application to inactive electrodes," *Industrial & Engineering Chemistry Research*, vol. 43, no. 9, pp. 1915–1922, 2004.

[49] P. Cañizares, J. García-Gómez, J. Lobato, and M. A. Rodrigo, "Modeling of wastewater electro-oxidation processes part II. Application to active electrodes," *Industrial & Engineering Chemistry Research*, vol. 43, no. 9, pp. 1923–1931, 2004.

[50] D. Fino, C. C. Jara, G. Saracco, V. Specchia, and P. Spinelli, "Deactivation and regeneration of Pt anodes for the electrooxidation of phenol," *Journal of Applied Electrochemistry*, vol. 35, no. 4, pp. 405–411, 2005.

[51] X.-Y. Li, Y.-H. Cui, Y.-J. Feng, Z.-M. Xie, and J.-D. Gu, "Reaction pathways and mechanisms of the electrochemical degradation of phenol on different electrodes," *Water Research*, vol. 39, no. 10, pp. 1972–1981, 2005.

[52] M. Li, C. Feng, W. Hu, Z. Zhang, and N. Sugiura, "Electrochemical degradation of phenol using electrodes of Ti/RuO_2-Pt and Ti/IrO_2-Pt," *Journal of Hazardous Materials*, vol. 162, no. 1, pp. 455–462, 2009.

[53] E. Chatzisymeon, S. Ferro, I. Karafyllis, D. Mantzavinos, N. Kalogerakis, and A. Katsaounis, "Anodic oxidation of phenol on Ti/IrO_2 electrode: experimental studies," *Catalysis Today*, vol. 151, no. 1-2, pp. 185–189, 2010.

[54] Y. Yavuz and A. S. Koparal, "Electrochemical oxidation of phenol in a parallel plate reactor using ruthenium mixed metal oxide electrode," *Journal of Hazardous Materials*, vol. 136, no. 2, pp. 296–302, 2006.

[55] A. M. Z. Ramalho, C. A. Martínez-Huitle, and D. R. D. Silva, "Application of electrochemical technology for removing petroleum hydrocarbons from produced water using a DSA-type anode at different flow rates," *Fuel*, vol. 89, no. 2, pp. 531–534, 2010.

[56] M. R. G. Santos, M. O. F. Goulart, J. Tonholo, and C. L. P. S. Zanta, "The application of electrochemical technology to the remediation of oily wastewater," *Chemosphere*, vol. 64, no. 3, pp. 393–399, 2006.

[57] F. Montilla, E. Morallón, and J. L. Vázquez, "Evaluation of the electrocatalytic activity of antimony-doped tin dioxide anodes toward the oxidation of phenol in aqueous solutions," *Journal of the Electrochemical Society*, vol. 152, no. 10, pp. B421–B427, 2005.

[58] Z.-C. Wu, M.-H. Zhou, Z.-W. Huang, and D.-H. Wang, "Electrocatalysis method for wastewater treatment using a novel beta-lead dioxide anode," *Journal of Zhejinag University Science*, vol. 3, no. 2, pp. 194–198, 2002.

[59] M. Zhou, Q. Dai, L. Lei, C. Ma, and D. Wang, "Long life modified lead dioxide anode for organic wastewater treatment: electrochemical characteristics and degradation mechanism," *Environmental Science and Technology*, vol. 39, no. 1, pp. 363–370, 2005.

[60] P.-A. Michaud, M. Panizza, L. Ouattara, T. Diaco, G. Foti, and C. Comninellis, "Electrochemical oxidation of water on synthetic boron-doped diamond thin film anodes," *Journal of Applied Electrochemistry*, vol. 33, no. 2, pp. 151–154, 2003.

[61] A. Kraft, M. Stadelmann, and M. Blaschke, "Anodic oxidation with doped diamond electrodes: a new advanced oxidation process," *Journal of Hazardous Materials*, vol. 103, no. 3, pp. 247–261, 2003.

[62] B. Marselli, J. García-Gómez, P.-A. Michaud, M. A. Rodrigo, and C. Comninellis, "Electrogeneration of hydroxyl radicals on boron-doped diamond electrodes," *Journal of the Electrochemical Society*, vol. 150, no. 3, pp. D79–D83, 2003.

[63] J. Iniesta, P. A. Michaud, M. Panizza, G. Cerisola, A. Aldaz, and C. Comninellis, "Electrochemical oxidation of phenol at boron-doped diamond electrode," *Electrochimica Acta*, vol. 46, no. 23, pp. 3573–3578, 2001.

[64] M. Panizza, P. A. Michaud, G. Cerisola, and C. Comninellis, "Electrochemical treatment of wastewaters containing organic pollutants on boron-doped diamond electrodes: prediction

of specific energy consumption and required electrode area," *Electrochemistry Communications*, vol. 3, no. 7, pp. 336–339, 2001.

[65] P. L. Hagans, P. M. Natishan, B. R. Stoner, and W. E. O'Grady, "Electrochemical oxidation of phenol using boron-doped diamond electrodes," *Journal of the Electrochemical Society*, vol. 148, no. 7, pp. E298–E301, 2001.

[66] P. Cañizares, M. Díaz, J. A. Domínguez, J. García-Gómez, and M. A. Rodrigo, "Electrochemical oxidation of aqueous phenol wastes on synthetic diamond thin-film electrodes," *Industrial & Engineering Chemistry Research*, vol. 41, no. 17, pp. 4187–4194, 2002.

[67] A. V. Diniz, N. G. Ferreira, E. J. Corat, and V. J. Trava-Airoldi, "Efficiency study of perforated diamond electrodes for organic compounds oxidation process," *Diamond and Related Materials*, vol. 12, no. 3–7, pp. 577–582, 2003.

[68] J.-F. Zhi, H.-B. Wang, T. Nakashima, T. N. Rao, and A. Fujishima, "Electrochemical incineration of organic pollutants on boron-doped diamond electrode, evidence for direct electrochemical oxidation pathway," *The Journal of Physical Chemistry B*, vol. 107, no. 48, pp. 13389–13395, 2003.

[69] A. M. Polcaro, A. Vacca, S. Palmas, and M. Mascia, "Electrochemical treatment of wastewater containing phenolic compounds: oxidation at boron-doped diamond electrodes," *Journal of Applied Electrochemistry*, vol. 33, no. 10, pp. 885–892, 2003.

[70] P. Cañizares, J. García-Gómez, C. Sáez, and M. A. Rodrigo, "Electrochemical oxidation of several chlorophenols on diamond electrodes. Part I. Reaction mechanism," *Journal of Applied Electrochemistry*, vol. 33, no. 10, pp. 917–927, 2003.

[71] P. Cañizares, J. García-Gómez, J. Lobato, and M. A. Rodrigo, "Electrochemical oxidation of aqueous carboxylic acid wastes using diamond thin-film electrodes," *Industrial & Engineering Chemistry Research*, vol. 42, no. 5, pp. 956–962, 2003.

[72] A. Morão, A. Lopes, M. T. P. de Amorim, and I. C. Gonçalves, "Degradation of mixtures of phenols using boron doped diamond electrodes for wastewater treatment," *Electrochimica Acta*, vol. 49, no. 9-10, pp. 1587–1595, 2004.

[73] P. Cañizares, C. Sáez, J. Lobato, and M. A. Rodrigo, "Electrochemical oxidation of polyhydroxybenzenes on boron-doped diamond anodes," *Industrial & Engineering Chemistry Research*, vol. 43, no. 21, pp. 6629–6637, 2004.

[74] P. Cañizares, J. Lobato, R. Paz, M. A. Rodrigo, and C. Sáez, "Electrochemical oxidation of phenolic wastes with boron-doped diamond anodes," *Water Research*, vol. 39, no. 12, pp. 2687–2703, 2005.

[75] C. Flox, J. A. Garrido, R. M. Rodríguez et al., "Degradation of 4,6-dinitro-*o*-cresol from water by anodic oxidation with a boron-doped diamond electrode," *Electrochimica Acta*, vol. 50, no. 18, pp. 3685–3692, 2005.

[76] M. J. Pacheco, A. Morão, A. Lopes, L. Ciríaco, and I. Gonçalves, "Degradation of phenols using boron-doped diamond electrodes: a method for quantifying the extent of combustion," *Electrochimica Acta*, vol. 53, no. 2, pp. 629–636, 2007.

[77] M. Mascia, A. Vacca, S. Palmas, and A. M. Polcaro, "Kinetics of the electrochemical oxidation of organic compounds at BDD anodes: modelling of surface reactions," *Journal of Applied Electrochemistry*, vol. 37, no. 1, pp. 71–76, 2007.

[78] X. Zhu, S. Shi, J. Wei et al., "Electrochemical oxidation characteristics of *p*-substituted phenols using a boron-doped diamond electrode," *Environmental Science and Technology*, vol. 41, no. 18, pp. 6541–6546, 2007.

[79] C. Flox, P.-L. Cabot, F. Centellas et al., "Solar photoelectro-Fenton degradation of cresols using a flow reactor with a boron-doped diamond anode," *Applied Catalysis B: Environmental*, vol. 75, no. 1-2, pp. 17–28, 2007.

[80] M. Mascia, A. Vacca, A. M. Polcaro, S. Palmas, J. R. Ruiz, and A. da Pozzo, "Electrochemical treatment of phenolic waters in presence of chloride with boron-doped diamond (BDD) anodes: experimental study and mathematical model," *Journal of Hazardous Materials*, vol. 174, no. 1–3, pp. 314–322, 2010.

[81] X. Zhu, J. Ni, H. Li, Y. Jiang, X. Xing, and A. G. L. Borthwick, "Effects of ultrasound on electrochemical oxidation mechanisms of *p*-substituted phenols at BDD and PbO_2 anodes," *Electrochimica Acta*, vol. 55, no. 20, pp. 5569–5575, 2010.

[82] X. Zhu, J. Ni, J. Wei, X. Xing, H. Li, and Y. Jiang, "Scale-up of BDD anode system for electrochemical oxidation of phenol simulated wastewater in continuous mode," *Journal of Hazardous Materials*, vol. 184, no. 1–3, pp. 493–498, 2010.

[83] J. Wei, X. Zhu, and J. Ni, "Electrochemical oxidation of phenol at boron-doped diamond electrode in pulse current mode," *Electrochimica Acta*, vol. 56, no. 15, pp. 5310–5315, 2011.

[84] J. Sun, H. Lu, H. Lin et al., "Electrochemical oxidation of aqueous phenol at low concentration using Ti/BDD electrode," *Separation and Purification Technology*, vol. 88, pp. 116–120, 2012.

[85] J. Lv, Y. Feng, J. Liu, Y. Qu, and F. Cui, "Comparison of electrocatalytic characterization of boron-doped diamond and SnO_2 electrodes," *Applied Surface Science*, vol. 283, pp. 900–905, 2013.

[86] G. Hurwitz, P. Pornwongthong, S. Mahendra, and E. M. V. Hoek, "Degradation of phenol by synergistic chlorine-enhanced photo-assisted electrochemical oxidation," *Chemical Engineering Journal*, vol. 240, pp. 235–243, 2014.

[87] X. Chen, G. Chen, F. Gao, and P. L. Yue, "High-performance Ti/BDD electrodes for pollutant oxidation," *Environmental Science and Technology*, vol. 37, no. 21, pp. 5021–5026, 2003.

[88] X. Chen, F. Gao, and G. Chen, "Comparison of Ti/BDD and Ti/SnO_2-Sb_2O_5 electrodes for pollutant oxidation," *Journal of Applied Electrochemistry*, vol. 35, no. 2, pp. 185–191, 2005.

[89] E. Weiss, K. Groenen-Serrano, and A. Savall, "A comparison of electrochemical degradation of phenol on boron doped diamond and lead dioxide anodes," *Journal of Applied Electrochemistry*, vol. 38, no. 3, pp. 329–337, 2008.

[90] A. Medel, E. Bustos, K. Esquivel, L. A. Godínez, and Y. Meas, "Electrochemical incineration of phenolic compounds from the hydrocarbon industry using boron-doped diamond electrodes," *International Journal of Photoenergy*, vol. 2012, Article ID 681875, 6 pages, 2012.

[91] J. H. Bezerra, M. M. Soares, N. Suely, D. Riveiro, and C. A. Martínez-Huitle, "Application of electrochemical oxidation as alternative treatment of produced water generated by Brazilian petrochemical industry," *Fuel*, vol. 96, pp. 80–87, 2012.

[92] A. J. C. da Silva, E. V. dos Santos, C. C. D. O. Morais, C. A. Martínez-Huitle, and S. S. L. Castro, "Electrochemical treatment of fresh, brine and saline produced water generated by petrochemical industry using Ti/IrO_2-Ta_2O_5 and BDD in flow reactor," *Chemical Engineering Journal*, vol. 233, pp. 47–55, 2013.

[93] R. B. A. Souza and L. A. M. Ruotolo, "Electrochemical treatment of oil refinery effluent using boron-doped diamond anodes," *Journal of Environmental Chemical Engineering*, vol. 1, no. 3, pp. 544–551, 2013.

[94] A. Medel, E. Bustos, L. M. Apátiga, and Y. Meas, "Surface activation of C-sp^3 in Boron-Doped diamond electrode," *Electrocatalysis*, vol. 4, no. 4, pp. 189–195, 2013.

[95] Mexican Regulation NMX-AA-050-SCFI-2001, "Analysis of water-determination of total phenols in natural, potable, residual and treated residual waters," 2001.

[96] A. Fakhru'l-Razi, A. Pendashteh, L. C. Abdullah, D. R. A. Biak, S. S. Madaeni, and Z. Z. Abidin, "Review of technologies for oil and gas produced water treatment," *Journal of Hazardous Materials*, vol. 170, no. 2-3, pp. 530–551, 2009.

[97] L. Wei, S. Guo, G. Yan, C. Chen, and X. Jiang, "Electrochemical pretreatment of heavy oil refinery wastewater using a three-dimensional electrode reactor," *Electrochimica Acta*, vol. 55, no. 28, pp. 8615–8620, 2010.

[98] E. V. dos Santos, S. F. M. Sena, D. R. da Silva, S. Ferro, A. de Battisti, and C. A. Martínez-Huitle, "Scale-up of electrochemical oxidation system for treatment of produced water generated by Brazilian petrochemical industry," *Environmental Science and Pollution Research*, vol. 21, pp. 8466–8475, 2014.

[99] M. Murugananthan, S. S. Latha, G. B. Raju, and S. Yoshihara, "Role of electrolyte on anodic mineralization of atenolol at boron doped diamond and Pt electrodes," *Separation and Purification Technology*, vol. 79, no. 1, pp. 56–62, 2011.

[100] A. Sánchez-Carretero, C. Sáez, P. Cañizares, and M. A. Rodrigo, "Electrochemical production of perchlorates using conductive diamond electrolyses," *Chemical Engineering Journal*, vol. 166, no. 2, pp. 710–714, 2011.

[101] Official Mexican Regulation NOM-001-SEMARNAT-1996, "Maximum limits allowed of pollutants in discharges of wastewaters and national resources," 1996.

[102] B. F. Giannetti, W. A. Moreira, S. H. Bonilla, C. M. V. B. Almeida, and T. Rabóczkay, "Towards the abatement of environmental mercury pollution: an electrochemical characterization," *Colloids and Surfaces A: Physicochemical and Engineering Aspects*, vol. 276, no. 1–3, pp. 213–220, 2006.

[103] U. Skyllberg, P. R. Bloom, J. Qian, C.-M. Lin, and W. F. Bleam, "Complexation of mercury(II) in soil organic matter: EXAFS evidence for linear two-coordination with reduced sulfur groups," *Environmental Science and Technology*, vol. 40, no. 13, pp. 4174–4180, 2006.

[104] D. T. Cestarolli and A. R. de Andrade, "Electrochemical oxidation of phenol at Ti/$Ru_{0.3}Pb_{(0.7-x)}Ti_xO_y$ electrodes in aqueous media," *Journal of the Electrochemical Society*, vol. 154, no. 2, pp. E25–E30, 2007.

[105] S. Balaji, S. J. Chung, R. Thiruvenkatachari, and I. S. Moon, "Mediated electrochemical oxidation process: electro-oxidation of cerium(III) to cerium(IV) in nitric acid medium and a study on phenol degradation by cerium(IV) oxidant," *Chemical Engineering Journal*, vol. 126, no. 1, pp. 51–57, 2007.

[106] D. Reyter, D. Bélanger, and L. Roué, "Nitrate removal by a paired electrolysis on copper and Ti/IrO_2 coupled electrodes—influence of the anode/cathode surface area ratio," *Water Research*, vol. 44, no. 6, pp. 1918–1926, 2010.

[107] B. H. Diya'Uddeen, W. M. A. W. Daud, and A. R. Abdul Aziz, "Treatment technologies for petroleum refinery effluents: a review," *Process Safety and Environmental Protection*, vol. 89, no. 2, pp. 95–105, 2011.

Hindawi Publishing Corporation
International Journal of Photoenergy
Volume 2015, Article ID 716853, 8 pages
http://dx.doi.org/10.1155/2015/716853

Research Article

Determination of Biological Treatability Processes of Textile Wastewater and Implementation of a Fuzzy Logic Model

Harun Akif Kabuk, Yasar Avsar, S. Levent Kuzu, Fatih Ilhan, and Kubra Ulucan

Environmental Engineering Department, Yildiz Technical University, Davutpasa Campus, Esenler, 34220 Istanbul, Turkey

Correspondence should be addressed to Yasar Avsar; yavsar@gmail.com

Received 9 September 2014; Accepted 7 December 2014

Academic Editor: Meenakshisundaram Swaminathan

This study investigated the biological treatability of textile wastewater. For this purpose, a membrane bioreactor (MBR) was utilized for biological treatment after the ozonation process. Due to the refractory organic contents of textile wastewater that has a low biodegradability capacity, ozonation was implemented as an advanced oxidation process prior to the MBR system to increase the biodegradability of the wastewater. Textile wastewater, oxidized by ozonation, was fed to the MBR at different hydraulic retention times (HRT). During the process, color, chemical oxygen demand (COD), and biochemical oxygen demand (BOD) removal efficiencies were monitored for 24-hour, 12-hour, 6-hour, and 3-hour retention times. Under these conditions, 94% color, 65% COD, and 55% BOD removal efficiencies were obtained in the MBR system. The experimental outputs were modeled with multiple linear regressions (MLR) and fuzzy logic. MLR results suggested that color removal is more related to COD removal relative to BOD removal. A surface map of this issue was prepared with a fuzzy logic model. Furthermore, fuzzy logic was employed to the whole modeling of the biological system treatment. Determination coefficients for COD, BOD, and color removal efficiencies were 0.96, 0.97, and 0.92, respectively.

1. Introduction

Due to their highly colored substance ingredient and hardly treatable characteristic, treatment studies on textile wastewater remain at the top of densely studied topics. As is known, textile wastewater has nonbiodegradable characteristics [1–3]. In general, textile wastewater is treated by chemical treatment techniques which are expensive and need many chemical applications [4, 5].

Due to the fact that textile industry effluents have a wide variety of pollutant parameters, diverse treatment techniques are required. Frequently used treatment processes, considered to be conventional chemical treatment methods, are used to remove COD and color. Alternatively, some of the oxidants presented in Table 1 are thought to be advanced oxidation process chemicals and are particularly used to increase biodegradability of textile wastewater that has high refractory organics. In particular, hydroxyl radicals occur as a result of using those kinds of oxidants and decompose the structure of refractory or resistive organics [6–8].

The ozonation of some industrial wastewaters increases their biological degradability [9, 10]. Ozone is a very effective substance, especially in color removal [11–14]. The observed COD removal efficiency of ozonation is not as high as color removal efficiencies. In some cases, such as industrial wastewaters having low BOD/COD rates, ozonation is used prior to biological treatment. Simple color removal can be achieved easily at low ozone doses and low operating costs [15]. In the literature, for different pH values, ozone doses, and durations, COD and color removal ranges vary between 37 and 60% and between 87 and 99%, respectively [16–21]. In particular, the effective elimination of toxic substances in textile effluents was observed with ozonation [22, 23].

Natural organic matter can affect the ozone stability in two ways: it can either directly react with ozone ((1) and (2)) or indirectly affect its stability through scavenging of OH radicals ((3) and (6)) [24]:

$$O_3 + NOM_1 \longrightarrow NOM_{1ox} \quad (1)$$

$$O_3 + OM_2 \longrightarrow NOM_2{}^{+\bullet} + O_3{}^{\bullet-} \quad (2)$$

Table 1: Oxidizing potential for conventional oxidizing agents [40].

Oxidizing agent	Electrochemical oxidation potential, volt
Fluorine	3.06
Hydroxyl radical	2.80
Ozone	2.08
Hydrogen peroxide	1.78
Hypochlorite	1.49
Chlorine	1.36
Chlorine dioxide	1.27

$$^{\bullet}OH + NOM_3 \longrightarrow NOM_3^{\bullet} + H_2O \quad \text{or} \quad NOM_3^{\bullet} + OH^- \tag{3}$$

$$NOM_3^{\bullet} + O_2 \longrightarrow NOM - O_2^{\bullet} \longrightarrow NOM_3^{+} + O_2^{\bullet -} \tag{4}$$

$$^{\bullet}OH + NOM_4 \longrightarrow NOM_4^{\bullet} + H_2O \tag{5}$$

$$NOM_4^{\bullet} + O_2 \longrightarrow NOM_4 + O_2^{\bullet} \longrightarrow \text{no } O_2^{\bullet -} \text{ formation} \tag{6}$$

One of the advanced treatment processes applied to domestic or industrial wastewater is membrane bioreactors (MBR) to obtain highly purified water or reuse [25, 26]. In recent years, the use of MBR systems and their implementation have increased rapidly. MBR systems are defined as biological and physical treatment process such as oxidation and separation of wastewater between biomass and water by membrane equipment [27]. These biological treatments and separation systems are applied either in two parts, aeration and sedimentation tanks in conventional activated sludge process, or in the same tank [28, 29]. In the MBR process, separation occurs by microfiltration (0.2 μm pore size) or ultrafiltration membrane (0.01 μm pore size) systems. In the course of the treatment time period, a biofilm bulk occurs on the surface of the membranes and occludes the pores of the membranes, thus leading to higher removal efficiencies, in other words, acquiring cleaner water [30–32].

The obtained experimental data set was subjected to artificial intelligence-based modeling. The three influent values (COD, BOD, and color) were utilized to predict the same effluent parameter concentrations. Fuzzy logic, developed by Zadeh, has some advantages over mathematical models where complicated equations are used [33]. Artificial intelligence-based tools are a suitable substitute to conventional methods such as curve fitting due to their speed, robustness, and nonlinear characteristics [34]. Due to its high precision ability and flexibility in use, fuzzy logic has been applied in many of the environmental engineering problems from air pollution to water treatment systems. Research in [35–37] stated that fuzzy logic is one of the methods to apply the expert knowledge to form an advanced control on various treatment processes.

In this study, a two-stage process was developed: an ozonation process followed by an aerobic membrane bioreactor (MBR) to provide the standard Turkish Water Pollution Control Regulations (SKKY) effluent discharge limits in a lab scale. The biodegradation, COD, and color removal performances of this combined system were studied using textile wastewater effluents. At present, the chemical addition processes alone cannot provide SKKY discharge criteria. In contrast to these methods, this two-stage process can meet the SKKY discharge standards. Therefore, this process is eligible as an alternative treatment process.

The main aim of this study is to display the biological treatability of the textile wastewater having low biodegradability and investigate its treatability by an MBR system. To prepare biological degradable wastewater prior to exposure to the MBR system, ozonation was applied to the wastewater. Implementation of the ozonation processes before MBR provides the advantage of acquiring better removal results. Without ozonation, textile wastewater cannot be treated by MBR effectively according to color, BOD, and COD parameters. The experimental results were also applied to the fuzzy logic system. With a short preliminary system demonstration implementation, it is possible to make effluent concentration predictions utilizing influent values with the fuzzy logic model. In addition, the fuzzy logic modeling of this study has the distinction of being first in MBR after biodegradation by ozonation.

2. Material and Methods

2.1. Experimental. The samples used in this study were gathered from the effluents of a wool textile plant. The characteristics of wastewater are shown in Table 2.

All of the experimental analyses, especially the initial pollution characteristics of the samples, were analyzed at Yildiz Technical University Environmental Engineering Department laboratory in accordance with Standard Methods [38]. The COD and color were determined using a Hach-Lange DR 5800 brand mark spectrophotometer. The ozonation experiments were carried out for 3 L samples in a 5-L cylindrical glass reactor as a batch system. All experiments were performed at room temperature (24 ± 0.5°C). Not all of the produced ozone gas reacts with the wastewater. Some parts of the ozone escaped without reacting with the wastewater. Due to health and environmental concerns, the excess ozone was absorbed in gas washing bottles filled with 2% w/w potassium iodide (KI) solution to capture and determine the excess ozone concentration. The ozone concentration was measured by the iodometric method proposed by IOA [39]. According to the ozonation equipment, 32 mg ozone/L air was applied to the wastewater.

Ozone gas was produced by an AZCO VMUS-4 model ozone generator. The system was fed with dried oxygen and ozone was produced by the corona discharge generation process. This system consumes 100 W electrical energy. Ozone gas was supplied to the bottom of the reactor with an AQUA pipe diffuser system at 0.4-bar pressure. The main aim of the diffuser system is to obtain fine ozone gas bubbles to mix homogenously with water. All of the connection parts from the generator to the reactor were made of Teflon to resist the ozone's corrosive effect.

In an MBR system, a 4.5 cm diameter cylindrical ceramic ultrafiltration and a 12.5 cm height membrane were placed into a 12 cm diameter/20 cm height Plexiglas reactor.

Table 2: Textile wastewater characteristics and discharge limits according to SKKY (wool scouring, finishing, weaving, and equivalents).

Parameter	Unit	Raw wastewater	Effluent of ozone process	Effluent of ozone-MBR system	SKKY limits
COD	mg/L	1600	1140	380	400
Color	Pt-Co	590	120	10	260
BOD	mg/L	544	785	330	—

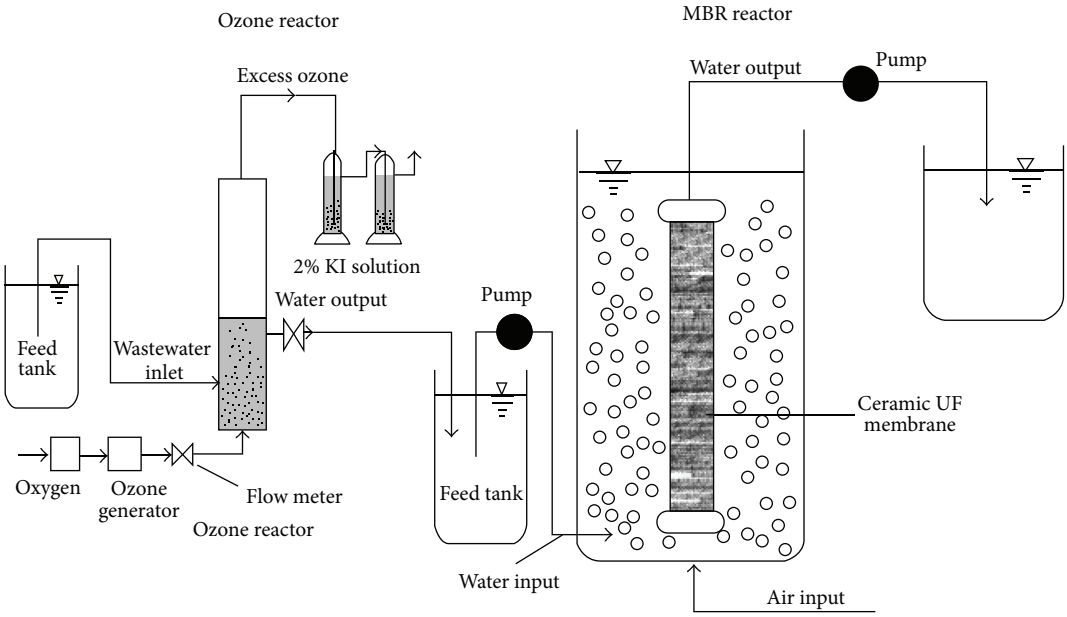

Figure 1: Schematic representation of the ozone and MBR system.

A Watson-Marlow 520S peristaltic pump was used to vacuum the wastewater. The schematic representation of the study is given in Figure 1.

3. Results and Discussions

In the first step of the study, the ozonation process was carried out to increase biodegradability of textile wastewater and to partially remove color. After the ozonation process, the BOD/COD value increased from 0.34 to 0.69, and 80% color removal was obtained. The ozonation process was studied at an initial pH 6.1 and 1-hour operation time.

The excess O_3 dose that was not used by the wastewater was determined by absorbing O_3 into a 2% KI solution, and results were as follows: applied O_3 dose, 640 mg; time, 20 min; O_3 dose, 64 mg/min; absorbed O_3 dose by KI, 45.6 ± 18.5 mg; absorbed O_3 dose by sample, 594.4 ± 18.5 mg; and O_3 concentration for 1 L sample, 198.1 ± 6.2 mg/L. Thus, the solubility of O_3 was only 198.1 mg/L at the optimal O_3 dose (32 mg/L) for a 3 L sample.

The focus of the study was MBR process and thus MBR application lasted for 81 days. Flux values during the experimental study period were examined daily. During an 81-day study period, no serious clogging problem occurred. During the experimental time period there was no need to clean the membrane parts. After 81 days, MBR application was terminated because the discharge standard of the Water Pollution Control Regulations (SKKY) [41] in Turkey for textile wastewater was achieved and is given in Table 2. While the flux value was 17.8 L/m^2-h at the beginning of the study, this parameter was determined as 8.9 L/m^2-h at the end of the 81-day time period. Figure 2 shows the flux variation obtained over time.

In the MBR system, removal efficiencies were investigated for different hydraulic retention times (HRT). According to the literature studies on textile wastewater that were examined, a 24-hour HRT was selected as the beginning [42, 43]. Then, this HRT value was decreased to 12 h, 6 h, and 3 h. Once the steady-state condition was reached for each HRT, the analyses were carried out. During the study, no sludge was removed from the reactor and therefore the MBR reactor was operated as endless sludge age.

Considering the whole study, the graphs of COD and BOD removal efficiencies are presented in Figures 3 and 4, respectively. When Figure 3 is investigated, three different curves can be seen. The breaking points indicated in Figure 3 show the changing HRT values. At the beginning of each breaking point, the COD removal rate decreased because of decreasing HRT values. Under the steady-state condition, COD removal efficiency increases over time. Ultimately, the COD removal efficiency was around 65% when the HRT of the study considered 3 h as the optimum time.

The organic loading rate (OLR) and, accordingly, the BOD removal efficiencies of the study are given in Figure 4.

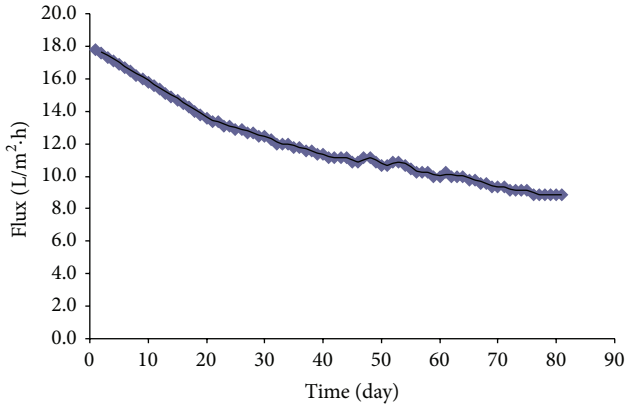

Figure 2: Flux variation obtained over time.

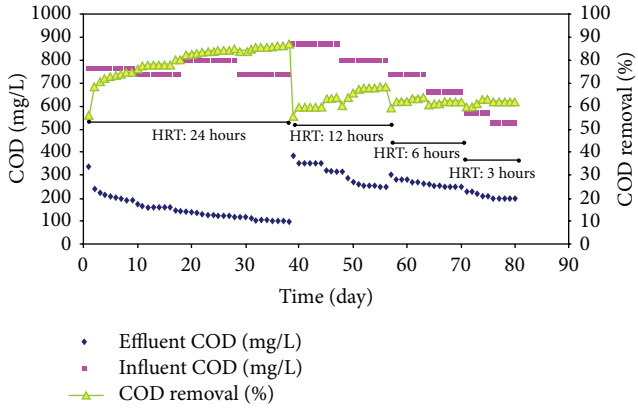

Figure 3: COD removal efficiency.

During the MBR system, various OLR values, ranging between 0.13 and 0.20 kg BOD/m^3 day, were worked. OLR values decreased with decreasing HRT values. BOD removal rates changed between 55% and 92%. BOD removal rates were high for high HRT and OLR values. The BOD removal rate decreased with decreasing HRT and OLR values. At the end of the study, BOD removal efficiency was around 55%.

3.1. Fuzzy Logic Modeling. Multiple-input and multiple-output fuzzy logic modeling was applied to the achieved experimental results. A fuzzy logic system consists of four essential components, which are fuzzification, fuzzy rule base, fuzzy inference engine, and defuzzification [44]. The interpretation of the dynamic behavior of the MBR system was accomplished by this four-step modeling algorithm. The fuzzy logic algorithm also provides a transparent relation between the rule bases and the results.

The discrete membership functions or a combination of them can be selected according to the nature of the problem to execute the modeling. Yetilmezsoy chose a combination of triangular and trapezoidal membership functions to predict Fenton's oxidation of anaerobically pretreated poultry manure wastewater [35]. Turkdogan-Aydinol and Yetilmezsoy stated that different types of membership functions such

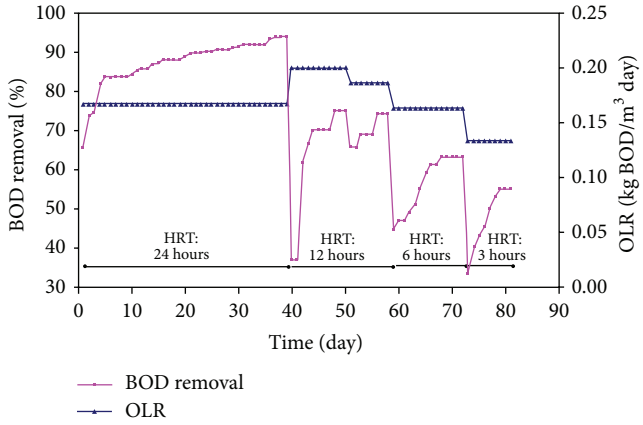

Figure 4: BOD removal efficiencies according to the different OLR values.

Table 3: The rules used during fuzzy logic process.

Input variables	Output variables
If COD is H and BOD is H and color is H	Then eCOD is L and eBOD is L and ecolor is L
If COD is M and BOD is MH and color is MH	Then eCOD is LM and eBOD is LM and ecolor is L
If COD is M and BOD is M and color is MH	Then eCOD is M and eBOD is M and ecolor is LM
If COD is LM and BOD is M and color is M	Then eCOD is MH and eBOD is MH and ecolor is M
If COD is LM and BOD is LM and color is LM	Then eCOD is MH and eBOD is MH and ecolor is MH
If COD is L and BOD is LM and color is LM	Then eCOD is H and eBOD is MH and ecolor is MH
If COD is L and BOD is LM and color is L	Then eCOD is H and eBOD is MH and ecolor is H
If COD is L and BOD is L and color is L	Then eCOD is H and eBOD is H and ecolor is H

as triangular, trapezoidal, bell-shaped, or other appropriate forms can be used for model prediction [45].

In this study, a combination of Gaussian and trapezoidal type membership functions was utilized to achieve the best fit with Mamdani's method by Matlab. Membership functions for both input and output variables are exhibited in Figure 5.

During the fuzzification of the input data sets, "minimum" operator produced better results than the "prod" operator. Thus, "min" operator was selected as the fuzzy inference operator. Aggregation was accomplished with the "maximum" operator. Defuzzification was completed with "centroid" operator.

Eight rules were formed to start model execution. These rules are shown in Table 3. Words with the capital letters of L, M, and H corresponded to low, medium, and high, respectively. The letter "e" was used to indicate effluent pollutant parameters. Input and output variables are connected to each other by an "if-then" expression.

As a consequence of the above selections, determination coefficients of 0.96, 0.97, and 0.92 were achieved for

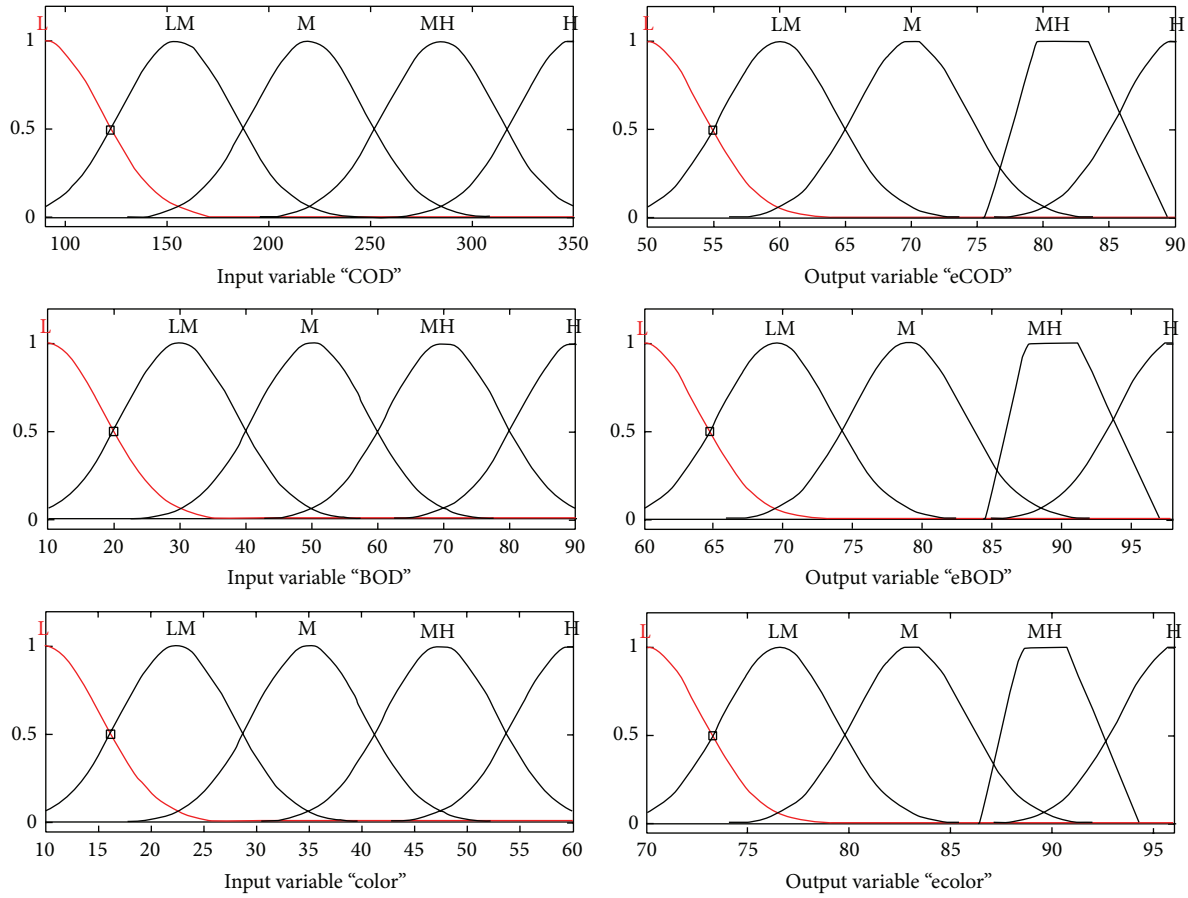

Figure 5: Membership functions.

COD, BOD, and color, respectively. Figure 6 shows the findings and statistical analysis results. COD, BOD, and color observed/predicted results are listed from top to bottom, respectively. On the left hand side of the figure, removal efficiencies are plotted as sample series. In the middle of the figure, observed values are plotted against predicted values to determine determination coefficients. On the right hand side of the figure, box-whisker plots are shown. The horizontal line inside the box refers to the median value, where the top and bottom of the box show 75% and 25%, respectively. The whiskers extending up and down show the maximum and minimum observed values, respectively.

COD removal rate and BOD removal rate are both effective on color removal efficiency. Multiple linear regression (MLR) was performed to determine the relative weight of COD and BOD removal rates on color removal. Based on 38 pieces of observation data, COD removal is the major factor inducing color removal ($P < 0.001$). However, BOD removal is not statistically significant ($P > 0.05$) in color removal. MLR predicted the coefficient of determination as 86%. This suggests that color forming compounds are hardly biodegradable. Thus, it can be inferred that a chemical preliminary treatment is essential before biological treatment.

A surface map of color removal rate according to influent COD and BOD concentrations was prepared by the fuzzy logic modeling results. The prepared map is illustrated in Figure 7.

It can be inferred from Figure 7 that the lower BOD and COD effluent concentrations, the higher color removal efficiencies. As one can expect, color removal rate decreased with the increasing COD and BOD concentrations. The lowest removal rate was observed when the highest BOD concentration and moderate COD concentration were present.

Constitution, strength, and volumetric flow rate of the raw wastewater fluctuate from time to time [37]. That is why modelling study becomes mandatory for optimum operation control. When the opening conditions deviate from the steady-state conditions, modelling results are going to yield the output parameters.

4. Conclusion

At the end of the study, the BOD/COD ratio of 0.34 was increased to 0.69 by ozonation as a pretreatment process of the wool textile wastewater. The results of the study were adequate for a 3-hour HRT in an MBR system. Under these conditions, 94% color, 65% COD, and 55% BOD removal efficiencies were obtained in the MBR system. COD, BOD, and color removal performances of the treatment system were modeled by fuzzy logic. The determination coefficient (R^2)

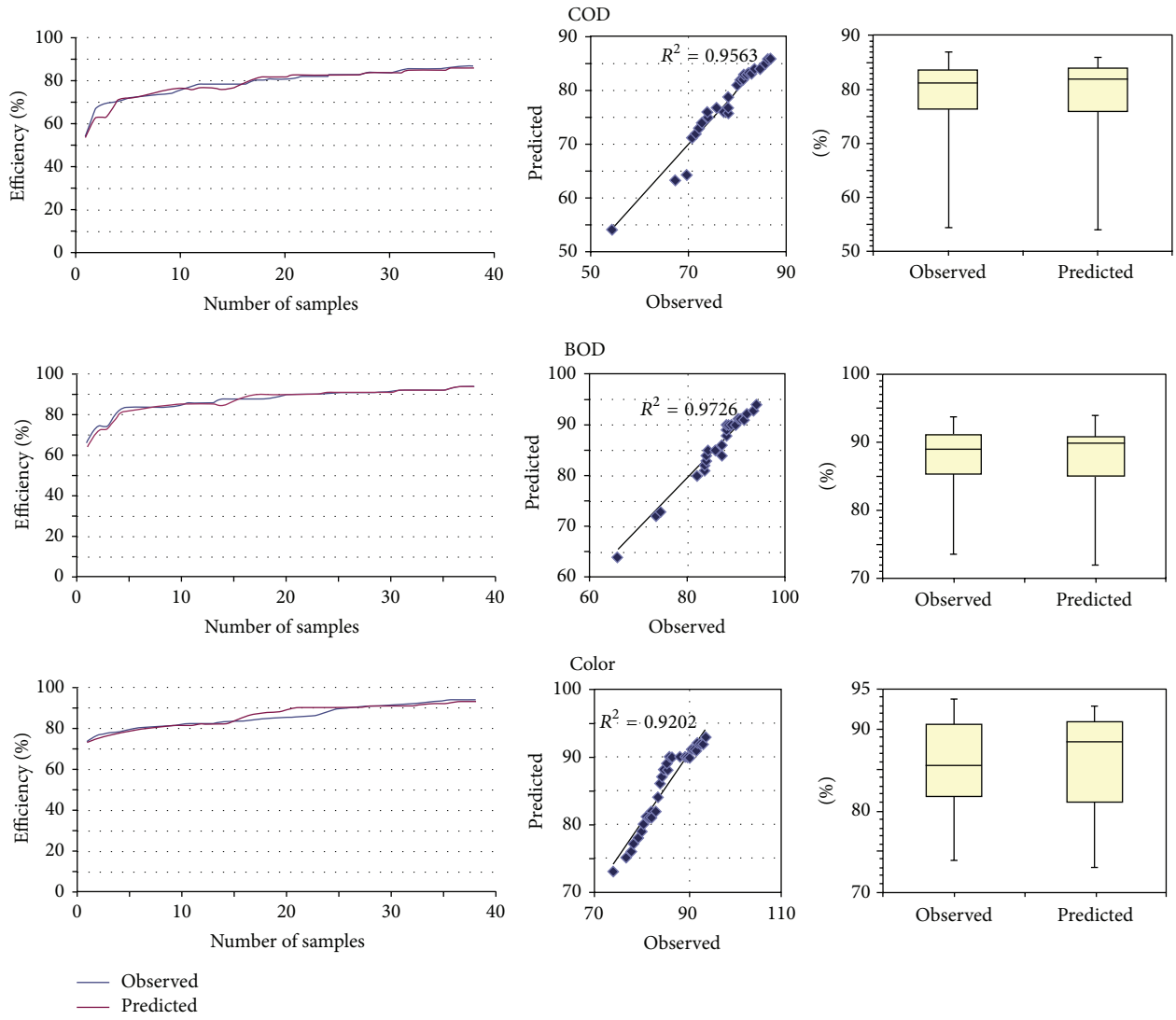

Figure 6: Observed-predicted plots.

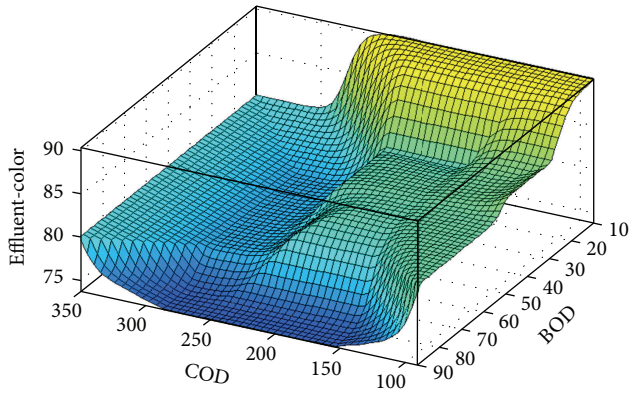

Figure 7: Surface map of color removal according to influent values.

was found to be 0.96, 0.97, and 0.92 for COD, BOD, and color, respectively. Multiple linear regressions suggested that the color removal rate is more dependent on the effluent COD value. Results of the estimation model exhibited favorable performance of the data set for predicting the MBR treatment system performance.

Conflict of Interests

The authors declare that there is no conflict of interests regarding the publication of this paper.

Acknowledgment

This research was supported by the Yildiz Technical University Scientific Research Projects Coordination Department, Project no. 2009-05-02-KAP01.

References

[1] Z. Zaroual, M. Azzi, N. Saib, and E. Chainet, "Contribution to the study of electrocoagulation mechanism in basic textile effluent," *Journal of Hazardous Materials*, vol. 131, no. 1–3, pp. 73–78, 2006.

[2] O. T. Can, M. Kobya, E. Demirbas, and M. Bayramoglu, "Treatment of the textile wastewater by combined electrocoagulation," *Chemosphere*, vol. 62, no. 2, pp. 181–187, 2006.

[3] N. O. Yigit, N. Uzal, H. Koseoglu et al., "Treatment of a denim producing textile industry wastewater using pilot-scale membrane bioreactor," *Desalination*, vol. 240, no. 1–3, pp. 143–150, 2009.

[4] S. Aoudj, A. Khelifa, N. Drouiche, M. Hecini, and H. Hamitouche, "Electrocoagulation process applied to wastewater containing dyes from textile industry," *Chemical Engineering and Processing: Process Intensification*, vol. 49, no. 11, pp. 1176–1182, 2010.

[5] N. Daneshvar, A. R. Khataee, and N. Djafarzadeh, "The use of artificial neural networks (ANN) for modeling of decolorization of textile dye solution containing C. I. Basic Yellow 28 by electrocoagulation process," *Journal of Hazardous Materials*, vol. 137, no. 3, pp. 1788–1795, 2006.

[6] M. Koch, A. Yediler, D. Lienert, G. Insel, and A. Kettrup, "Ozonation of hydrolyzed azo dye reactive yellow 84 (CI)," *Chemosphere*, vol. 46, no. 1, pp. 109–113, 2002.

[7] J. Sanz, J. I. Lombraña, A. M. De Luis, and F. Varona, "UV/H_2O_2 chemical oxidation for high loaded effluents: a degradation kinetic study of LAS surfactant wastewaters," *Environmental Technology*, vol. 24, no. 7, pp. 903–911, 2003.

[8] S. K. A. Solmaz, A. Birgül, G. E. Üstün, and T. Yonar, "Colour and COD removal from textile effluent by coagulation and advanced oxidation processes," *Coloration Technology*, vol. 122, no. 2, pp. 102–109, 2006.

[9] M. Mänttäri, M. Kuosa, J. Kallas, and M. Nyström, "Membrane filtration and ozone treatment of biologically treated effluents from the pulp and paper industry," *Journal of Membrane Science*, vol. 309, no. 1-2, pp. 112–119, 2008.

[10] Y. Avsar, H. A. Kabuk, U. Kurt, M. Cakmakci, and B. Ozkaya, "Biological treatability processes of textile wastewaters using electrocoagulation and ozonation," *Journal of Scientific and Industrial Research*, vol. 71, no. 7, pp. 496–500, 2012.

[11] E. Lee, H. Lee, Y. K. Kim, K. Sohn, and K. Lee, "Hydrogen peroxide interference in chemical oxygen demand during ozone based advanced oxidation of anaerobically digested livestock wastewater," *International Journal of Environmental Science and Technology*, vol. 8, no. 2, pp. 381–388, 2011.

[12] L. Bijan and M. Mohseni, "Novel membrane pretreatment to increase the efficiency of ozonation-biooxidation," *Environmental Engineering Science*, vol. 25, no. 2, pp. 229–237, 2008.

[13] S. K. A. Solmaz, A. Birgül, G. E. Üstün, and T. Yonar, "Colour and COD removal from textile effluent by coagulation and advanced oxidation processes," *Coloration Technology*, vol. 122, no. 2, pp. 102–109, 2006.

[14] A. Baban, A. Yediler, D. Lienert, N. Kemerdere, and A. Kettrup, "Ozonation of high strength segregated effluents from a woollen textile dyeing and finishing plant," *Dyes and Pigments*, vol. 58, no. 2, pp. 93–98, 2003.

[15] L. Szpyrkowicz, C. Juzzolino, and S. N. Kaul, "A comparative study on oxidation of disperse dyes by electrochemical process, ozone, hypochlorite and fenton reagent," *Water Research*, vol. 35, no. 9, pp. 2129–2136, 2001.

[16] S. Barredo-Damas, M. I. Iborra-Clar, A. Bes-Pia, M. I. Alcaina-Miranda, J. A. Mendoza-Roca, and A. Iborra-Clar, "Study of preozonation influence on the physical-chemical treatment of textile wastewater," *Desalination*, vol. 182, no. 1–3, pp. 267–274, 2005.

[17] A. Bes-Piá, A. Iborra-Clar, J. A. Mendoza-Roca, M. I. Iborra-Clar, and M. I. Alcaina-Miranda, "Nanofiltration of biologically treated textile effluents using ozone as a pre-treatment," *Desalination*, vol. 167, no. 1-3, pp. 387–392, 2004.

[18] O. S. G. P. Soares, J. J. M. Órfão, D. Portela, A. Vieira, and M. F. R. Pereira, "Ozonation of textile effluents and dye solutions under continuous operation: influence of operating parameters," *Journal of Hazardous Materials*, vol. 137, no. 3, pp. 1664–1673, 2006.

[19] N. Azbar, T. Yonar, and K. Kestioglu, "Comparison of various advanced oxidation processes and chemical treatment methods for COD and color removal from a polyester and acetate fiber dyeing effluent," *Chemosphere*, vol. 55, no. 1, pp. 35–43, 2004.

[20] G. Ciardelli and N. Ranieri, "The treatment and reuse of wastewater in the textile industry by means of ozonation and electroflocculation," *Water Research*, vol. 35, no. 2, pp. 567–572, 2001.

[21] M. Muthukumar, D. Sargunamani, N. Selvakumar, and J. Venkata Rao, "Optimisation of ozone treatment for colour and COD removal of acid dye effluent using central composite design experiment," *Dyes and Pigments*, vol. 63, no. 2, pp. 127–134, 2004.

[22] K. Sarayu, K. Swaminathan, and S. Sandhya, "Assessment of degradation of eight commercial reactive azo dyes individually and in mixture in aqueous solution by ozonation," *Dyes and Pigments*, vol. 75, no. 2, pp. 362–368, 2007.

[23] H. Selcuk, "Decolorization and detoxification of textile wastewater by ozonation and coagulation processes," *Dyes and Pigments*, vol. 64, no. 3, pp. 217–222, 2005.

[24] U. von Gunten, "Ozonation of drinking water: part I. Oxidation kinetics and product formation," *Water Research*, vol. 37, no. 7, pp. 1443–1467, 2003.

[25] F. Zanetti, G. de Luca, and R. Sacchetti, "Performance of a full-scale membrane bioreactor system in treating municipal wastewater for reuse purposes," *Bioresource Technology*, vol. 101, no. 10, pp. 3768–3771, 2010.

[26] E. Atasoy, S. Murat, A. Baban, and M. Tiris, "Membrane bioreactor (MBR) treatment of segregated household wastewater for reuse," *Clean—Soil, Air, Water*, vol. 35, no. 5, pp. 465–472, 2007.

[27] M. Brik, P. Schoeberl, B. Chamam, R. Braun, and W. Fuchs, "Advanced treatment of textile wastewater towards reuse using a membrane bioreactor," *Process Biochemistry*, vol. 41, no. 8, pp. 1751–1757, 2006.

[28] J. R. Banu, D. K. Uan, S. Kaliappan, and I. T. Yeom, "Effect of sludge pretreatment on the performance of anaerobic/ anoxic/ oxic membrane bioreactor treating domestic wastewater," *International Journal of Environmental Science and Technology*, vol. 8, no. 2, pp. 281–290, 2011.

[29] E. Marti, H. Monclús, J. Jofre, I. Rodriguez-Roda, J. Comas, and J. L. Balcázar, "Removal of microbial indicators from municipal wastewater by a membrane bioreactor (MBR)," *Bioresource Technology*, vol. 102, no. 8, pp. 5004–5009, 2011.

[30] F. Meng, S. R. Chae, H. S. Shin, F. Yang, and Z. Zhou, "Recent advances in membrane bioreactors: configuration development, pollutant elimination, and Sludge Reduction," *Environmental Engineering Science*, vol. 29, no. 3, pp. 139–160, 2012.

[31] P. Schoeberl, M. Brik, R. Braun, and W. Fuchs, "Treatment and recycling of textile wastewater—case study and development of a recycling concept," *Desalination*, vol. 171, no. 2, pp. 173–183, 2005.

[32] Z. Badani, H. Ait-Amar, A. Si-Salah, M. Brik, and W. Fuchs, "Treatment of textile waste water by membrane bioreactor and reuse," *Desalination*, vol. 185, no. 1-3, pp. 411–417, 2005.

[33] L. A. Zadeh, "Fuzzy sets," *Information and Computation*, vol. 8, pp. 338–353, 1965.

[34] A. Akkoyunlu, K. Yetilmezsoy, F. Erturk, and E. Oztemel, "A neural network-based approach for the prediction of urban SO_2 concentrations in the Istanbul metropolitan area," *International Journal of Environment and Pollution*, vol. 40, no. 4, pp. 301–321, 2010.

[35] K. Yetilmezsoy, "Fuzzy-logic modeling of Fenton's oxidation of anaerobically pretreated poultry manure wastewater," *Environmental Science and Pollution Research*, vol. 19, no. 6, pp. 2227–2237, 2012.

[36] K. Yetilmezsoy and S. A. Abdul-Wahab, "A prognostic approach based on fuzzy-logic methodology to forecast PM_{10} levels in Khaldiya residential area, Kuwait," *Aerosol and Air Quality Research*, vol. 12, no. 6, pp. 1217–1236, 2012.

[37] E. Yel and S. Yalpir, "Prediction of primary treatment effluent parameters by Fuzzy Inference System (FIS) approach," *Procedia Computer Science*, vol. 3, pp. 659–665, 2011.

[38] American Public Health Association (APHA), *Standard Methods for the Examination of Water & Wastewater*, American Public Health Association (APHA), Washington, DC, USA, 21st edition, 2005.

[39] Anonymous, "Iodometric method for the determination of ozone in a process gas," IOA Standardization Committee-Europe 001/87-F, International Ozone Association, Brussels, Belgium, 1987.

[40] G. Tchobanoglous, F. Burton, and H. D. Stensel, *Wastewater Engineering: Treatment and Reuse*, McGraw-Hill, 4th edition, 2001.

[41] Water Pollution Control Regulation, "Table 10: The discharge standards of textile industry waste water," The Ministry of Forest and Water, 2004.

[42] S.-J. You and J.-Y. Teng, "Anaerobic decolorization bacteria for the treatment of azo dye in a sequential anaerobic and aerobic membrane bioreactor," *Journal of the Taiwan Institute of Chemical Engineers*, vol. 40, no. 5, pp. 500–504, 2009.

[43] F. I. Hai, K. Yamamoto, F. Nakajima, and K. Fukushi, "Bioaugmented membrane bioreactor (MBR) with a GAC-packed zone for high rate textile wastewater treatment," *Water Research*, vol. 45, no. 6, pp. 2199–2206, 2011.

[44] J. Jantzen, "Design of fuzzy controllers," Tech. Rep. 98 -E864, Department of Automation, Technical University of Denmark, Lyngby, Denmark, 1998.

[45] F. I. Turkdogan-Aydinol and K. Yetilmezsoy, "A fuzzy-logic-based model to predict biogas and methane production rates in a pilot-scale mesophilic UASB reactor treating molasses wastewater," *Journal of Hazardous Materials*, vol. 182, no. 1–3, pp. 460–471, 2010.

Hindawi Publishing Corporation
International Journal of Photoenergy
Volume 2015, Article ID 623492, 9 pages
http://dx.doi.org/10.1155/2015/623492

Research Article

Removal of Polyvinyl Alcohol in Aqueous Solutions Using an Innovative Paired Photoelectrochemical Oxidative System in a Divided Electrochemical Cell

Kai-Yu Huang,[1] Chih-Ta Wang,[2] Wei-Lung Chou,[3] and Chi-Min Shu[1]

[1] *Department of Safety, Health and Environmental Engineering, National Yunlin University of Science and Technology, Yunlin 64002, Taiwan*
[2] *Department of Safety, Health and Environmental Engineering, Chung Hwa University of Medical Technology, Tainan 717, Taiwan*
[3] *Department of Safety, Health and Environmental Engineering, Hungkuang University, Sha-Lu, Taichung 433, Taiwan*

Correspondence should be addressed to Wei-Lung Chou; wlchou@sunrise.hk.edu.tw

Received 23 July 2014; Accepted 2 October 2014

Academic Editor: Bashir Ahmmad

This study evaluates the performance of an innovative paired photoelectrochemical oxidative system fabricated in our laboratory to determine the removal efficiency of polyvinyl alcohol (PVA) in aqueous solutions. An innovative paired photoelectrochemical oxidative system employed metal redox mediators with high redox potential for anodic oxidation (MEO process) and UV assisted photoelectrochemical oxidation (PEO process) for cathodic oxidation in a divided electrochemical cell. Several parameters were investigated to characterize the removal efficiency of PVA, such as the current density, initial Ce(III) concentration, nitric acid concentration, oxygen flow rate, and UV irradiation intensity. The effects of these parameters on the specific energy consumption were also investigated. Additionally, the conversion yield of Ce(IV) concentration and the electrogeneration of H_2O_2 were calculated in this study. The optimum current density, initial Ce(III) concentration, nitric acid concentration, oxygen flow rate, and UV irradiation intensity were found to be 3 mA cm^{-2}, 0.01 M, 0.3 M, 500 cm^3 min^{-1}, and 1.2 mW cm^{-2}, respectively. The synergistic effect of combination process of MEO and PEO would be as a promising alternative for the removal efficiency of PVA.

1. Introduction

Due to rapid development of industrial, polymers are increasingly used in various industrial products, polyvinyl alcohol especially. Polyvinyl alcohol (PVA) is widely used as warp sizes for cotton-synthetic blends in the textile industry and the molecular structure of $[-CH_2-CH(OH)]_n$ makes it possess of well water solubility [1]. The global production of PVA is almost over 650,000 tons/year. It is also used for polarizing film light in liquid crystal displays (LCDs) [2]. However, discharging of a large quantity of PVA influences both human health and natural environment [3] and leads to high chemical oxygen demand (COD) in the industrial effluents. It is difficult to convert wastewaters containing PVA to generate harmless end-products like water and carbon dioxide. Therefore, PVA adversely can affect the ecosystem and accumulates in the human body through the food chain [4]. Conventional biological technologies do not provide an efficacious treatment of wastewaters containing PVA, because most microorganisms degradation ability for PVA is extremely specific and restricted [5]. An effective method for the treatment of wastewaters containing PVA has to be developed. For the treatment of PVA wastewater, a number of chemical processes have been investigated, including adsorption [1, 6, 7], photocatalysis degradation process [8–11], chemical oxidation [12, 13], electrocoagulation [14], and electro-Fenton [15]. However, to date, there is little research on the development of a paired photoelectrochemical oxidative system treatment for the removal of PVA.

In recent years, electrochemical treatment technology has been applied in various ways to clean the environment such as anodic oxidation, cathodic reduction, and electro-Fenton process [16–18]. Advanced oxidation processes (AOPs) and mediated electrochemical oxidation (MEO) are new

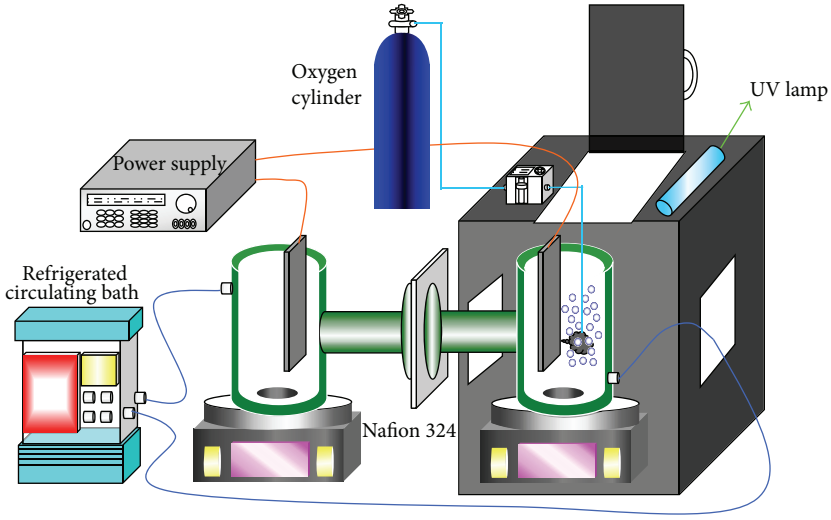

Figure 1: Schematic diagram of the paired photoelectrochemical oxidative equipment.

technology for the treatment of industrial wastewater containing organic compounds. Both promising technologies can mineralize the organics into nontoxic carbon dioxide and water [19, 20]. AOPs are based on generation strong oxidant of hydroxyl radicals that can nonselectively degrade organic contaminants rapidly [21]. Among all AOPs methods, hydrogen peroxide often has been used as a powerful oxidant to generate $OH^{\bullet}$ for oxidizing wastewater of organic compounds [9, 22–24]. A combination UV irradiation and H_2O_2 process can effectively increase the oxidative power of hydrogen peroxide due to the production of hydroxyl free radicals, as shown in the reaction $H_2O_2 + UV \rightarrow 2OH^{\bullet}$. The UV/$H_2O_2$ process also has been proven to be efficient in degrading organic compounds [25, 26]. Therefore, the hydroxyl free radicals were produced by photoelectrochemical oxidation (PEO) process in the cathodic compartment.

MEO technique presents several advantages: easy operations, simple equipment, less sludge production, the oxidant can conveniently be reused, and avoided production of secondary wastes. In the MEO process, the mediator ion is a transition metal, such as cobalt, cerium, and silver [27–30]. These mediators can be oxidized from lower oxidation state to higher oxidation state to mineralize organic complexes. Among these mediators, cerium (IV) has good oxidizing property because of its higher redox potential ($E^0 = 1.62$ V). However, in the traditional electrochemical anodic oxidation system, the cathodic compartment usually only reduces the water and generate hydrogen gas. Thus, the removal efficiency of organic substance cannot be effectively increased to result in energy waste. In order to improve the overall current efficiency, we will combine the MEO process of the anodic compartment with PEO reaction to generate hydroxyl free radicals at the cathodic compartment to form a paired photoelectrochemical oxidative system. To the best of our knowledge, very little work has been reported in the literature to date on PVA removal by an innovative paired photoelectrochemical oxidative system.

In the present study, parameters such as current density, initial Ce(III) concentration, nitric acid concentration, oxygen flow rate, and UV irradiation intensity were investigated in terms of the PVA removal efficiency. A technically effective process must be economically feasible with regard to its specific energy consumption (SEC) and practically applicable to environmental problems. The effects of the main operational parameters (current density, initial Ce(III) concentration, nitric acid concentration, oxygen flow rate, and UV irradiation) on SEC under the optimum conditions were evaluated. The yield of the Ce(IV) concentration and the electrogeneration of H_2O_2 on the different operational parameters by MEO process of the anodic compartment and PEO process of the cathodic compartment were also investigated in this study.

2. Experimental

2.1. Chemicals and Apparatus. Cerium(III) nitrate hexahydrate was obtained from Alfa Aesar (USA). Polyvinyl alcohol (PVA, molecular weight in the range of 13,000 to 23,000 g mol^{-1}) was obtained from Sigma-Aldrich (USA) with a hydrolysis degree ranging from 98 to 99%. Na_2SO_4 was purchased from Merck (Germany), and HNO_3 (65%) was obtained from Scharlau (Spain). Titanium(IV) sulfate (24%) was purchased from SHOWA (Japan). Boric acid (99.5%) was supplied by Merck, and potassium iodide (99.5%) and iodine (99.5%) were obtained from Union Chemical Work Ltd. (Taiwan) and Toyobo Co. Ltd. (Japan), respectively. All chemicals were analytical grade reagents and were prepared by dilution with deionized water to the desired concentrations. The activated carbon fiber (ACF), PAN-based rigid composite carbon felt series, was obtained from Taiwan carbon Technology Co. Ltd. (Taiwan).

Figure 1 is a schematic diagram of the paired photoelectrochemical system and the electrode assembly used in this work. The anodic and cathodic electrolytic cell was 0.5 L glass reactor equipped with a water jacket and a magnetic stirrer.

The electrolytic cell consisted of an anode and a cathode separated by a Nafion 324 membrane. The temperature of the electrolytic cell was controlled by continuously circulating water jacket from a refrigerated circulating bath (Model BL-720, Taiwan). A magnetic stirrer bar (Suntex SH-301, Taiwan) was spun at the center of the bottom of the reactor. The platinum anode (6 cm^2) and ACF cathode (20 cm^2) were immersed in the PVA aqueous solution at a depth of 5 cm. In the following, all experiments were conducted using a Pt/ACF electrode combination. The oxygen gas from an oxygen cylinder was dispersed at the bottom of the cathode. The electric current was supplied by a DC power supply (PSM-6003, Taichung, Taiwan). A UV lamp (8 W, UV-C, λ_{max} = 254 nm, manufactured by Sankyo denski, Japan) was used as a radiation source and placed above a cathodic reactor. The UV-light intensity was measured by a Digital Ultraviolet Radiometer (Rixen Technology, Taiwan).

2.2. Methods and Analysis. The experiments were conducted in a divided glass vessel. Before each experiment, the electrodes were cleaned with deionized water. During each test run, two circular containers with 0.4 L of synthetic wastewater containing polyvinyl alcohol were as the reactor. Then, the magnetic stirrer was turned on and set at 300 rpm; this stirrer speed was sufficient for good mixing in the electrolytic cell. The ACF felt was saturated with 1000 mg L^{-1} PVA solution for 24 h to exclude the adsorption reaction of PVA on the ACF felt. The direct current power source was operated with a constant current density of 1, 2, 3, 4, and 5 mA cm^{-2}. A constant Ce(III) concentration (0.001 M to 0.02 M) and HNO_3 concentration (0.1 M to 0.5 M) were adjusted in the anodic compartment during the experiments. The cathodic compartment was fed with an oxygen gas flow rate of 100 to 900 cm^3 min^{-1}, and the UV light intensity (0 to 1.2 mW cm^{-2}) was controlled by UV lamps during the experiments. The paired photoelectrochemical system treatment run lasted 120 min in all experiments. Prior to the electrolysis, the oxygen gas was bubbled for 10 min to saturate the aqueous solution; then, the electric power was turned on, and the paired photoelectrochemical reactions started simultaneously. Samples were drawn out from the reactor at default time intervals and then analyzed.

The H_2O_2 concentration was determined using the $Ti(SO_4)_2$ titration method and spectrophotometric analysis at λ = 410 nm [31]. Ce(IV) concentration was quantitatively determined using ferrous ammonium sulfate dissolved in 0.005 M nitric acid [32]. The amount of Ce(IV) generated theoretically is dependent on the quantity of applied electricity. According to Faraday's laws of electrolysis, the theoretical production of Ce(IV) amount (m_t) at electrolysis time t can be calculated as follows [33]:

$$m_t = \frac{MIt}{zF}, \tag{1}$$

where M is molecular weight of Ce; I is the applied current; z is the electrons transferred per Ce(III) ion (z = 1 in Ce(III) → Ce(IV) + e^-); and F is the Faraday's constant.

Quantitative determination of PVA concentration in the aqueous solutions was carried out using a HACH Model DR2800 spectrophotometer (USA) after addition of boric acid and iodine solutions according to the procedure described by Finley [34]. A calibration curve was obtained by plotting the absorbance value at 680 nm against polyvinyl alcohol concentration. The calculation of the PVA destruction efficiency after the paired photoelectrochemical treatment was performed using the following formula:

$$\text{RE}\,(\%) = \frac{C_0V_0 - C_tV_t}{C_0V_0} \times 100, \tag{2}$$

where C_0 is the initial concentration in mg L^{-1}, C_t is the concentration value at time t in mg L^{-1}, V_0 is the initial volume of the treated wastewater in liters, and V_t is the volume of the treated wastewater at time t in liters. All of the samples were evaluated at least fifth to ensure data reproducibility, and an additional measurement was carried out if necessary.

3. Results and Discussion

3.1. Effect of Current Density. Current density is an important operating factor that strongly controls the reaction rate in the electrochemical engineering. It determines the electrogeneration of Ce(IV) from the initial Ce(III) by the anodic MEO process and electrogeneration of H_2O_2 by the cathodic PEO process in the paired photoelectrochemical oxidative system. The mechanism of the anodic MEO process and the cathodic PEO process removal of PVA may be expressed as follows.

For the anodic process:

$$Ce^{3+} \longrightarrow Ce^{4+} + e^- \tag{3}$$

$$\text{PVA} + \text{Ce (IV)} \longrightarrow \text{intermediates} \longrightarrow CO_2 + H_2O \tag{4}$$

For the cathodic process:

$$\begin{gathered} H_2O_2 + \text{UV} \longrightarrow 2OH^{\bullet} \\ \text{PVA} + OH^{\bullet} \longrightarrow \text{intermediates} \longrightarrow CO_2 + H_2O \end{gathered} \tag{5}$$

The effect of the current density on the PVA removal efficiency in the anodic and cathodic compartment was studied at 1, 2, 3, 4, and 5 mA cm^{-2}. Figure 2(a) indicated the effect of different current density on the removal efficiency of PVA in the anodic and cathodic compartment. As the current density increased, the PVA removal efficiencies increased. After 120 min of electrolysis, it can be seen from Figure 2(a) that the removal efficiency of PVA in the anodic compartment was 51.2%, 62.7%, 77.8%, 79.3%, and 80.4% and cathodic compartment was 20.8%, 27.7%, 29.4%, 31.6%, and 32.8% for the current densities of 1, 2, 3, 4, and 5 mA cm^{-2}, respectively. According to (3), the reduced Ce(III) can be electrooxidized to Ce(IV) in the anodic compartment, as shown in Table 1. Therefore, the Ce(IV) can be reused as the oxidant for the continuous removal of PVA and avoided the generation of secondary waste. In the cathodic compartment, the

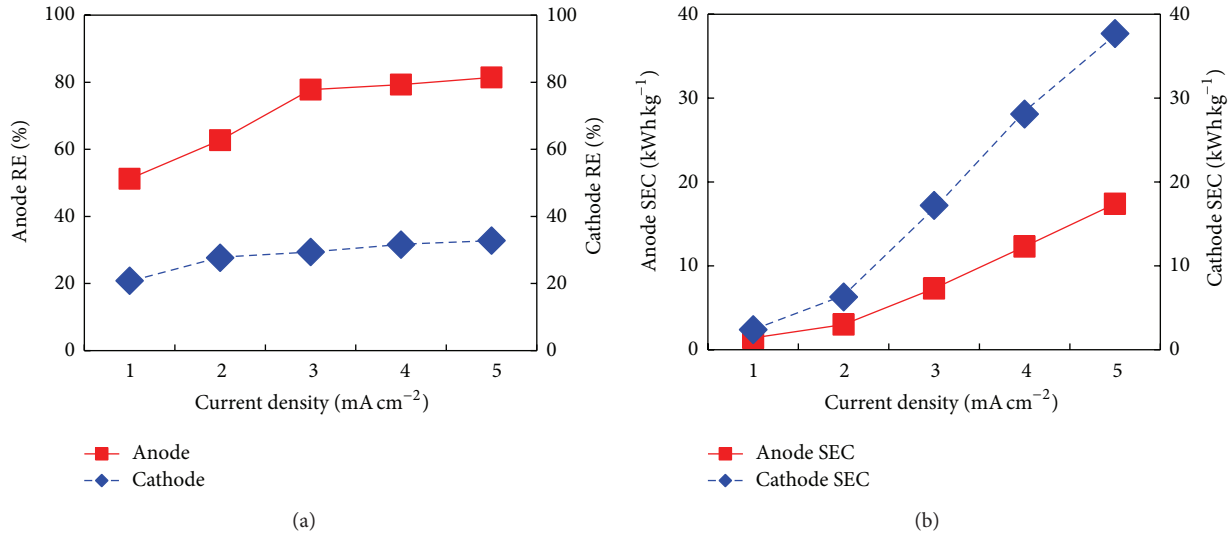

Figure 2: Effect of current density: (a) anodic and cathodic compartment removal efficiency of PVA and (b) SEC of anodic and cathodic compartment removal of PVA (temperature = 323 K, anodic compartment: PVA = 50 mg L^{-1}, Ce(III) = 0.01 M, HNO_3 = 0.2 M; cathodic compartment: PVA = 50 mg L^{-1}, Na_2SO_4 = 0.05 M, pH = 3, oxygen flow rate = 500 cm^3 min^{-1}, and UV-light intensity = 0.4 mW cm^{-2}).

Table 1: Effect of the current density on the Ce(IV) and H_2O_2 electrogeneration during a paired photoelectrochemical oxidative system.

Current density (mA cm^{-2})	Yield of Ce(IV) concentration (%)	Concentration of H_2O_2 generation (mg L^{-1})
1	5	9
2	8.7	9.6
3	12.3	14.5
4	13.3	16.6
5	16	20.3

electrogenerated H_2O_2 was catalyzed into hydroxyl radicals by UV light, which were very powerful oxidizing species. These hydroxyl radicals can effectively oxidize the PVA. As shown in Table 1, a significant increase in the H_2O_2 yield was observed with increasing current density; thus there was more generation of hydroxyl radicals to oxidize PVA. However, no significant improvement in the PVA removal efficiency was observed while the current density increased from 3 to 5 mA cm^{-2}.

In order to obtain the optimum current density when concerning the energy efficiency, the specific energy consumption (SEC) [35] for removing 1 Kg PVA at a specified certain electric current was calculated by the following:

$$\mathrm{SEC}\ \left(\mathrm{kWh\,kg^{-1}}\right) = \frac{\int U \times I\,dt}{(C_0V_0 - C_tV_t) \times 3.6} = \frac{I\int U\,dt}{(C_0V_0 - C_tV_t) \times 3.6}, \quad (6)$$

where U, I, t were the applied voltage (V), current (A), and electrolysis time (min), respectively. In addition, C_0 (mg L^{-1}) is the initial concentration, C_t (mg L^{-1}) is the concentration value at time t, V_0 (L) is the initial volume of the treated wastewater, and V_t (L) is the volume of the treated wastewater at time t. A reasonable removal efficiency and relatively low energy consumption were determined below. Figure 2(b) also shows the SEC values of anodic and cathodic compartment after 120 min of electrolysis at different current densities. It can be obviously seen that increasing current density had a significant effect on SEC. When the current density varied from 1 to 5 mA cm^{-2}, we observed a dramatic increase in the SEC value from 1.4 kWh kg^{-1} to 17.4 kWh kg^{-1} in the anodic compartment and 2.4 kWh kg^{-1} to 37.7 kWh kg^{-1} in the cathodic compartment for PVA removal. However, as the current density was increased from 3 to 5 mA cm^{-2}, the anodic and cathodic PVA removal efficiency increased slightly, whereas the corresponding electric energy consumption increased by almost 2 times. Consequently, when considering both the electric energy consumption and the PVA removal efficiency, 3 mA cm^{-2} offers the best compromise, providing a reasonable PVA removal efficiency and relatively low electrical energy consumption.

3.2. Removal of PVA in the Anodic Compartment

3.2.1. Effect of Initial Ce(III) Concentration. In this study, the effect of initial Ce(III) concentration on the PVA removal efficiency was studied at 0.001, 0.0025, 0.005, 0.01, and 0.02 M, as shown in Figure 3(a). After 120 min of electrolysis, we observed that the PVA removal efficiencies reached 38.6%, 51%, 56%, 77.8%, and 80.1% for initial Ce(III) concentrations of 0.001, 0.0025, 0.005, 0.01, and 0.02 M, respectively. This phenomenon was probably derived from the increasing of driving force for Ce(III) mass transfer and electrolyte conductivity while increasing initial Ce(III) concentration. When the initial Ce(III) concentration was increased, the Ce(IV)

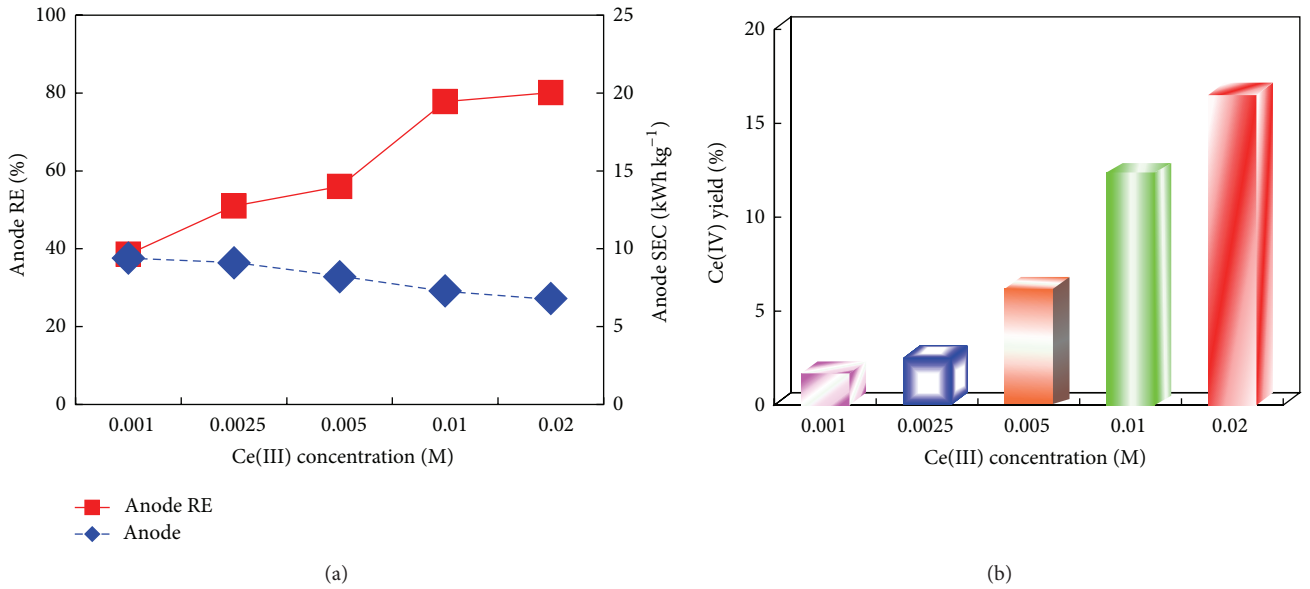

FIGURE 3: Effect of initial Ce(III) concentration: (a) removal efficiency and SEC of PVA and (b) Ce(IV) yield with different initial Ce(III) concentration in the anodic compartment (current density = 3 mA cm^{-2}, temperature = 323 K, anodic compartment: PVA = 50 mg L^{-1}, HNO_3 = 0.2 M; cathodic compartment: PVA = 50 mg L^{-1}, Na_2SO_4 = 0.05 M, pH = 3, oxygen flow rate = 500 cm^3 min^{-1}, and UV-light intensity = 0.4 mW cm^{-2}).

ion concentration also increased, as shown in Figure 3(b). However, if the initial Ce(III) concentration was higher than 0.01 M, the PVA removal efficiency did not increase significantly.

In order to evaluate the effect of initial Ce(III) concentration on the specific energy consumption and PVA removal efficiency, a number of experiments were performed after 120 min of electrolysis while keeping the current density, solution temperature, and anodic supporting electrolyte at 3 mA cm^{-2}, 323 K, and 0.2 M HNO_3 in the anodic compartment; oxygen flow rate, UV light intensity, and cathodic supporting electrolyte at 500 cm^3 min^{-1}, 0.4 mW cm^{-2}, and 0.05 M Na_2SO_4 in the cathodic compartment. Figure 3(b) also shows the effect of the initial Ce(III) concentration on the SEC during the paired photoelectrochemical oxidative system. As shown in the figure, the SEC decreased from 9.4 kWh kg^{-1} to 6.8 kWh kg^{-1} when the initial Ce(IV) concentration increased from 0.001 to 0.02 M. Although there was a significant downward trend for the SEC while the initial Ce(III) concentration increased, the SEC was not significantly changed by increasing Ce(III) ion concentration from 0.01 to 0.02 M. Consequently, the initial Ce(III) concentration of 0.01 M provides the optimum performance for this system; it provides a reasonable PVA removal efficiency and a relatively low electrical energy consumption.

3.2.2. Effect of Nitric Acid Concentration. Electrochemical treatments need salts or acid for supporting the electrolytes that make the solution more conductive. In comparison with low solubility of sulfuric acid on the cerium, nitric acid is often chosen in the past references [20, 29, 36]. Therefore, nitric acid was used as the anodic supporting electrolyte to increase the solution conductivity and thus reduce the SEC in the present study. In order to decrease environmental pollutions, we used a comparatively lower acid concentration in this study. The effect on the PVA removal efficiency of varying the nitric acid from 0.1 to 0.5 M was studied, as shown in Figure 4(a). It was observed that the removal efficiency increased as the concentration of nitric acid was increased in the anodic compartment. After 120 min of electrolysis, 40.8%, 77.8%, 80.1%, 82.2%, and 83.5% of the original PVA were removed at nitric acid concentrations of 0.1, 0.2, 0.3, 0.4, and 0.5 M, respectively. Nitric acid is a strong oxidant and in favor of the generation of Ce(IV). Figure 4(b) also indicated that Ce(IV) yield increased with increasing nitric acid concentration. As the Ce(IV) yield increased, the PVA removal efficiency also increased. However, if the concentration of nitric acid was higher than 0.3 M, the PVA removal efficiency did not increase significantly.

The concentration of the supporting electrolyte was adjusted by adding a suitable amount of nitric acid to the anodic compartment. Figure 4(a) also indicates the effect of the nitric acid concentration on the PVA removal efficiency and SEC during the paired photoelectrochemical oxidative system. Figure 4(a) also indicates that SEC decreased from 13.1 kWh kg^{-1} to 5.4 kWh kg^{-1} when the concentration of the nitric acid increased from 0.1 to 0.5 M. It was observed that the SEC was significantly decreased almost 60%. Although there was a significant downward trend for the SEC when the nitric acid concentration increased, the SEC did not significantly vary by increasing acid concentration from 0.3 to 0.5 M. Consequently, 0.3 M nitric acid concentration provided the optimum balance between the removal efficiency at the specific energy consumption.

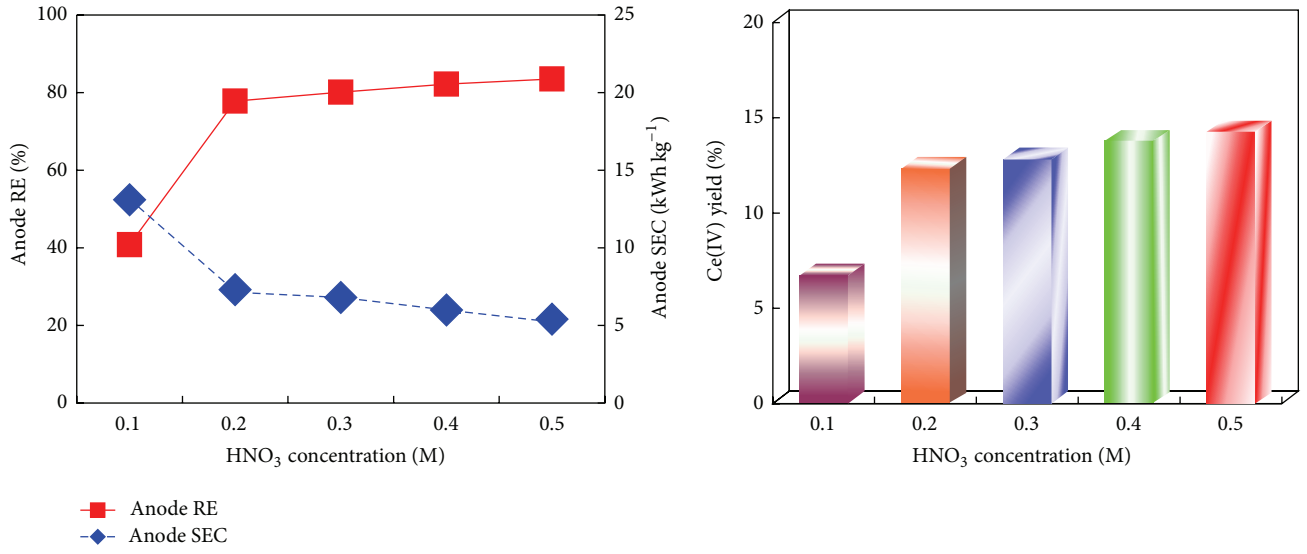

Figure 4: Effect of HNO_3 concentration: (a) removal efficiency and SEC of PVA and (b) Ce(IV) yield with different HNO_3 concentration in the anodic compartment (current density = 3 mA cm^{-2}, temperature = 323 K, anodic compartment: PVA = 50 mg L^{-1}, Ce(III) = 0.01 M; cathodic compartment: PVA = 50 mg L^{-1}, Na_2SO_4 = 0.05 M, pH = 3, oxygen flow rate = 500 cm^3 min^{-1}, and UV-light intensity = 0.4 mW cm^{-2}).

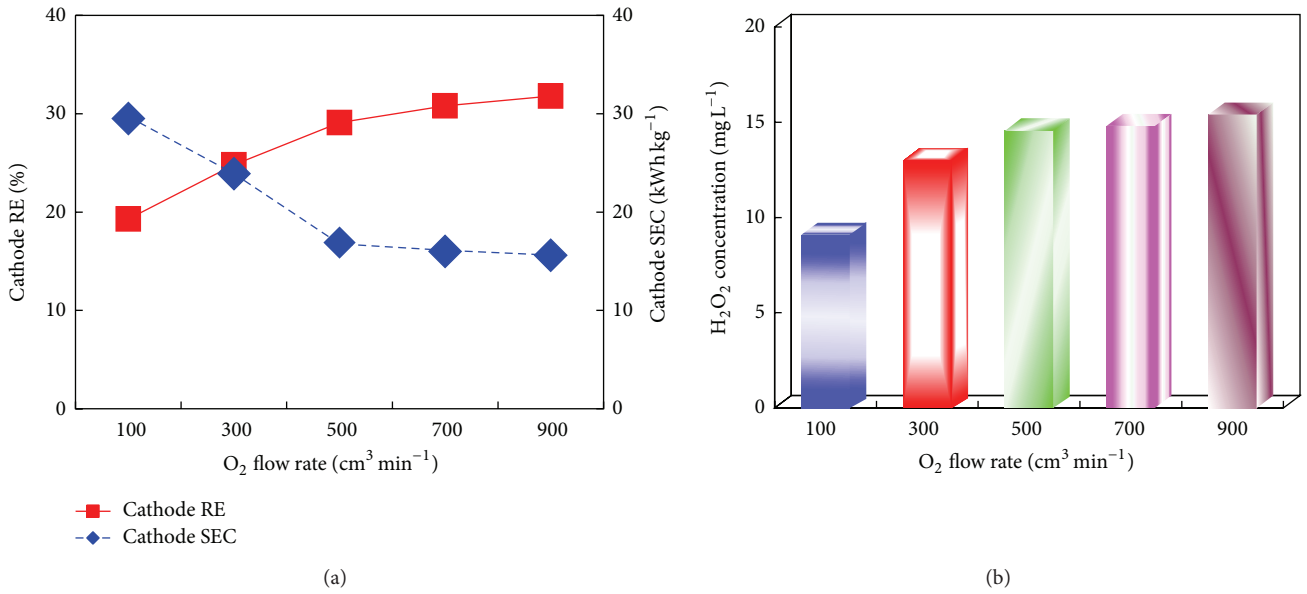

Figure 5: Effect of oxygen flow rate: (a) removal efficiency and SEC of PVA and (b) concentration of H_2O_2 generation with different oxygen flow rate in the cathodic compartment (current density = 3 mA cm^{-2}, temperature = 323 K, anodic compartment: PVA = 50 mg L^{-1}, Ce(III) = 0.01 M, HNO_3 = 0.3 M; cathodic compartment: PVA = 50 mg L^{-1}, Na_2SO_4 = 0.05 M, pH = 3, and UV-light intensity = 0.4 mW cm^{-2}).

3.3. Removal of PVA in the Cathodic Compartment

3.3.1. Effect of Oxygen Flow Rate. In this study, the yield of H_2O_2 electrogeneration via oxygen reduction at the cathode significantly affects the PVA removal efficiency of cathodic compartment. The effect of the oxygen flow rate on the PVA removal efficiency was studied at 100 to 900 cm^3 min^{-1}, as shown in Figure 5(a). For increased oxygen flow rate, significant increases in the PVA removal efficiency were observed, suggesting that the increase of the oxygen flow rate improves PVA removal rate. After 120 min of electrolysis, while the oxygen flow rate increased from 100, 300, 500, 700, and 900 cm^3 min^{-1}, the concentration of PVA was removed significantly, increasing from 19.3, 24.8, 29.1, 30.8, and 31.8%, respectively. This reason was that when the oxygen flow rate was increased, the concentration of dissolved oxygen and mass transfer rate of dissolved oxygen were increased, thereby accelerating the electrogeneration of H_2O_2 which

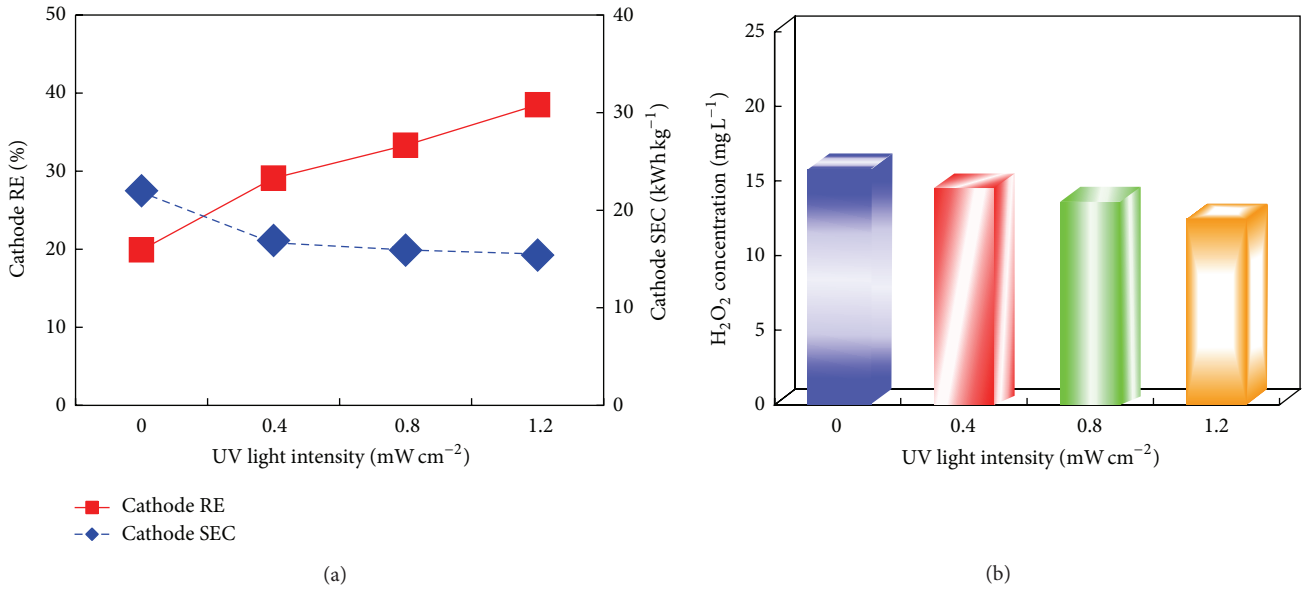

Figure 6: Effect of UV-light intensity: (a) removal efficiency and SEC of PVA and (b) concentration of H_2O_2 generation with different UV-light intensity in the cathodic compartment (current density = 3 mA cm^{-2}, temperature = 323 K, anodic compartment: PVA = 50 mg L^{-1}, Ce(III) = 0.01 M, HNO_3 = 0.3 M; cathodic compartment: PVA = 50 mg L^{-1}, Na_2SO_4 = 0.05 M, pH = 3, and oxygen flow rate = 500 cm^3 min^{-1}).

was dissociated into more hydroxyl radicals. Therefore, the hydroxyl radicals can oxidize PVA to improve removal efficiency. Figure 5(b) demonstrated that the electrogeneration of H_2O_2 increased with increasing of the oxygen flow rate. However, above an oxygen flow rate of 500 cm^3 min^{-1}, the oxygen and H_2O_2 concentration followed a steady trend. The results illustrated that the saturated solubility of oxygen in aqueous solutions was nearly accomplished at the oxygen flow rate of 500 cm^3 min^{-1} [37]. To investigate the optimum oxygen flow rate, the performance of the specific energy consumption at a certain oxygen flow rate during this system was evaluated; these results were given in the following section.

PVA solutions were treated using paired photoelectrochemical oxidative system at oxygen flow rates in the range of 100 to 900 cm^3 min^{-1} to determine the optimal removal efficiency and specific energy consumption. The effect of the oxygen flow rate on removal efficiency and specific energy consumption was shown in Figure 5(a). The specific energy consumption decreased significantly by approximately 50%, when the oxygen flow rate was increased from 100 to 900 cm^3 min^{-1}, whereas the corresponding PVA removal efficiency in the cathodic compartment increased from 19.3% to 31.8%. However, when the oxygen flow rate was increased from 500 to 700 and 900 cm^3 min^{-1}, the specific energy consumption decreased slightly from 16.9 to 16 and 15.6 kWh kg^{-1}, respectively, whereas the corresponding PVA removal efficiency in the cathodic compartment increased from 29.1% to 31.8%, respectively. Consequently, on consideration of the removal efficiency and specific energy consumption values for PVA removal in the cathodic compartment, an oxygen flow rate of 500 cm^3 min^{-1} offers the best performance with reasonable removal efficiency and relatively low specific energy consumption.

3.3.2. Effect of UV Irradiation Intensity. The UV irradiation intensity is an important factor that strongly controls the concentration of hydroxyl radicals generated. In this study, the effect of the UV light intensity on PVA removal efficiency and SEC was investigated at 0, 0.4, 0.8, and 1.2 mW cm^{-2}, as shown in Figure 6(a). After 120 min of electrolysis, it was observed that the maximum PVA removal efficiency was found at 1.2 mW cm^{-2}. The PVA removal efficiency reached 19.9%, 29.1%, 33.3%, and 38.5% for UV light intensities of 0, 0.4, 0.8, and 1.2 mW cm^{-2}, respectively. It appears that increasing UV light intensity increases the PVA removal efficiency. This experimental results explained that higher UV light intensity can improve the generation of hydroxyl radicals to remove PVA from the solution [22, 23]. On the one hand, the rate of photolysis of hydrogen was limited at lower UV light intensity, resulted in decreased PVA removal efficiency. Figure 6(b) shows the concentration of hydrogen peroxide generation at various UV light intensities. As shown in Figure 6(b), after 120 min of electrolysis, 15.8%, 14.5%, 13.6%, and 12.4% of the hydrogen peroxide was generated for UV light intensities of 0, 0.4, 0.8, and 1.2 mW cm^{-2}, respectively. It is clear that increasing the UV light intensity can effectively increase the generation of hydroxyl radicals, result in the hydrogen peroxide decreased. Therefore, at a higher UV light intensity the amount of hydroxyl radicals generation in the reaction cell was found well.

Figure 6(a) also shows the effect of UV light intensity on the PVA removal efficiency and specific energy consumption after 120 min of electrolysis by paired photoelectrochemical oxidative system. The SEC values decreased from 22 kWh kg^{-1} to 15.4 kWh kg^{-1} when the UV light intensities were increased from 0 to 1.2 mW cm^{-2}, whereas the corresponding PVA removal efficiency increased significantly from 19.9% to 38.5%. Consequently, when considering both

the SEC values and the PVA removal efficiency in the cathodic compartment, a UV light intensity of 1.2 mW cm^{-2} offers the best overall performance with a reasonable PVA removal efficiency and relatively low SEC values.

4. Conclusions

Electrooxidation of Ce(III) in nitric acid medium for the anodic MEO process and electrogeneration of H_2O_2 in acid medium for the cathodic PEO process were performed using the divided electrochemical cell fabricated in our study. The removal efficiency of PVA tin aqueous solutions via this innovative paired photo-electrochemical oxidative system was investigated in anodic compartment and cathodic compartment conditions, respectively. Various operating parameters such as the current density, the initial Ce(III) concentration, nitric acid concentration, oxygen flow rate, and UV irradiation intensity were investigated in this study. The yield of the Ce(IV) concentration and H_2O_2 on the different operational parameters by MEO process of the anodic compartment and PEO process of the cathodic compartment were also calculated. The current density of 3 mA cm^{-2} was regarded as optimum for a reasonable PVA removal efficiency with a relatively low specific energy consumption. Considering the removal efficiency and SEC, an initial Ce(III) concentration of 0.1 M, nitric acid concentration of 0.3 M, oxygen flow rate of 500 cm^3 min^{-1}, and UV irradiation of 1.2 mW cm^{-2} were found be the optimum values for the present study. The results indicate that an innovative paired photoelectrochemical oxidative system, combining anodic MEO process and cathodic PEO process, would be regarded as a potential alternative to remove PVA in aqueous solutions.

Conflict of Interests

The authors declare that there is no conflict of interests with any financial organization regarding the material discussed in this study.

Acknowledgments

The authors would like to thank the National Science Council of Taiwan, ROC, for financially supporting this study under contract no. NSC101-2628-E-241-013-MY3.

References

[1] X.-Y. Pang, "Adsorption characteristics of polyvinyl alcohols in solution on expanded graphite," *E-Journal of Chemistry*, vol. 9, no. 1, pp. 240–252, 2012.

[2] J. B. Chang, J. H. Hwang, J. S. Park, and J. P. Kim, "The effect of dye structure on the dyeing and optical properties of dichroic dyes for PVA polarizing film," *Dyes and Pigments*, vol. 88, no. 3, pp. 366–371, 2011.

[3] J. A. Giroto, R. Guardani, A. C. S. C. Teixeira, and C. A. O. Nascimento, "Study on the photo-Fenton degradation of polyvinyl alcohol in aqueous solution," *Chemical Engineering and Processing*, vol. 45, no. 7, pp. 523–532, 2006.

[4] K. Yoo, *Sequential biological treatment including ozonation for persistent organic compounds [Ph.D. thesis]*, Korea Advanced Institute of Science and Technology, Daejeon, South Korea, 1999.

[5] J. G. Lim and D. H. Park, "Degradation of polyvinyl alcohol by Brevibacillus laterosporus: metabolic pathway of polyvinyl alcohol to acetate," *Journal of Microbiology and Biotechnology*, vol. 11, no. 6, pp. 928–933, 2001.

[6] A. K. Bajpai and N. Vishwakarma, "Adsorption of polyvinylalcohol onto Fuller's earth surfaces," *Colloids and Surfaces A: Physicochemical and Engineering Aspects*, vol. 220, no. 1–3, pp. 117–130, 2003.

[7] S. K. Behera, J.-H. Kim, X. Guo, and H.-S. Park, "Adsorption equilibrium and kinetics of polyvinyl alcohol from aqueous solution on powdered activated carbon," *Journal of Hazardous Materials*, vol. 153, no. 3, pp. 1207–1214, 2008.

[8] Y. Chen, Z. Sun, Y. Yang, and Q. Ke, "Heterogeneous photocatalytic oxidation of polyvinyl alcohol in water," *Journal of Photochemistry and Photobiology A: Chemistry*, vol. 142, no. 1, pp. 85–89, 2001.

[9] L.-J. Hsu, L.-T. Lee, and C.-C. Lin, "Adsorption and photocatalytic degradation of polyvinyl alcohol in aqueous solutions using P-25 TiO_2," *Chemical Engineering Journal*, vol. 173, no. 3, pp. 698–705, 2011.

[10] C.-C. Lin, L.-T. Lee, and L.-J. Hsu, "Performance of UV/$S_2O_8^{2-}$ process in degrading polyvinyl alcohol in aqueous solutions," *Journal of Photochemistry and Photobiology A: Chemistry*, vol. 252, no. 1, pp. 1–7, 2013.

[11] K.-Y. Huang, C.-T. Wang, W.-L. Chou, and C.-M. Shu, "Removal of polyvinyl alcohol using photoelectrochemical oxidation processes based on hydrogen peroxide electrogeneration," *International Journal of Photoenergy*, vol. 2013, Article ID 841762, 9 pages, 2013.

[12] A. M. T. Silva, R. N. P. Vaz, R. M. Quinta-Ferreira, and J. Levec, "Gas-liquid-solid reactions of polyvinyl alcohol on oxidation treatments for environmental pollution remediation," *The Canadian Journal of Chemical Engineering*, vol. 81, no. 3-4, pp. 566–573, 2003.

[13] S. Kim, T.-H. Kim, C. Park, and E.-B. Shin, "Electrochemical oxidation of polyvinyl alcohol using a RuO2/Ti anode," *Desalination*, vol. 155, no. 1, pp. 49–57, 2003.

[14] W.-L. Chou, C.-T. Wang, C.-W. Hsu, K.-Y. Huang, and T.-C. Liu, "Removal of total organic carbon from aqueous solution containing polyvinyl alcohol by electrocoagulation technology," *Desalination*, vol. 259, no. 1–3, pp. 103–110, 2010.

[15] W.-L. Chou, L.-S. Chen, C.-T. Wang, and S.-R. Lee, "Electro-fenton removal of polyvinyl alcohol from aqueous solutions using an activated carbon fiber cathode," *Fresenius Environmental Bulletin*, vol. 21, no. 12, pp. 3735–3742, 2012.

[16] X. Chen and G. Chen, "Anodic oxidation of orange II on Ti/BDD electrode: variable effects," *Separation and Purification Technology*, vol. 48, no. 1, pp. 45–49, 2006.

[17] S. Ammar, R. Abdelhedi, C. Flox, C. Arias, and E. Brillas, "Electrochemical degradation of the dye indigo carmine at boron-doped diamond anode for wastewaters remediation," *Environmental Chemistry Letters*, vol. 4, no. 4, pp. 229–233, 2006.

[18] C.-T. Wang, J.-L. Hu, W.-L. Chou, and Y.-M. Kuo, "Removal of color from real dyeing wastewater by Electro-Fenton technology using a three-dimensional graphite cathode," *Journal of Hazardous Materials*, vol. 152, no. 2, pp. 601–606, 2008.

[19] E. Neyens and J. Baeyens, "A review of classic Fenton's peroxidation as an advanced oxidation technique," *Journal of Hazardous Materials*, vol. 98, no. 1–3, pp. 33–50, 2003.

[20] S. Balaji, S. J. Chung, R. Thiruvenkatachari, and I. S. Moon, "Mediated electrochemical oxidation process: electro-oxidation of cerium(III) to cerium(IV) in nitric acid medium and a study on phenol degradation by cerium(IV) oxidant," *Chemical Engineering Journal*, vol. 126, no. 1, pp. 51–57, 2007.

[21] A. R. Khataee, V. Vatanpour, and A. R. Amani Ghadim, "Decolorization of C.I. Acid Blue 9 solution by UV/Nano-TiO_2, Fenton, Fenton-like, electro-Fenton and electrocoagulation processes: a comparative study," *Journal of Hazardous Materials*, vol. 161, no. 2-3, pp. 1225–1233, 2009.

[22] M. Muruganandham and M. Swaminathan, "Photochemical oxidation of reactive azo dye with UV-H_2O_2 process," *Dyes and Pigments*, vol. 62, no. 3, pp. 269–275, 2004.

[23] N. Modirshahla and M. A. Behnajady, "Photooxidative degradation of Malachite Green (MG) by UV/H_2O_2: influence of operational parameters and kinetic modeling," *Dyes and Pigments*, vol. 70, no. 1, pp. 54–59, 2006.

[24] M. A. Fard, B. Aminzadeh, M. Taheri, S. Farhadi, and M. Maghsoodi, "MBR excess sludge reduction by combination of electrocoagulation and Fenton oxidation processes," *Separation and Purification Technology*, vol. 120, no. 1, pp. 378–385, 2013.

[25] C. Zhou, N. Gao, Y. Deng, W. Chu, W. Rong, and S. Zhou, "Factors affecting ultraviolet irradiation/hydrogen peroxide (UV/H_2O_2) degradation of mixed N-nitrosamines in water," *Journal of Hazardous Materials*, vol. 231-232, no. 1, pp. 43–48, 2012.

[26] X. He, M. Pelaez, J. A. Westrick et al., "Efficient removal of microcystin-LR by UV-C/H_2O_2 in synthetic and natural water samples," *Water Research*, vol. 46, no. 5, pp. 1501–1510, 2012.

[27] J. C. Farmer, F. T. Wang, P. R. Lewis, and L. J. Summers, "Destruction of chlorinated organics by cobalt(III)-mediated electrochemical oxidation," *Journal of the Electrochemical Society*, vol. 139, no. 11, pp. 3025–3029, 1992.

[28] V. V. Kokovkin, S. J. Chung, S. Balaji, M. Matheswaran, and I.-S. Moon, "Electrochemical cell current requirements for toxic organic waste destruction in Ce(IV)-mediated electrochemical oxidation process," *Korean Journal of Chemical Engineering*, vol. 24, no. 5, pp. 749–756, 2007.

[29] S. Balaji, S. J. Chung, M. Matheswaran, K. V. Vasilivich, and I. S. Moon, "Destruction of organic pollutants by cerium(IV) MEO process: a study on the influence of process conditions for EDTA mineralization," *Journal of Hazardous Materials*, vol. 150, no. 3, pp. 596–603, 2008.

[30] S. J. Chung, K. Chandrasekara Pillai, and I. S. Moon, "A sustainable environmentally friendly NO_x removal process using Ag(II)/Ag(I)-mediated electrochemical oxidation," *Separation and Purification Technology*, vol. 65, no. 2, pp. 156–163, 2009.

[31] M. Sudoh, H. Kitaguchi, and K. Koide, "Electrochemical production of hydrogen peroxide by reduction of oxygen," *Journal of Chemical Engineering of Japan*, vol. 18, no. 5, pp. 409–414, 1985.

[32] Y. Wei, B. Fang, T. Arai, and M. Kumagai, "Electrolytic oxidation of Ce(III) in nitric acid and sulfuric acid media using a flow type cell," *Journal of Applied Electrochemistry*, vol. 35, no. 6, pp. 561–566, 2005.

[33] T. Raju and C. A. Basha, "Electrochemical cell design and development for mediated electrochemical oxidation Ce (III)/Ce (IV) system," *Chemical Engineering Journal*, vol. 114, no. 1–3, pp. 55–65, 2005.

[34] J. H. Finley, "Spectrophotometric determination of polyvinyl alcohol in paper coatings," *Analytical Chemistry*, vol. 33, no. 13, pp. 1925–1927, 1961.

[35] W. L. Chou, C. T. Wang, and K. Y. Huang, "Investigation of process parameters for the removal of polyvinyl alcohol from aqueous solution by iron electrocoagulation," *Desalination*, vol. 251, no. 1–3, pp. 12–19, 2010.

[36] K.-L. Huang, T.-S. Chen, and K.-J. C. Yeh, "Regeneration of Ce(IV) in simulated spent Cr-etching solutions using an undivided cell," *Journal of Hazardous Materials*, vol. 171, no. 1–3, pp. 755–760, 2009.

[37] A. Özcan, Y. Şahin, A. S. Koparal, and M. A. Oturan, "Carbon sponge as a new cathode material for the electro-Fenton process: comparison with carbon felt cathode and application to degradation of synthetic dye basic blue 3 in aqueous medium," *Journal of Electroanalytical Chemistry*, vol. 616, no. 1-2, pp. 71–78, 2008.